AN INTEGRATED SYSTEM FOR FIRE AND EXPLOSION CONSEQUENCE ANALYSIS OF OFFSHORE PROCESS FACILITIES

RAVI CHANDRA PULA

AN INTEGRATED SYSTEM FOR FIRE AND EXPLOSION CONSEQUENCE ANALYSIS OF OFFSHORE PROCESS FACILITIES

BY

RAVI CHANDRA PULA© B. Eng. (Hons)

A thesis

submitted to the School of Graduate Studies

in partial fulfillment of the requirements for the degree of

MASTER OF ENGINEERING

FACULTY OF ENGINEERING AND APPLIED SCIENCE

MEMORIAL UNIVERSITY OF NEWFOUNDLAND

St. John's, Newfoundland, Canada

July 2005

Abstract

Offshore oil and gas platforms are well known for their compact geometry, high degree of congestion, limited ventilation and difficult escape routes. A small mishap under such conditions can quickly escalate into a catastrophe. Among all the loss producing events occurring offshore, fires and explosions are the most frequently reported process related accidents. They have potential to cause serious injury to personnel, major damage to equipment and structure, and disruption of operations. It is therefore necessary to study the characteristics of fires and explosions and thereby quantify the hazards/consequences posed by them in order to complete a detailed quantitative risk assessment study. This can eventually form a basis for the implementation of appropriate mitigation measures and emergency response plans to protect personnel in case of any eventuality.

While there are many consequence models available to predict fire and explosion hazards – varying from simple empirical models to highly complex computational fluid dynamic models – only a few have been validated for the unique conditions found offshore. Furthermore, the complexity involved in simulating these models for quantifying the consequences makes the use of computer programs inevitable. Although, there are a few commercial software

packages available for offshore quantitative risk assessment and consequence studies, they are very expensive and there is ample scope for technical improvements in these packages.

This work is, therefore, focused on developing a scientifically sound tool for offshore consequence analysis. Technical improvements were incorporated by carrying out an extensive literature review on the existing consequence models (such as source models, dispersion models, ignition models, and fire and explosion models) and selecting the state-of-the-art ones most suitable for offshore conditions. Also, the implementation of a grid based methodology for impact assessment is innovative and is the highlight of this work. This work is considered to have produced a significant contribution in the areas of fire and explosion consequence modeling due to the development of additional models for predicting fire overpressures and analyzing the possibility of accident escalation (Domino effects analysis).

Acknowledgements

I wish to express my deep gratitude towards my supervisors Dr. Faisal I Khan, Dr. Brian Veitch and Dr. Paul R. Amyotte for their financial and moral support, and the invaluable guidance provided throughout the period of my study. I would never forget to thank their remarkable character of encouraging students to persistently focus on research, draft papers and attend technical conferences which form the stepping stones for any researcher. The time we spent at IIT Kanpur and Halifax conferences are the most stimulating moments of my life. Special thanks for everything you have done to me.

I would like to gratefully acknowledge the financial support from NSERC and School of Graduate Studies, Memorial University. I am also thankful to Faculty of Engineering and Applied Science, for giving me an opportunity to pursue my Master's degree and providing me with the best of the resources and a friendly atmosphere.

Heartfelt thanks to Christian uncle, Priya aunty, Howse family and everyone in St.John's who cared for me and helped me when I was in need. You are all wonderful. My endless gratitude towards my parents and brothers for bestowing their unconditional love, affection and friendship, and for the immense trust they have in me.

Lastly to all my friends: Ram, Manoj, Joseph, Jay, Chandru, Sachin, Vikrant and many more, who have made the last two years most enjoyable and unforgettable especially the moments we had during our trips to Grosmorne, Terranova, and many other places in Newfoundland. You are the best.

Contents

List of Figures

List of Tables

Nomenclature

a	Proportion of time for which source is active.
A	Area of the hole, m^2
b	Flame lift-off , m
C_d	Discharge coefficient (0.60 for liquids, ~0.8 for gases)
d	Cloud depth, m
d_j	Diameter of the expanded jet, m
D	Diameter of the pool, m
D'	Diameter of the dragged flame, m
D_s	Combustion source diameter, m
D_t	Diameter of the spherical target object, m
E	Expansion ratio, $\frac{\rho_u}{\rho_b}$
E_{ki}	Kinetic energy imparted to the fragment, Joule
Fr	Froude number
$F_{s\infty}$	Fraction of the overall heat emitted as radiation
g	Acceleration due to gravity, 9.81 m/s^2
h	Release height, m
h_s	Static head of liquid, m

H	Height of the cloud, m
H_f	Visible flame height, m
k	Burning rate size coefficient, m^{-1}
k_m	Extinction coefficient
L	Length of the flame, m
L_c	Clear layer length, m
L_P	Path length through the atmosphere, m
L_{bo}	Length of the flame in still air, m
$\dot{m}$	Mass burning rate, kg/m^2s
m_l	Mass of fluid released, kg
M	Quantity of gas released instantaneously, kg
$\dot{M}$	Mass discharge rate, kg/s
M_e	Mass of gas emitted from the main vent, kg
M_f	Mass of the fragment, kg
M_u	Mass of unburned gas, kg
MW	Molecular weight, kg/kmol
MW_{air}	Molecular weight of air, kg/kmol
n	Moles of combustion gases in the compartment, moles
p	Ignition potential of a source (0-1)

P	Pressure, N/m^2
P_o	Overpressure, N/m^2
P_a	Ambient pressure, Pa
P_g	Absolute pressure of the gas, Pa
P_l	Absolute pressure at which the liquid is stored, Pa
PI	Probability of ignition
PI_n	Probability of no ignition
P_t	Pressure at the target, Pa
$\overline{P_t}$	Non-dimensional overpressure at the target
q	Radiation heat flux, kW/m^2
Q	Net heat released by combustion, kW
Q_e	Volumetric flow of air entrained at the edge of the cloud
Q_t	Total volumetric flow of air entrained at the top of the cloud
r'	Distance from the edge of the cloud to the receiver, m
R	Cloud radius, m
Ri_*	Richardson number
R_g	Ideal gas constant,
R_H	Relative humidity expressed as a fraction
R_L	Length of the frustum, m

R_0	Radius of the explosion source gas cloud, m
SEP	Average surface emissive power, kW/m^2
SEP_∞	Maximum surface emissive power of a fuel, kW/m^2
SEP_S	Surface emissive power of smoke (approx. 20 kW/m^2)
SEP_L	Average surface emissive power of the lower clear flame
SEP_U	Average surface emissive power of the upper smoke obscured layer, kW/m^2
SEP_{side}	Average surface emissive power from the side of the jet flame, kW/m^2
SEP_{end}	Average surface emissive power from the end of the jet flame, kW/m^2
sA	Flame area, m^2
S	Cloud burning speed, m/s
S_{mm}	Saturated water vapor pressure in mm Hg at the ambient temperature, K
t	Time, s
t_a	Average time for which source is active, s
t_i	Average time between source activations, s
t_{lo}	Lift off time, s
T_{cc}	Temperature at one end of the compartment, K

T_o	Initial compartment temperature (15° C)
T_{flame}	Flame temperature, K
T_{gases}	Average gas temperature, K
u	Wind velocity, m/s
u'	Root mean square burning velocity, m/s
u_*	Friction velocity, 5-10% of the wind speed at a height of 10m
u_c	Mean velocity of the cloud, m/s
u_j	Velocity of the expanded jet, m/s
u_r	Mean wind velocity at a reference height, m/s
u_1	Specific internal energy of the fluid in the initial state, Joule
u_2	Specific internal energy in the expanded state, Joule
U_R	Unobscured ratio
U_t	Turbulent burning velocity, m/s
U_x	Wind velocity in the downwind direction, m/s
U_z	Wind velocity in the crosswind direction, m/s
U_{xz}	Wind velocity vector, m/s
U_v	Velocity of the unburned gas through the vent, m/s
v_i	Initial fragment velocity, m/s
V	Total volume of the gas cloud, m^3

V_b	Volume of burnt gas, m^3
V_0	Volume of the explosion source gas cloud, m^3
V_{room}	Volume of the compartment under study, m^3
$\dot{V}_L$	Volumetric spill rate, m^3/s
VF	Geometric view factor
W	Flame width, m
W_1	Width of the frustum base, m
W_2	Width of the frustum tip, m
x	Distance along the plume centerline, m
y	Lateral displacement from plume centerline, m
z	Height above ground, m
z_o	Roughness length, m
z_r	Reference height, 10 m
γ	Isentropic expansion factor (Cp/Cv)
γ_i	Fragment angle of trajectory, degrees
μ	Average number of ignition sources per unit area
λ	Rate of activation of the source, s^{-1}
θ	Pool fire flame angle from the vertical (degrees)
τ	Atmospheric transmissivity
ρ_c	Density of the cloud, kg/m^3

ρ_a	Density of the ambient air (1.23 kg/m^3)
ρ_l	Density of the liquid, kg/m^3
ρ_0	Fuel-air mixture density, kg/m^3
ρ_j	Density of the expanded jet, kg/m^3
ρ_u	Unburned gas density, kg/m^3
ρ_b	Burned gas density, kg/m^3
α	Tilt of the jet flame with the vertical axis, degrees
r	Stiochiometric mixture air-fuel mass ratio
α	Constant pressure expansion ratio for stoichiometric combustion (typically 8 for hydrocarbons)
ϕ	Fuel-air mixture composition (fuel volume ratio)
ϕ_{st}	Stoichiometric mixture composition (fuel volume ratio)
σ	Stefan-Boltzmann constant ($5.669*10^{-8}$ W/m^{2}K^4)

Chapter 1

INTRODUCTION

1.1. OFFSHORE PROCESS OPERATIONS

An offshore oil and gas platform is usually divided into a number of modules for operations, such as separation, water injection, high-pressure compression, and seawater de-aeration, as well as local and main electrical rooms and an accommodations block. Most of the process modules are highly congested with the presence of obstacles in the form of pipelines, barriers and other equipment necessary for process operations. The level of risk in such conditions, while operating in a remote and harsh marine environment, is high.

A study by the UK Health and Safety Executive (HSE, 1996 and Mansfield et al., 1996a) showed that process and structural failure incidents account for almost 80% of the risk to personnel offshore. Potential risks offshore include blowouts, riser and process leaks, fires, explosions, vessel collisions, helicopter accidents, dropped objects, structural failures, and capsizing. The past few

decades have seen a wide range of major accidents with a number of fatalities, economic losses, and damage to the environment. Examples of accidents in the offshore oil and gas industry includes the flooding and capsize of the *Ocean Ranger* on the Grand Banks (1982), a blowout on the *Vinland* off Sable Island (1984), the structural failure and loss of the *Alexander Kielland* in Norway (1980), the process leak leading to fires and explosions on the *Piper Alpha* in the UK (1988), the explosion and sinking of the *P-36* production semi-submersible off Brazil (2001), and the recent helicopter accident en route to the Bombay High offshore platform. An examination of incidents such as *Piper Alpha* in the North Sea and the *P-36* production semi-submersible off Brazil reveals that most offshore incidents are in fact process-related.

Experience shows that operational failures and human errors are the most common initiating events for accidents offshore. While operational failures could be arrested by safety-instrumented systems (through monitoring and restriction to the desirable limits of Safety Integrity Level or SIL), human errors are difficult to identify and quantify. Recently DiMattia et al. (2004) developed a unique human error probability calculation index for offshore mustering. The operational failures can be mainly attributed to design faults or improper inspection and maintenance.

1.2. QUANTITATIVE RISK ASSESSMENT

An offshore development can never be completely safe, but the degree of inherent safety (Mansfield et al., 1996b and Khan & Amyotte, 2002) can be increased by selecting the optimum design in terms of the installation/field configuration, layout, and operation. This is done in an attempt to reduce the risk to a level that is As Low As Reasonably Practicable (ALARP) without resorting to costly protective systems. This requires the identification and assessment of major risk contributors, which could be accomplished using Quantitative Risk Assessment (QRA) techniques early in the project life cycle. If a structured approach of identification and assessment is not carried out early in the project, it is possible that the engineering judgment approach will fail to identify all of the major risks, and that loss prevention expenditures will be targeted in areas where there is little benefit. This may result in expensive remedial actions later during the life of the project (Vinnem, 1998).

QRA involves four main steps (Figure 1.1): hazard identification, consequence assessment, probability calculation, and risk quantification (Khan et al., 2002). Consequence assessment, which is central to QRA, involves quantification of the likely loss or damage due to anticipated eventualities. Among the various possible loss-producing events on offshore production

facilities, fires and explosions are the most frequently reported process-related incident (Chamberlain, 2002). They may result in anything from no damage or loss, up to catastrophic damage or loss, depending upon their characteristics.

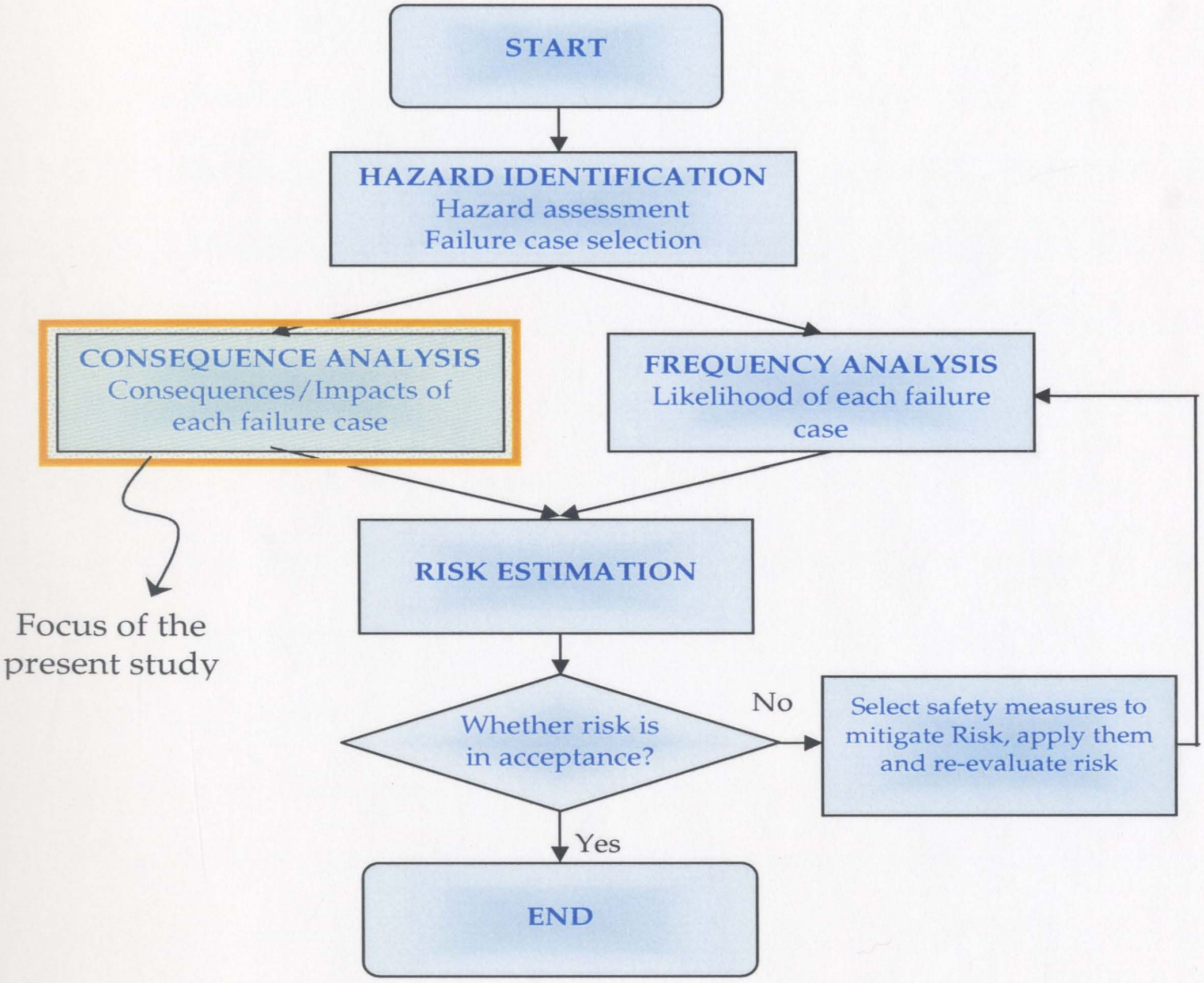

Figure 1.1. Flow chart for Quantitative Risk Assessment

Since the *Piper Alpha* disaster, the offshore industry has carried out a great deal of research work directed towards understanding the characteristics of hydrocarbon fires and explosions. This research has resulted in the development of numerous fire and explosion consequence models varying from simple empirical models to highly complex computational fluid dynamics models. The complexity involved in using these models for quantification of consequences has led to the evolution of computer-automated toolkits. There are many commercial software packages available for a detailed analysis of fire and explosion consequences, which includes COMEX, VENTEX, CLICHÉ, FRED, SCOPE, ARAMAS, FIREX, MAXCRED, PLATO, DAMAGE, OHRAT, PHAST, SAFETI, SUPERCHEMS, and CANARY etc. These packages use empirical, semi-empirical and phenomenological models for analyzing the characteristics of accidents. The advantage of using simple models is less computational time, thus aiding the design engineers to carry out numerous 'what if' runs, and testing the effect of design modifications. It also aids in conducting a detailed quantitative risk assessment study in less time. Complex computer models (mainly based on computational fluid dynamics) such as FLACS, EXSIM, COBRA, CFX, AUTOREAGAS, Imperial College code etc. are also available. However, the limiting factors in their applicability are related to high computational time and user expertise. Further, the input details required by models are very high, thus being inappropriate for use in the early design phase.

Although, the above mentioned packages serve the purpose of performing a QRA and consequence analysis, only a few deal with offshore process operations. The ones that consider offshore conditions are very expensive, for example, OHRAT (offshore hazard and risk analysis tool kit), now known as NEPTUNE supplied by DNV costs more than $100,000. Further, there is ample scope of technical improvements in these commercial software packages. Thus, there is a need for an economically viable, easy to use, scientifically sound tool for offshore QRA, particularly consequence assessment. The present work is an attempt to fulfill these requirements.

1.3. OBJECTIVES OF THE CURRENT WORK

The overall objective of this work is "**To develop an integrated computer automated toolkit for Consequence Analysis of process accidents on offshore oil and gas platforms".**

In the process of achieving this objective, the work has been planned in such a way that the existing knowledge of Offshore Consequence Analysis can be enhanced through the following advancements:

- **Release, Dispersion and Ignition modeling:** Available release models and gas dispersion models have been reviewed and the models most

suitable to conditions offshore have been identified. An enhanced model for estimating onsite ignition probability has also been identified and embedded in the consequence assessment process to enable better prediction of impact and risk.

- **Fire Consequence Modeling:** A comprehensive literature review has been carried out to analyze the modeling techniques available to model fire radiation hazards. For each of the offshore fires, most appropriate model has been identified and selected for the current application. Further, the models were refined by making revisions wherever necessary by incorporating wind and confinement effects, which are unique to offshore process facilities.
- **Fire Overpressure impact:** The importance of overpressure caused due to fire in a confined or semi-confined space has been highlighted by Wighus (1994). However, there appears to have been no attempt to quantify this phenomenon. A model has therefore been developed to study the overpressure impact. This model is embedded in the basic fire consequence modeling methodology described herein.
- **Explosion Consequence Modeling:** Available explosion modeling techniques were reviewed and suitable one was selected for the specific

requirements imposed. Appropriate models for offshore gas explosions and BLEVE were identified.

- **Missile impact model:** A new model has been developed to determine the probability of impact of missiles on objects in the neighborhood by employing statistical distributions for stochastic and uncertain parameters. This model can also be used to analyze the possibility of escalation of events, the phenomenon often termed as domino effect analysis.
- **Radiation and blast consequence modeling:** Instead of point/area modeling, a grid-based approach has been developed and employed to enable better modeling and analysis of radiation and overpressure impact at different locations in the process area, plotting the results as contours.

1.4. STRUCTURE OF THESIS

The thesis is divided into eight chapters. This first chapter has provided an introduction to the characteristics of offshore oil and gas process operations and an overview of the previous accidents. Importance of QRA for the offshore industry, various software packages currently available for consequence analysis and their features were also discussed, followed by the objectives set out for this research.

Chapter 2: This chapter provides an overview of offshore consequence analysis. Particularly, process accidents such as fires and explosions are emphasized and the procedures to analyze the consequences from these accidents have been discussed. Also, the necessary models to carry out such analyses are identified and discussed.

Chapter 3: Release, dispersion and ignition form the major initiatives for any process related accidents such as fires and explosions. This chapter presents the details of the release, gas dispersion and ignition models adopted in the present study.

Chapter 4: This chapter elaborates the extensive literature review carried out in fire consequence modeling to select the state-of-the-art consequence models that are necessary for performing a fire consequence study as identified in chapter 2. Modeling details of the selected ones are discussed as well. In addition, a model for fire overpressure impact assessment has been developed and discussed.

Chapter 5: This chapter focuses on the extensive literature review carried out in explosion consequence modeling to select the state-of-the-art consequence models that are necessary for performing an explosion consequence study as identified in chapter 2. Modeling details of the selected ones are discussed as

well. Additionally, a new probabilistic model has been developed, to analyze the damage caused by missiles to the people and the process area.

Chapter 6: With the successful selection of the necessary and appropriate models for offshore conditions, as discussed in chapters 3, 4 and 5, computer codes were developed in MATLAB for fire and explosion consequence analysis. This task was achieved by simulating the suite of fire consequence models and explosion consequence models for various accident scenarios. A grid based approach has been introduced and employed during the simulation process, details of which are provided in this chapter.

Chapter 7: This chapter discusses the simulation results of various fire and explosion accident scenarios. The results are in the form of hazard potentials and the corresponding consequences to people. With the help of a grid based approach the result were plotted more interactively in the form of contours over a predefined process area. The comparison and validation of these results with those obtained by the models used in commercial software packages has also been discussed.

Chapter 8: The final conclusions of this work and future recommendations for the research have been provided in this chapter.

Chapter 2

OFFSHORE CONSEQUENCE ANALYSIS

This chapter provides an overview of offshore consequence analysis. Different types of offshore accidents considered in this study have been discussed. The procedures to analyze the consequences from these accidents have been formulated and the models required to carry out consequence studies have been identified and discussed herein.

2.1. INTRODUCTION

As discussed in Section 1.2 and shown in Figure 1.1, QRA involves four main steps: hazard identification, consequence analysis, probability calculation and finally risk quantification. Consequence analysis, which is considered to be central to QRA, involves quantification of the likely loss or damage due to anticipated eventualities. The main aim of performing a consequence analysis is to identify the personnel, equipment, plant and structure that are exposed to the initial and escalating events, and to assess the likely effects and failures. Assessing the consequences from various loss-producing events on offshore

platforms is referred to as offshore consequence analysis. Nevertheless, the methodology of consequence analysis remains the same irrespective of offshore or onshore conditions, only the models used to perform the analysis would vary.

Offshore accidents are usually classified as process accidents, non-process fires, blowouts, collision accidents, structural failures, earthquakes, helicopter accidents, dropped objects, diving accidents and construction accidents. Among all, process accidents pose higher percentage of risk to the personnel onboard (HSE, 1996 and Mansfield et al., 1996a). Therefore, in the present study only process related accidents are considered. Among the process related accidents fires and explosions are the most frequently reported hazardous events. They have a potential to cause major damage to the personnel, equipment, structure and the environment. This fact is reflected from the *Piper Alpha* disaster (6 July 1988), the worst ever disaster in the history of offshore accidents. It was initiated by a condensate leak in the gas compression module, which ignited and exploded leading to pool fires and jet fires on the platform that in turn escalated through secondary explosions and fires eventually destroying the whole platform and killing 167 people (Spouge, 1999).

Since this incident, the offshore industry, along with the regulatory agencies of most of the countries, has come up stringent rules, making QRA compulsory with the risk associated with the platform be reduced to ALARP, for new as well as existing offshore platforms. With QRA being made compulsory, in recent times a great deal of research work has been carried out (Johnson et al., 1994, 1997, Cracknell et al., 1994, Rew et al., 1997, 1998, Chamberlain, 1996, Chamberlain & Persaud, 1997, Van den Berg, et al. 1997, 2000, Baker et al. 1998, 2000, 2004, Puttock, 1999, 2000 and Lea et al. 2002) that was directed towards understanding the characteristics of hydrocarbon fires and explosions. This research has resulted in the development of numerous fire and explosion models for consequence studies that can be further used for risk assessment studies. However, due to increased complexity involved in solving these models, the use of computer-automated toolkits becomes inevitable.

The present study is focused on developing one such toolkit to perform fire and explosion consequence analysis by embedding the state-of-the-art fire and explosion consequence models in it. However, in order to develop the computer codes successfully, two things are considered very important:

(i) Formulation of the procedures for fire and explosion consequence analysis, and

(ii) Identification of the necessary consequence models required to perform such analyses.

The following sections emphasize these two points. Fire and explosion consequence analyses are considered as two separate entities, hence are dealt with in two different sections. The details of fire consequence analysis are dealt within Section 2.2, whereas that of explosion is dealt within Section 2.3.

2.2. FIRE CONSEQUENCE ANALYSIS

Fire consequence analysis is defined as the process of analyzing the consequences from fires (Phillips, 1994, Ditali et al., 2000, CCPS, 2000, and Krueger et al., 2003, Pula et al., 2005). Consequences from fires are evaluated in terms of damage to personnel, equipment, structure and the environment. Only consequences to personnel (injury to the people) are considered in this work.

Fires occur when a leakage or spillage of flammable material is triggered by one of any number of potential ignition sources (sparks, open flames, etc.). Depending on the type of material released, nature of the release and the time of ignition, offshore fires are mainly classified into four types: pool fires, jet fires,

fireballs and flash fires (Lees, 1996 and Pula et al., 2004). A brief description follows:

i) **Pool fire** – a burning pool of hydrocarbon liquid released in a blowout or from oil leaks. Heat radiation from this type of fire can be lethal to personnel. An oil pool fire often results in a large smoke plume, which can also prove to be lethal if inhaled. Also, excess smoke causes impaired visibility along escape routes, leading to deaths during mustering. Toxicity effects from the gases such as carbon dioxide, carbon monoxide and traces of other gases, released during combustion are also significant.

ii) **Jet fire** – a burning jet of gas or spray of vapor released from high pressure equipment. This represents a significant element of risk to the personnel on offshore installations. Radiation heat flux and the impingement characteristics are the main sources of damage to personnel.

iii) **Fireball** – a spherical fire resulting from sudden release of pressurized liquid or gas that is immediately ignited. Although it may only last a few seconds, this can be lethal for personnel at distances close to the fireball due to its high radiation effects.

iv) **Flash fire** – a fire that propagates through a cloud of gas. This may be lethal for anyone within it, but is unlikely to damage steel structures.

Although there are additional fires like flares, fires on the sea surface and running liquid fires, they are in one way or the other modeled as one of the above defined types. For example, flares are treated as vertical jet fires, and fires on the water surface and running liquid fires are treated as pool fires. Therefore only these four fires have been considered within this work.

The damage to the personnel from these fires is mainly caused due to the hazard potentials such as external thermal radiation, smoke and toxicity effects and overpressure impacts. Overpressure impact from fires in confined spaces is one of the important hazards often neglected in fire consequence modeling that has been highlighted by Wighus (1994). With only small openings in a compartment, the highly energized combustion products released from these fires can generate pressures greater than ambient. This is considered to be significant. As there was no attempt to quantify the possible impacts from fire overpressures, a model has been developed and used in the present work.

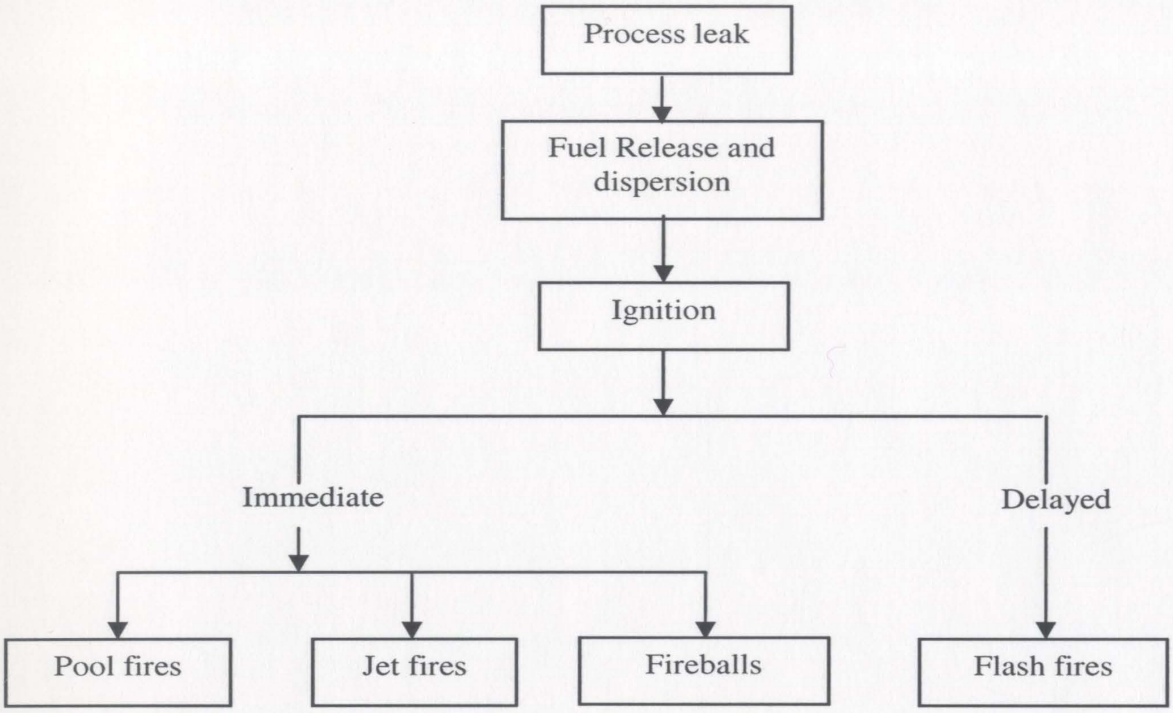

Figure 2.1: Scenario for the occurrence of variety of fires

The scenario for the occurrence of the four types of fires mentioned earlier is presented in Figure 2.1. It is apparent that any fire event begins with an incident leading to loss of fuel from the process. Typical incidents include the rupture or break of a pipeline, leak in a tank or pipe etc. The procedure for analyzing the consequences initiating from such incidents and the necessary models required to perform the analysis are the topics of the subsequent sections.

2.2.1. Procedure For Fire Consequence Analysis

As is evident from the earlier discussion, any process related accident initiates from a process leak. Fuel released due to such a leak starts dispersing and results in a fire upon ignition of the dispersing cloud. The procedure to analyze consequences from this scenario (CCPS, 2000) is described as follows:

1. Upon fuel discharge, the first step is to estimate the rate of discharge of the fuel or the total quantity discharged. Source/release models are then selected based on the phase of release and can be effectively used to serve the purpose.

2. The second step is to determine how the released material is transported downwind and dispersed to some concentration levels. Dispersion models can be used to predict these characteristics.

3. The third step is to predict the probable chances for the dispersing cloud to get ignited. An ignition model can be used to estimate the probability of ignition of the dispersing cloud.

4. Fuel ignition leads to a fire. The fourth step is then to determine the characteristics of the resultant fire such as the burning properties, flame dimensions, etc. Individual fire models for the corresponding fires can be used to predict these features.

5. The possible hazards from fires are external thermal radiation, smoke, toxicity effects and overpressure impacts. In the fifth step, the hazard potentials associated with each hazard are quantified. Radiation models, smoke and toxicity models and fire overpressure models can be used for this purpose.

6. The sixth step is to translate the incident specific results or the hazards potentials of radiation, smoke, toxic gases and fire overpressure into effects on people (injury or fatality). Human impact models can be used to quantify this effect. Finally, a grid based model can be used to analyze these consequence results in a better way.

The procedure described so far is represented in the form of a flowchart shown in Figure 2.2.

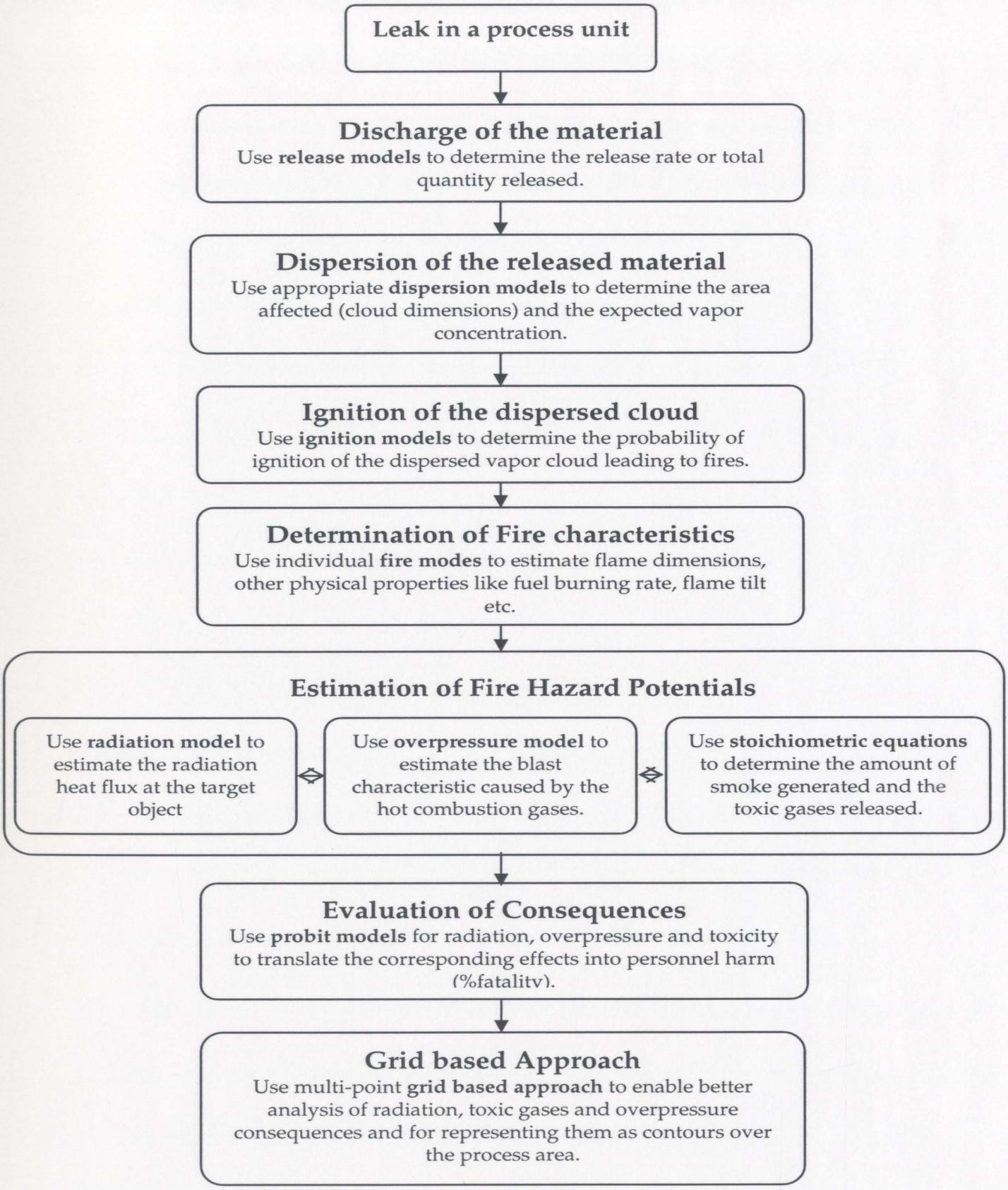

Figure 2.2. Procedure for Fire consequence analysis

2.2.2. CONSEQUENCE MODELS REQUIRED

Based on the procedure described in the previous section, it is apparent that the models required to perform a fire consequence analysis are release models, dispersion models, ignition models, individual fire models, radiation model, overpressure model, smoke and toxicity models and human impact models. All the models together form a comprehensive **fire consequence model suite**. A brief description of each of the models follows:

i) **Release models:** These models determine the rate of fuel release or the amount of fuel released. Release models are very significant; as this is the initial step for consequence analysis, improper selection may prove highly sensitive for the overall consequences estimated. Details about these models are elaborated in Section 3.1.

ii) **Dispersion models:** The gases or vapor released as a result of a leak start dispersing. These models can predict the dispersion characteristics of the vapor cloud in terms of estimating the area affected (cloud dimensions) and the expected vapor concentration. Details are provided in Section 3.2.

iii) **Ignition models:** Ignition models are used to carry out a probabilistic analysis to evaluate the probability of ignition of the dispersed vapor cloud. Modeling details are presented in Section 3.3.

iv) **Fire models:** These models estimate the characteristics of the fires which are later used to evaluate the radiation heat flux. For example, in the case of a pool fire, the model estimates the fire diameter, flame length, flame drag, flame tilt etc. Details of fire modeling for pool fires, jet fires, fireballs and flash fires are provided in Sections 4.1.1, 4.2.1, 4.3.1, 4.4.1 respectively.

v) **Radiation models**: These models are used to quantify the radiation heat flux at a target object. Each type of fire has a specific set of equations for estimating the radiation heat flux. These equations are based on the flame dimensions and fire characteristics, which are obtained from the fire models. Details of radiation models for all the four types of fires are provided in Sections 4.1.2, 4.2.2, 4.3.2, 4.4.2.

vi) **Smoke and Toxicity (CO and CO_2) models**: A large amount of smoke is released due to combustion of heavy hydrocarbons on offshore platforms. In addition, incomplete combustion of fuels will result in the release of toxic gases. These models estimate the amount of smoke and toxic gases released, details of which are presented in Section 4.5.

vii) **Overpressure model**: This model is used to quantify the overpressures and investigate possible blast effects caused by the hot combustion gases released in a confined environment. A model has been developed for quantifying this effect and is discussed in Section 4.6.

viii) **Human impact models**: Probit models are used to translate the fire hazard potentials such as radiation heat flux, blast overpressure and toxicity effects into damage to assets and harm to personnel. Details of individual probit models are provided in Section 4.7.

ix) **Grid based model:** A multipoint grid based model has been developed and employed to enable better modeling and analysis of radiation impact at various locations in the process area. The radiation and fatality results are eventually plotted as contours, a more user friendly way of representation than the conventional method where the results are represented as line plots. Details are discussed in chapter 6.

2.3. EXPLOSION CONSEQUENCE ANALYSIS

Explosion consequence analysis is defined as the process of analyzing the consequences from a variety of explosions (Ditali et al., 2000, CCPS, 1994, 1996, 1998, 2000, and Pula et al., 2005). The explosions that commonly occur on an offshore platform are classified as (Spouge, 1999):

i) Gas explosions

- Explosions in unconfined, congested areas (e.g. on the deck of an FPSO)
- Explosions in confined areas (e.g. within a compartment or module)

- External explosions (e.g. following a confined, vented explosion)

ii) Boiling Liquid Expanding Vapor Explosions (BLEVE).

The scenario for the occurrence of these explosions is presented in Figure 2.3. Other types of explosions include physical explosions (caused by excess pressure in a vessel), internal explosions (within a flare stack), mist explosions and solid phase explosions (e.g. associated with the use of well completion explosives). The modeling of internal explosions, mist explosions, and solid phase explosions is not well understood and needs further research efforts. Hence, only gas explosions and BLEVE are discussed within this work.

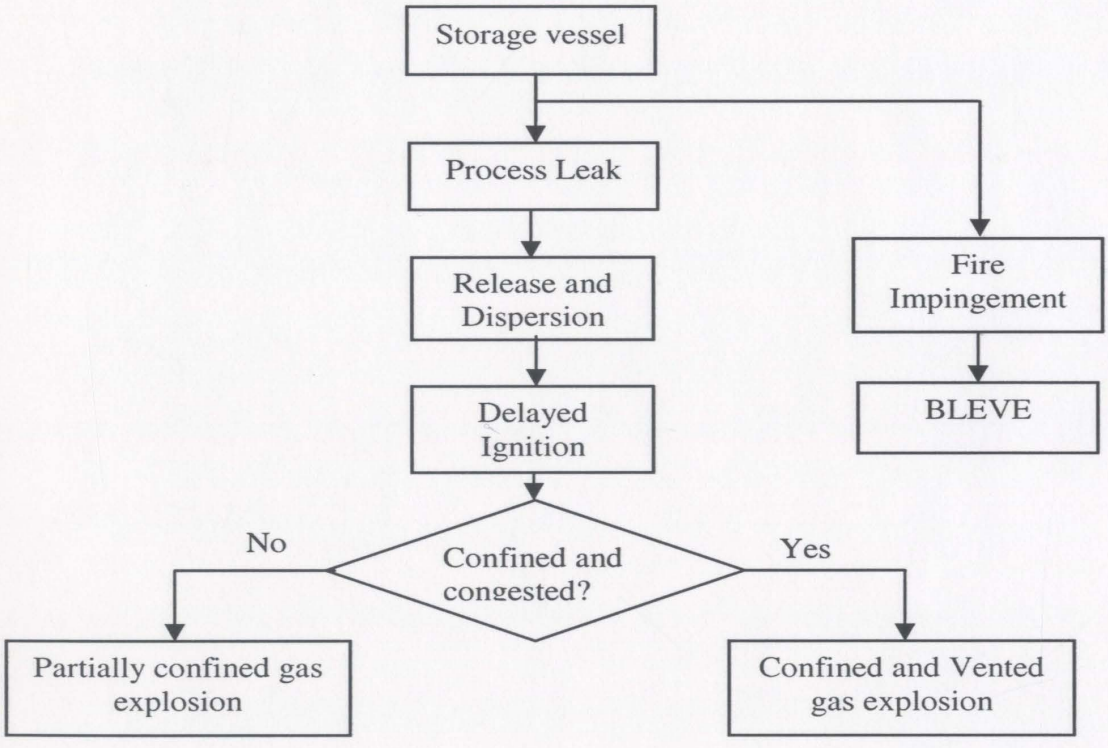

Figure 2.3: Scenario for the occurrence of variety of explosions

Again, only consequences to the people are considered. The consequences from explosions are either in the form of direct blast effects such as lung or ear drum ruptures or indirect effects such as impact from missiles projected by the explosion. The procedure for analyzing these consequences and the necessary models required to perform the analysis are the topics of the subsequent sections.

2.3.1. Procedure For Explosion Consequence Analysis

A gas explosion occurs due to delayed ignition of the vapor cloud subject to the fact that the gas is released in a congested area that is capable enough to enhance the flame speed. The procedure to analyze consequences from this scenario (CCPS, 2000 and Ditali et al., 2000) is described as follows:

1. Upon fuel discharge, the first step is to estimate the rate of discharge of the fuel or the total quantity discharged. Source/release models are then selected based on the phase of release and can be effectively used to serve the purpose.

2. The second step is to determine how the released material is transported downwind and dispersed to some concentration levels. Dispersion models can be used to predict these characteristics.

3. The third step is to predict the probable chances for the dispersing cloud to get ignited. An ignition model can be used to estimate the probability of ignition of the dispersing cloud.

4. Ignition of the dispersing cloud leads to an explosion under specific conditions such as delayed ignition of the cloud in congested environment. The fourth step is to determine the explosion characteristics like source overpressure, pressure pulse duration, decay etc. Gas explosion models can be used to predict these features.

5. The hazards from explosions are blast overpressure and missile effects. In the fifth step, the hazard potentials associated with each hazard are quantified. Blast dissipation and missile effects models can be used for this purpose.

6. The sixth step is to translate the incident specific results such as the hazards potentials of blast overpressure and missiles into effects on people (injury or fatality). Human impact models can be used to quantify this effect. Finally, a grid based model can be used to analyze these consequence results in a better way.

The procedure described so far is represented in the form of a flowchart shown in Figure 2.4. It should be noted that the first three steps in the

consequence analysis for gas explosions are the same as those for fire consequence analysis. For the case of a BLEVE scenario, the consequence analysis procedure is not as complex as gas explosions. It involves only three steps, similar to those explained in steps 4, 5, 6 above in which source overpressure, pressure pulse duration and decay are estimated, followed by estimation of hazard potentials and corresponding consequences.

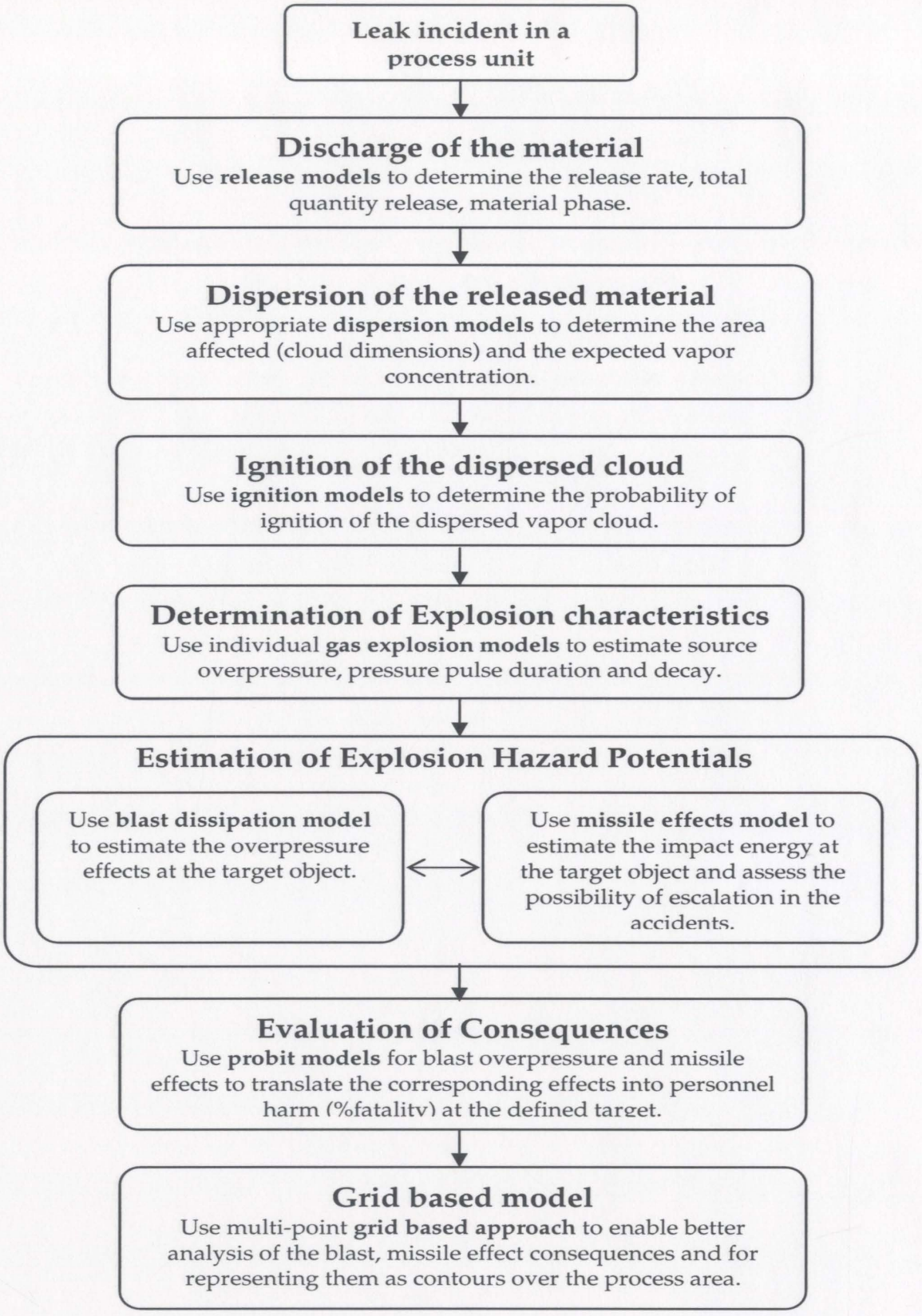

Figure 2.4: Procedure for gas explosion consequence analysis

2.3.2. CONSEQUENCE MODELS REQUIRED

Based on the procedure described in the previous section, it is apparent that the models required to perform an explosion consequence analysis are release models, dispersion models, ignition models, explosion models, blast dissipation models, missile effects model and human impact models. All the models together form an **explosion consequence model suite**. A brief description of each of the models follows:

i) **Release models:** These models are used to determine the amount of fuel released or the rate of fuel release. Details are elaborated in Section 3.1.

ii) **Dispersion models:** These models predict the dispersion characteristics of the vapor cloud in terms of estimating the dimensions and the physical properties of the gas cloud. Literature review, modeling details are provided in Section 3.2.

iii) **Ignition models:** Ignition models are used to carry out a probabilistic analysis to evaluate the probability of ignition of the dispersed vapor cloud. Modeling details are presented in Section 3.3.

iv) **Explosion models:** These models estimate the explosion characteristics and predict certain parameters like source overpressure, pressure pulse duration and decay. Details of gas explosion models for partially confined

and totally confined cases are presented in Sections 5.1.1, 5.1.2 respectively. BLEVE details are provided in 5.2.

v) **Blast dissipation model**: This model is used to quantify the blast overpressure at a target object located at a certain distance from the explosion source. It remains the same for all the types of gas explosions. Overpressure dissipation model details are provided in Sections 5.1.1.

vi) **Missile Effects model:** A new probabilistic model has been developed to analyze the damage caused by missiles to the process area. It can also be used to assess the possible chances of escalation of accidental events. Details are discussed in Section 5.3.

vii) **Human impact models**: Probit models are used to translate the fire hazard potentials such as radiation heat flux, blast overpressure and toxicity effects into damage to assets and harm to personnel. Details of individual probit models are provided in Section 5.4.

viii) **Grid based model:** A multipoint grid based model has been developed and employed to enable better modeling and analysis of overpressure impact. This model helps in plotting the blast dissipation and fatality results as contours. Details are provided in chapter 6.

2.4. SUMMARY

This chapter has provided an overview of offshore consequence analysis. Particularly, process accidents such as fires and explosions were emphasized and the procedures to analyze the consequences from these accidents were discussed. Also, the necessary models to carry out such analyses were identified.

The subsequent chapters will present the details of the extensive literature review that has been carried out for selecting the state-of-the-art consequence models that are suitable to be used in offshore conditions. The selected models were further revised wherever possible. In case of unavailability of certain models in the literature, new models were developed and discussed. Chapter 3 deals with source/release, dispersion and ignition modeling, whereas chapters 4 and 5 deal with fire and explosion consequence models respectively. The literature review was followed by selection and revision of models, then computer codes were developed utilizing the procedures provided in this chapter and the revised models. Results obtained by simulating various credible accident scenarios were finally discussed in chapter 7.

Chapter 3

RELEASE, DISPERSION AND IGNITION MODELS

As discussed in the previous chapter, release, gas dispersion and ignition models form the major initiatives for the overall consequence analysis. In this chapter a comprehensive literature review of available models has been carried out and the modeling details of adopted models are elaborated. Models are adopted considering their appropriateness to offshore process conditions, flexibility to map different scenarios and validation against experimental observations.

3.1. RELEASE MODELS

Source models or release models (CCPS, 2000 and Crowl & Louvar, 2002) are used to estimate the amount of fuel released, or the rate of fuel release. These models are crucial in the risk assessment process as the release rate and quantity of fuel released determine the size of the resulting cloud and hence the probability of ignition.

The initial release rate through a leak depends mainly on the chemical characteristics, pressure inside the equipment, and size of the hole and the phase of release. Offshore hydrocarbon releases are usually gaseous, liquid and two-phase. Among these, the gaseous hydrocarbons range from C1 to C4, while liquids are crude oil, diesel oil, aviation fuel, and others. Condensate is considered to be two-phase as it is a mixture of hydrocarbons mainly C4 to C6 that condense from the gas during compression. This material is liquid while it is held under pressure but becomes gas if the pressure is released. Identification of the appropriate phase and its corresponding model is essential, as, this being the initial step for risk assessment, it may prove to be highly sensitive to the risk estimated. Models for two phase releases are not considered in the present study as it demands further research and experimental validation. However, the details of release models for liquid and gaseous releases (as a result of holes in process equipment), used in this work are described in the subsequent sections.

3.1.1 Liquid Release Model

For liquid releases, the driving force for the discharge is pressure, with the pressure energy being converted into kinetic energy during the discharge. Therefore, the mass flow rate of liquid from a leak in a vessel below the liquid

level can be calculated using the Bernoulli equation (Crowl & Louvar, 2002) given as,

$$\dot{m} = C_d \times \rho \times A \sqrt{2 \times \left(\frac{P_1 - P_a}{\rho} + g \times h_s \right)} \qquad (3.1)$$

where $\dot{m}$ is the mass discharge rate, C_d is the discharge coefficient (0.60 recommended for liquids), ρ is the density of the liquid, A is the area of leak, P_1 is the absolute pressure at which the liquid is stored, P_a is the ambient pressure, g is the acceleration due to gravity and h_s is the static head of liquid.

3.1.2 Gas/Vapor Release Model

Gaseous releases through holes can be sonic or subsonic depending on the pressure inside the equipment in relation with the critical pressure. The critical pressure, P_{crit}, is calculated as,

$$P_{crit} = P_a \left(\frac{2}{\gamma + 1} \right)^{\gamma - 1/\gamma} \qquad (3.2)$$

If the pressure inside the equipment P_g is above the critical pressure P_{crit}, the flow is ***sonic.*** This is also known as choked flow condition. The mass flow rate for choked flow condition can be calculated using:

$$\dot{m}_{choked} = C_d \times A \times P_g \times \sqrt{\frac{\gamma \times MW}{R_g T_g} \times \left(\frac{2}{\gamma+1}\right)^{\frac{\gamma+1}{\gamma-1}}} \quad (3.3)$$

If the flow is ***subsonic*** (P_g is below the critical pressure P_{crit}) the mass flow rate can be calculated as,

$$\dot{m}_{nonchoked} = C_d \times A \times \Psi_o \times P_g \times \sqrt{\frac{\gamma \times MW}{R_g T_g} \times \left(\frac{2}{\gamma+1}\right)^{\frac{\gamma+1}{\gamma-1}}} \quad (3.4)$$

$$\Psi_o = \left(\frac{P_a}{P_g}\right)^{\frac{1}{\gamma}} \times \sqrt{1-\left(\frac{P_a}{P_g}\right)^{\frac{\gamma-1}{\gamma}}} \times \sqrt{\left(\frac{2}{\gamma-1}\right)\left(\frac{\gamma+1}{2}\right)^{\frac{\gamma+1}{\gamma-1}}} \quad (3.5)$$

where, γ is the isentropic expansion factor (Cp/Cv), $\dot{m}$ is the mass discharge rate, C_d is the discharge coefficient (~0.8 for gases), A is the leak area, MW is the molecular weight, T_g is the temperature of the vessel, R_g is the ideal gas constant, P_a is the ambient pressure and P_g is the absolute pressure of the gas.

3.2. GAS DISPERSION MODELS

The gas (or vapor flashed from liquid releases) that is released during an accident, form clouds and are dispersed by the initial momentum of the release,

turbulence around the obstructions, natural ventilation and the wind. Dispersion models are used to estimate the dimensions of these clouds, varying with time and space in an unobstructed uniform field (CCPS 1996), or a highly obstructed field (CCPS, 1998).

The main categories of releases encountered offshore are release in confined, congested areas of the platform, release in open areas or outside the platform, and release under water. The modeling of gas dispersion in the presence of obstacles demands the use of highly complex computational fluid dynamic (CFD) models, which are supposed to give good results, but are highly sensitive and need validation with the experimental data. Moreover there is a necessity for expertise to use the CFD models for simulating the gas dispersion. On the other hand, for dispersion in uniform wind fields without any obstructions, box or slab models (Lees, 1996) and the Pascal Gifford model (Crowl and Louver, 2002) can be used for dense gas releases and neutrally buoyant releases, respectively. These models are employed in the present study and are described as follows.

3.2.1 Dense Gas Dispersion Model

A Box model (Cox and Carpenter, 1980) predicts the dense gas dispersion behavior quite efficiently and has few limitations, such as its applicability for

only open and flat terrain and inability to handle obstacles. However these limitations can be overcome by adopting a grid based model, discussed elsewhere in chapter 6.

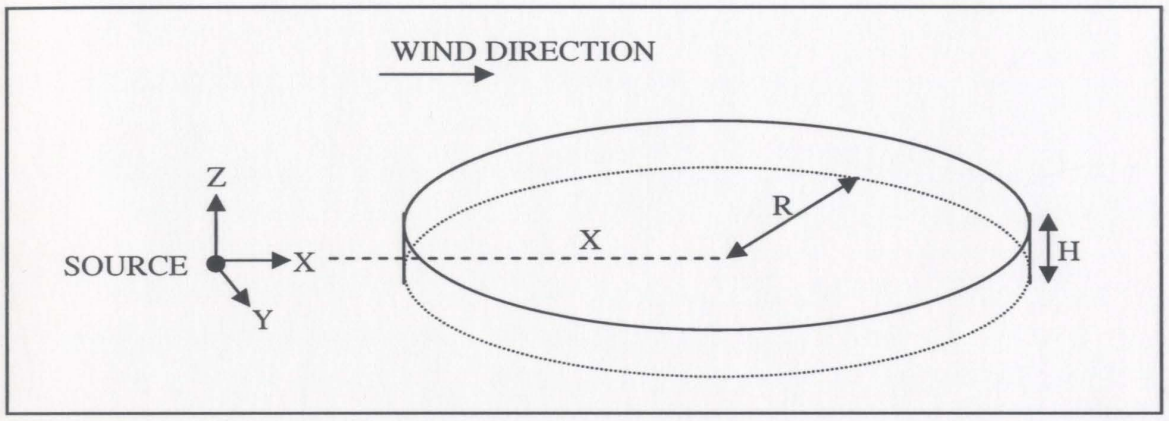

Figure 3.1. Vapor cloud dimensions for an instantaneous release of gas.

For instantaneous gaseous releases, the cloud formed is assumed as a circular cylinder as shown in Figure 3.1. Box model for these releases is based on three simultaneous differential equations for the downwind distance 'x' of the cloud, the radius 'R' of the cloud and the volume 'V' of the cloud. The corresponding equations are:

i) The rate of change of downwind distance of the center of the cloud is given as:

$$\frac{dx}{dt} = u_c(t) \qquad (3.6)$$

$$u_c(t) = u_r \frac{\ln(H/2z_o)}{\ln(z_r/z_o)} \tag{3.7}$$

where, $u_c(t)$ is the mean velocity of the cloud, u_r is the mean wind velocity at a reference height, H is height of the cloud (m), z_r is the reference height (10m) and z_o is the roughness length. Roughness length varies from 0.001 to 0.01 for normal flat surfaces and is 1 for industrial areas (CCPS, 1996).

ii) Rate of change of the cloud radius is given as:

$$\frac{dR}{dt} = c_E \left(g' \frac{V}{\pi R^2} \right)^{1/2} \tag{3.8}$$

where, $c_E = 1.15$

iii) Rate of change of volume is given as:

$$\frac{dV}{dt} = Q_e + Q_t \tag{3.9}$$

$$Q_e = 0 \tag{3.10}$$

$$Q_t = \pi R^2 u_e \tag{3.11}$$

$$u_e = \frac{0.6u_*}{(1+0.8Ri_*)^{1/2}}, \quad Ri_* = g' \frac{H}{{u_*}^2}, \quad g' = g \frac{\rho_c - \rho_a}{\rho_a} \tag{3.12 a, b, c}$$

where, V is total volume of the cloud, Q_e is the volumetric flow of air entrained at the edge of the cloud, which is assumed to be negligible, Q_t is the total volumetric flow of air entrained at the top of the cloud, u_* is friction velocity, usually equal to about 5-10% of the wind speed at a height of 10m, Ri_* is the Richardson number, ρ_c is density of the cloud and ρ_a is density of the ambient air.

These three differential equations and the corresponding algebraic equations are solved simultaneously to obtain the movement of the cloud, change in the radius of the cloud and volume of the cloud varying with time. The analytical solution is:

$$x = t \times u_c(t) \tag{3.13}$$

$$R^2 = R_o^2 + 2c_E\left(\frac{g'}{\pi}V_i\right)^{\frac{1}{2}} \times t \tag{3.14}$$

$$V_i = \pi R^2 u_e t \tag{3.15}$$

3.2.2 Passive Gas Dispersion Model

A standard gas dispersion model, which is used in many commercial software packages for the dispersion of neutrally buoyant gases, is the "Gaussian model". This model assumes, on the basis of empirical data, that a Gaussian

distribution can adequately describe the concentration profiles in both horizontal and vertical directions. Among the Gaussian models, Pasquill-Gifford plume and puff models (Lees, 1996 and Crowl & Louver, 2002) are widely used. It has similar limitations as Box models, and can be handled in the same way as mentioned earlier. Despite these limitations, they predict conservative estimates of the downwind gas concentration in the plume and the puff for continuous and instantaneous release respectively.

The puff model for an instantaneous point source at height h above ground is given as,

$$C(x,y,z,t)=\frac{m}{(2\pi)^{\frac{3}{2}}\times\sigma_x\times\sigma_y\times\sigma_z}exp\left[\frac{-y^2}{2\sigma_y^2}\right]\times\left\{exp\left[\frac{-(z-h)^2}{2\sigma_z^2}\right]+exp\left[\frac{-(z+h)^2}{2\sigma_z^2}\right]\right\} \quad (3.16)$$

Similarly, plume model defines the concentration at any point (x, y, z) downwind of an elevated source as,

$$C(x,y,z)=\frac{\dot{m}}{2\pi\times u\times\sigma_y\times\sigma_z}exp\left[\frac{-y^2}{2\sigma_y^2}\right]\times\left\{exp\left[\frac{-(z-h)^2}{2\sigma_z^2}\right]+exp\left[\frac{-(z+h)^2}{2\sigma_z^2}\right]\right\} \quad (3.17)$$

where, σ_x, σ_y, σ_z are the dispersion coefficients in the downwind, crosswind and vertical (x, y, z) directions (Lees 1996, Crowl & Louver, 2002), m is the

quantity of gas released instantaneously, the $\dot{m}$ is the gas release rate, u is the wind velocity, h is the release height, x is distance along the plume centerline, z is height above ground and y is the lateral displacement from plume centerline. For ground level releases substitute h equal to 0 in both the cases.

3.3. IGNITION MODEL

Among the currently available models, a few are based on the assumption that ignition probability is solely a function of size of the flammable gas cloud (CCPS, 1998 and Spencer & Rew, 1997), while the others incorporate some additional features (Rew et. al. 2000, 2004) such as multiple ignition sources, density of ignition sources, different land use types, ignition potential of each source etc. The model developed by Rew et al. (2004) for onsite ignition probability estimation is relatively sophisticated and is formulated in such a way that it can be implemented within risk analysis models. This model was employed for the present study. The equations used in the model are described below.

3.3.2 ONSITE IGNITION MODEL

For a flammable cloud of area A, containing a random distribution of ignition sources with parameters λ, p and a, the probability of no ignition at time t in a given type of scenario is

$$Q(t) = exp\left(-\mu A\left\{1-(1-ap)e^{-\lambda pt}\right\}\right) \tag{3.18}$$

where, μ is the average number of ignition sources per unit area, p is the ignition potential of a source (0-1), a is the rate of activation of the source, and λ is the proportion of time that the source is active.

$$a = \frac{t_a}{t_a + t_i} \tag{3.19}$$

$$\lambda = \frac{1}{t_a + t_i} \tag{3.20}$$

If there are n different ignition sources in a given scenario, the probability of no ignition is given as:

$$Q(t) = \prod_{i=1}^{n} Q_i \tag{3.21}$$

For m scenario types, the probability of the cloud not having ignited at time t is given as:

$$Q(t) = \prod_{j=1}^{m} \prod_{i=1}^{n} Q_{ji}(t) \tag{3.22}$$

Hence, the probability of ignition is:

$$P_I(t) = 1 - Q(t) \tag{3.23}$$

The details of scenario types, ignition sources and ignition source parameters used in the model are listed in Table 3.1, Rew et al. (2004).

Table 3.1. Ignition source parameters for various sources in different land use types

Scenario type	Ignition sources	Ignition source parameters					
		p	t_a	t_i	a	λ	μ
Flames	Continuous	1.00	-	0	1.00	0.000	1
	Infrequent	1.00	60	420	0.13	0.002	2
	Intermittent	1.00	5	55	0.08	0.017	2
Accommodation	Smoking	1.00	5	115	0.04	0.008	2
Kitchen facilities	Cooking equipment	0.25	5	25	0.17	0.033	1
Boiler house	Boiler	1.00	120	360	0.25	0.002	1
Process area	Heavy equipment	0.50	-	-	1.00	0.028	2
	Medium equipment	0.25	-	-	1.00	0.035	2
	Light equipment	0.10	-	-	1.00	0.056	2
Office	Light equipment levels	0.05	-	-	1.00	0.056	2
Storage	Materials handling	0.10	10	20	0.333	0.033	1

Chapter 4

FIRE CONSEQUENCE MODELING

This chapter provides an overview of consequence modeling of fires which commonly occur on offshore platforms, e.g. pool fires, jet fires, fireballs and flash fires. A comprehensive literature review carried out related to each fire consequence model has been discussed in their respective sections. Additionally, fire overpressure impact and human impact models are also discussed in detail.

By reviewing the predictive models for modeling fire hazards, it was found that many models exist – varying from point source techniques to more complex computational fluid dynamic (CFD) calculations. Such predictive models can be categorized as: *semi-empirical models* (*point source models* (Lees, 1996) and *solid flame models* (Johnson et al., 1994, Cracknell et al., 1994, and Rew et al., 1997, 1998)), *field models* (Johnson et al., 1997), *integral models* (Wilcox, 1975 and Vachon & Champion, 1986), and *zone models* (Chamberlain, 1996 and Chamberlain & Persaud, 1997).

Among all these models, the well-validated solid flame models provide a better prediction of flame geometry and external thermal radiation for offshore fires. Also, these models are mathematically simple and can be easily computer programmed with short run times. In recent times, these models have been successfully used for fire consequence analysis and further, for Quantitative Risk Assessment (Rew et al., 1997, 1998, Johnson et al., 1994, and Cracknell et al., 1994). Therefore, semi-empirical *solid flame models* have been chosen to be the basis for selecting fire models and subsequently using them in the development of a consequence analysis toolkit. As identified earlier, the fires that commonly occur on offshore platforms are categorized as pool fires, jet fires, fireballs and flash fires (vapor cloud fires). In the subsequent sections, a literature review carried out for individual fire models has been provided followed by the description of modeling details of the selected ones.

4.1. POOL FIRES

"A pool fire is a turbulent diffusion flame burning above a pool of vaporizing hydrocarbon fuel where the fuel vapor has negligible initial momentum" (Rew et al., 1997).

Liquid fuel released accidentally during overfilling of storage tanks, rupture of pipes and tanks etc., forms a pool on the surface, vaporizes, and upon

ignition, results in a pool fire. Consequence models for pool fires in open spaces have been well documented over the past few years (Rew et al., 1997, Pritchard & Binding, 1992, and Johnson, 1992). After reviewing the pool fire models available in the literature, the model described by Rew et al. (1997) was judged to be most suitable for the current work because of the following reasons:

a) This model (POOLFIRE6) was developed after an extensive review of literature followed by undertaking full-scale measurements to assess the current status of pool fire modeling.

b) It has been compared with the existing models developed by Pritchard & Binding (1992) and Johnson (1992) and found to have obtained superior results.

c) Upon performing model validation and uncertainty analysis, it was found that the model predicts with a 90% confidence level, which seems to be reasonable for risk assessment studies.

Wind effects are significant in deciding certain parameters such as flame drag, flame tilt and flame length. In the selected model, flame drag and flame tilt were modeled as a function of wind parameters; however flame length was considered independent of wind parameters. Therefore, the model has been

revised using the work of Thomas (1963) to account for the wind effect on flame length. A description of the selected radiation model (Rew et al., 1997) follows.

4.1.1 POOL FIRE MODEL

A pool fire is usually modeled as a sheared elliptical cylinder which is assumed to radiate in two layers – a high emissive power, clean burning zone at the base, with a smoky obscured layer above as shown in Figure 4.1.

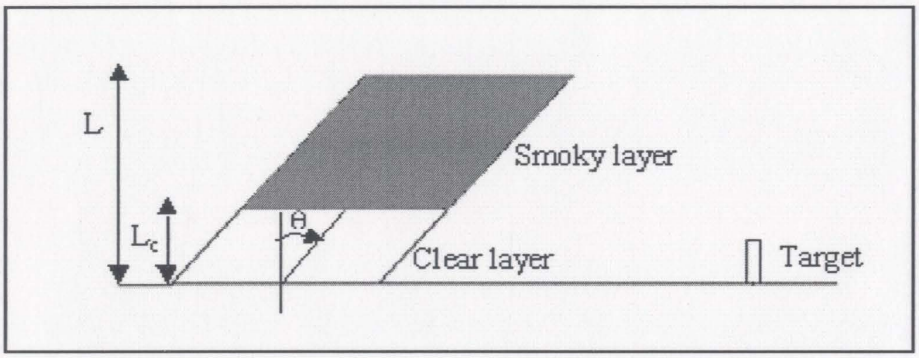

Figure 4.1. Flame geometry for a tilted pool fire

The parameters that can capture the characteristics of a pool fire and their corresponding correlations are given below.

i) **Size of Liquid pool**

Liquid pool size is a function of leak/spill rate, duration of spill, and burning rate. Pool size is particularly important as most of the correlations

depend on pool diameter (D). The correlation for maximum possible diameter is given as,

$$D_{max} = 2\sqrt{\frac{\dot{V}_L}{\pi \dot{m}}} \tag{4.1}$$

where, $\dot{V}_L$ is the volumetric spill rate and $\dot{m}$ is the mass burning rate.

ii) **Liquid Burning Rate**

In general the burning rate increases with pool diameter as the surface to volume ratio of the flame decreases and more heat is available to evaporate liquid from the surface of the pool. The correlation widely used is,

$$\dot{m} = \dot{m}_{\infty}\left(1 - e^{-kD}\right) \tag{4.2}$$

where, $\dot{m}_{\infty}$ is the maximum burning rate, k is the burning rate size coefficient and D is diameter of the pool.

iii) **Flame Length**

The flame length from a pool fire is related to the burning rate, pool size and ambient air density. Effect of wind on flame length was accounted for in this correlation by using the work of Thomas (1963).

$$\frac{L}{D} = 55\left(\frac{\dot{m}}{\rho_{air}\sqrt{gD}}\right)^{0.67}\left(\frac{u}{u_c}\right)^{-0.21} \tag{4.3}$$

$$u_c = \left(\frac{g\dot{m}D}{\rho_v} \right)^{1/3} \tag{4.4}$$

where, L is the flame length, u is the wind velocity, ρ_{air} is the density of air and ρ_v is the density of vapor.

iv) **Flame Tilt and Drag**

Strong wind often causes the flame of a pool fire to tilt and can drag the base in the downwind direction. Hence, a pool fire is modeled as a sheared elliptical cylinder instead of a circular cylinder. This feature has been captured in the following correlations.

$$\frac{\tan\theta}{\cos\theta} = 3.13(Fr)^{0.431} \tag{4.5}$$

$$\frac{D'}{D} = 1.5(Fr)^{0.069} \tag{4.6}$$

$$Fr = \frac{u^2}{gD} \tag{4.7}$$

Where, θ is flame angle from the vertical, u is the wind velocity, Fr is Froude number and D' is the diameter of the dragged flame

4.1.2 THERMAL RADIATION MODEL

i) **Surface Emissive Power**

A pool fire is modeled to radiate in two different layers as mentioned earlier. The surface emissive power for each of the layers is correlated separately. Therefore, the Surface Emissive Power of the lower clear flame, SEP_L, and the upper, smoke obscured layer SEP_U is given by,

$$SEP_L = SEP_\infty \left(1 - e^{-k_m D}\right) \tag{4.8}$$

$$SEP_U = U_R \times SEP_L + (1 - U_R) \times SEP_S \tag{4.9}$$

where, SEP_∞ is the maximum surface emissive power of a fuel, k_m is the extinction coefficient, U_R is unobscured ratio and SEP_S is the surface emissive power of smoke (approximately 20 kW/m^2).

ii) **Radiation Heat flux**

The thermal radiative flux at a target object is given as:

$$q = q_L + q_U = \tau_L \times VF_L \times SEP_L + \tau_U \times VF_U \times SEP_U \tag{4.10}$$

where, τ is atmospheric transmissivity, VF is the geometric view factor and SEP is average surface emissive power. The subscripts L and U refer to values

calculated for the clear lower layer and smoky upper layer of the model flame shape, respectively.

Atmospheric transmissivity is calculated using an algorithm developed by Wayne (1991). This calculation is based on the assumptions that the flame is a black body source at 1500 K, with CO_2 and H_2O vapor being the only molecules that absorb radiation in the pathway between the fire and the target. The atmospheric transmissivity is given by the formula:

$$\tau = 1.006 - 0.01171 \log_{10} X(H_2O) - 0.02368 (\log_{10} X(H_2O))^2 - 0.03188 \log_{10} X(CO_2) + 0.001164 (\log_{10} X(CO_2))^2 \quad (4.11)$$

$$X(H_2O) = R_H P_L S_{mm} (288.65 / T_a) \quad (4.12)$$

$$X(CO_2) = P_L (273 / T_a) \quad (4.13)$$

where, R_H is the relative humidity expressed as a fraction, P_L is path length through the atmosphere and S_{mm} is the saturated water vapour pressure in mm Hg at the ambient temperature.

The view factor (Davis & Bagster, 1989) represents the fraction of the overall heat output that strikes the target, and is dependent upon the geometry of both the flame and the target. For radiation from a finite flame to a differential

receiving element, the view factor is given by the integral over the flame surface:

$$VF = \int_s \frac{\cos \beta_1 \cos \beta_2}{\pi d^2} \tag{4.14}$$

where β_1 and β_2 are the angles between the normals to the fire surface and the receiving element, respectively, and d is the distance from the receiver point to the flame center.

4.2. JET FIRES

"A jet fire is a turbulent diffusion flame resulting from the combustion of a fuel continuously released with some significant momentum in a particular direction" (Johnson et al., 1994).

Jet fires represent a significant element of risk associated with major incidents on offshore installations, with the fuels ranging from light flammable gases to two-phase crude oil releases. Between horizontal and vertical jet fires, the former is the most dangerous because of the high probability of impingement on objects downwind (Carsley, 1994). This can lead to structural, storage vessel, and pipe-work failures, and can cause further escalation of the event (i.e. domino effect). The heat fluxes released from these fires are very high, ranging from 200 – 400 kW/m^2 depending on the type of fuel. Almost all the fuels handled offshore

can form jet fires provided that the release occurs under conditions such that the fluid has some initial momentum (such as a leak from a pressurized gas line).

Vertical jet fire models (e.g. Chamberlain, 1987) are commonly used to assess the hazards from flares. The model of Chamberlain (1987) has been extended to horizontal jet fires by Johnson et al. (1994). This model has been chosen as the base jet fire model in the current work because of the following reasons:

i) It was developed with offshore conditions in mind and provides the required information for all the parameters used in the model.

ii) This is the only solid flame model available for horizontal jet fires.

Description of the horizontal jet fire model (Johnson et al., 1994) follows.

4.2.1 Horizontal Jet Fire Model

A horizontal jet fire is modeled as the truncated frustum of a cone, which emits thermal radiation from its surface as shown in Figure 4.2 (Johnson et al., 1994). For horizontal releases, the buoyancy of the flame dominates over wind momentum, causing the flame to rise above the horizontal plane. Because objects in the direction of the release receive radiation from emitting paths roughly equal to the flame length (which is much larger than the flame width), a different

surface emissive power is assigned to the ends of the solid flame from the surface emissive power used for the sides of the flame. The important correlations to predict the flame shape are mass release rate, flame length, flame lift off, maximum and minimum flame widths, angle of tilt etc., all of which are shown in Figure 4.2 and described as follows.

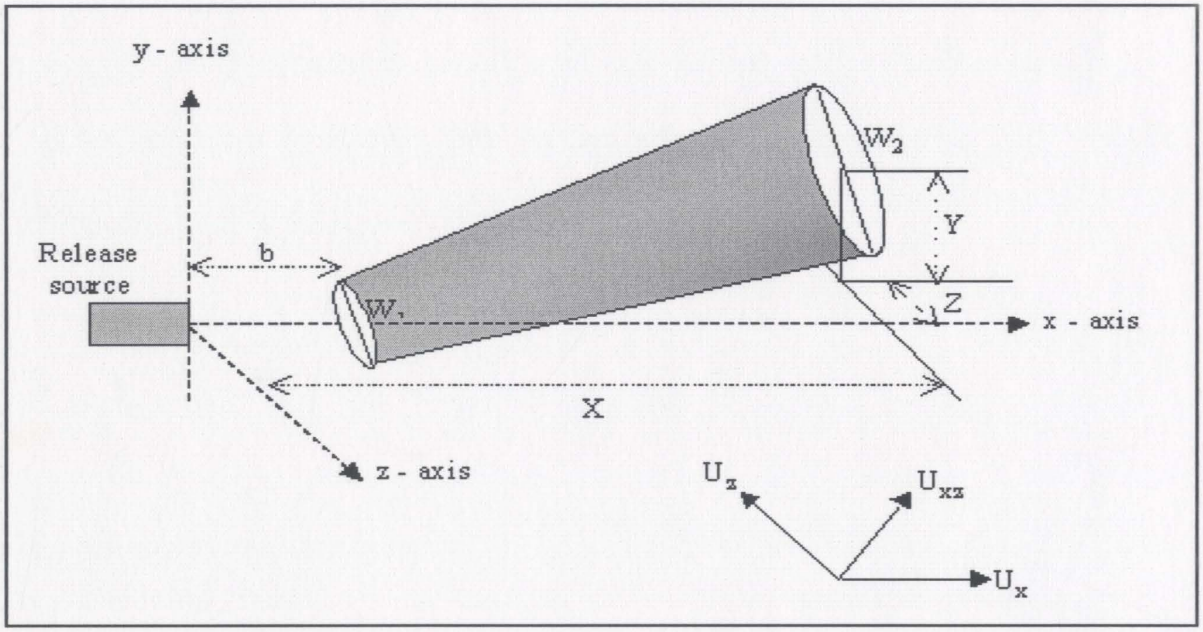

Figure 4.2. Flame geometry for a horizontal jet fire (from Johnson et al., 1994)

i) **Momentum flux**

The initial jet behavior for horizontal releases, when the gas expands down to atmospheric pressure, is calculated in the same way as described for

vertical releases (Chamberlain, 1987). The expanded jet momentum flux G is given by:

$$G = \frac{\pi \rho_j u_j^2 d_j^2}{4} \tag{4.15}$$

where, ρ_j is the expanded jet density, u_j is the expanded jet velocity and d_j is the expanded jet diameter.

The balance between the initial jet momentum flux and buoyancy is characterized by the Richardson number.

$$\xi(L) = \left[\frac{\pi \rho_{air} g}{4G}\right]^{1/3} L \tag{4.16}$$

ii) **Flame length in still air**

Length of the flame in still air is used as a basis to estimate the flame length in wind conditions. It is correlated with parameters such as the Richardson number, source diameter and mass fraction of fuel in a stoichiometric mixture of air using a nonlinear algebraic equation, which needs to be solved iteratively. The correlations are given as

$$\left[\frac{2.85 D_s}{L_{bo} MW_{air}}\right]^{2/3} = 0.2 + 0.2\xi(L_{bo}) \tag{4.17}$$

$$D_s = d_j \left[\frac{\rho_j}{\rho_{air}} \right]^{1/2} \tag{4.18}$$

where, Ds is the combustion source diameter, MW_{air} is the molecular weight of air and L_{bo} is the flame length in still air.

iii) **Flame length under wind conditions**

The flame length Lb_{xy} depends on two main parameters X, Y which are defined as the lengths in x and y directions as shown in the Figure 4.2.

$$Lb_{xy} = \left(X^2 + Y^2 \right)^{1/2} \tag{4.19}$$

The correlations to evaluate X are given as:

$$\frac{X}{L_{bo}} = f(\xi)(1 + r(\xi)\Omega_x) \tag{4.20}$$

where,

$$f(\xi) = \begin{cases} 0.55 + (1 - 0.55)exp(-0.168\xi) & \xi \le 5.11 \\ 0.55 + (1 - 0.55)exp\left(-0.168\xi - 0.3(\xi - 5.11)^2\right) & \xi > 5.11 \end{cases} \tag{4.21a, b}$$

$$r(\xi) = \begin{cases} 0 & \xi \le 3.3 \\ 0.02(1 - exp(-0.5(\xi - 3.3))) & \xi > 3.3 \end{cases} \tag{4.22a, b}$$

The parameters used to characterize the effect of the wind on the flame length are:

$$\Omega_x = \left[\frac{\pi\rho_{air}}{4G}\right]^{1/2} L_{bo} u_{air} \tag{4.23}$$

$$\Omega_z = \left[\frac{\pi\rho_{air}}{4G}\right]^{1/2} L_{bo} w_{air} \tag{4.24}$$

where, Ω_x indicates the extent to which the wind is blowing along or against the release direction and is used respectively to elongate and flatten the flame or to shorten and raise-up the flame, and Ω_z indicates the extent to which the flame is blown to either side of the release direction.

Correlations for Y are given as,

$$\frac{Y}{L_{bo}} = h(\xi)(1 - c(\xi)\Omega_x) \tag{4.25}$$

$$h(\xi) = \frac{1}{(1 + 1/\xi)^{8.78}} \tag{4.26}$$

$$c(\xi) = 0.02\xi \tag{4.27}$$

iv) **Flame lift-off**

A jet with high initial momentum entrains more air per unit length in the initial convection dominated part of the jet and burns as a premixed flue flame. The lift-off of this flame '*b*' is given as,

$$b = 0.141(G_{air})^{1/2} \tag{4.28}$$

v) **Maximum width of the flame**

The maximum flame width W_2 is correlated with the flame length and the wind effecting parameters and is given as,

$$W_2/Lb_{xy} = -0.004 + 0.0396\xi - \Omega_x\left(0.0094 + 9.5\times10^{-7}\,\xi^5\right) \qquad (4.29)$$

vi) **Minimum width of the flame**

Similarly the minimum flame width W_1 is given as

$$W_1/b = -0.18 + 0.081\xi \qquad (4.30)$$

vii) **Angle of tilt**

As buoyancy of the flame dominates over wind momentum, it causes the flame to rise above the horizontal plane. The tilt of the flame α with the vertical axis is, therefore given as

$$tan(\alpha) = Z/(X-b) = 0.178\,\Omega_z \qquad (4.31)$$

4.2.2 THERMAL RADIATION MODEL

i) **Surface Emissive power**

The surface emissive powers for the side and end of the model flame are given as,

$$SEP_{side} = SEP_{\infty}\left(1 - e^{-kW_2}\right) \tag{4.32}$$

$$SEP_{end} = SEP_{\infty}\left(1 - e^{-kR_L}\right) \tag{4.33}$$

$$SEP_{\infty} = \frac{F_{s\infty}Q}{A} \tag{4.34}$$

$$F_{s\infty} = 0.21exp\left(-0.00323u_j\right) + 0.14 \tag{4.35}$$

where, the factor k is the gas absorption coefficient, W_2 is the maximum width of the flame, R_L is the length of the frustum, Q is the net heat released by combustion, SEP_{∞} is the maximum surface emissive power, A is the surface area of the flame, $F_{s\infty}$ is the fraction of the overall heat emitted as radiation and u_j is the velocity of the jet.

ii) **Radiation Heat flux**

The thermal radiative flux at a target object is given as:

$$q = \left(VF_{side} * SEP_{side} + VF_{end} * SEP_{end}\right) * \tau \tag{4.36}$$

where *SEP* is the average surface emissive power, *VF* is the geometric view factor and the subscripts *side* and *end* refer to values calculated for the side and end of the model flame shape. Geometric view factors (*VF*) and atmospheric transmissivity (τ) are calculated in the same way as described in Section 4.1.2.

4.3. FIREBALL MODEL

"A fireball is a rapid turbulent combustion of fuel, usually in the form of a rising and expanding radiant ball of flame" (Roberts et al., 2000).

When a fire such as a pool or jet fire impinges on a vessel containing pressure-liquefied gas, the pressure in the vessel rises and the vessel wall weakens. This can eventually lead to catastrophic failure of the vessel with the release of the entire inventory. This phenomenon is known as a boiling liquid expanding vapor explosion (BLEVE). In such releases, the liquefied gas released to the atmosphere flashes due to the sudden pressure drop. If the released material is flammable, it will ignite; in addition to missile and blast hazards, there is thus a thermal radiation hazard from the fireball produced. It is this thermal radiation which dominates in the near field. Although the duration of the heat pulse from a fireball is typically of the order of 10 – 20 s, the damage potential is high due to the fireball's massive surface emissive power. In the present approach (Roberts et al., 2000) a fireball is modeled as a sphere as shown in Figure 4.3.

Modeling of fireballs has been carried out by several researchers (e.g. Prugh, 1994, Cracknell & Carsley 1997, and Roberts et al., 2000). An alternative

fireball scenario to the one described in the previous paragraph, i.e. fireballs from delayed ignition of continuous jet releases, has also been dealt with by Cracknell & Carsley (1997). For the present study, the model of Roberts et al. (2000) was selected as the base fireball model because of the following reasons:

a) This model was extensively validated against full-scale experimental data.

b) Fireballs from ignition of instantaneous releases are more common than those from continuous jet releases.

c) This is the only solid flame fireball model developed to date.

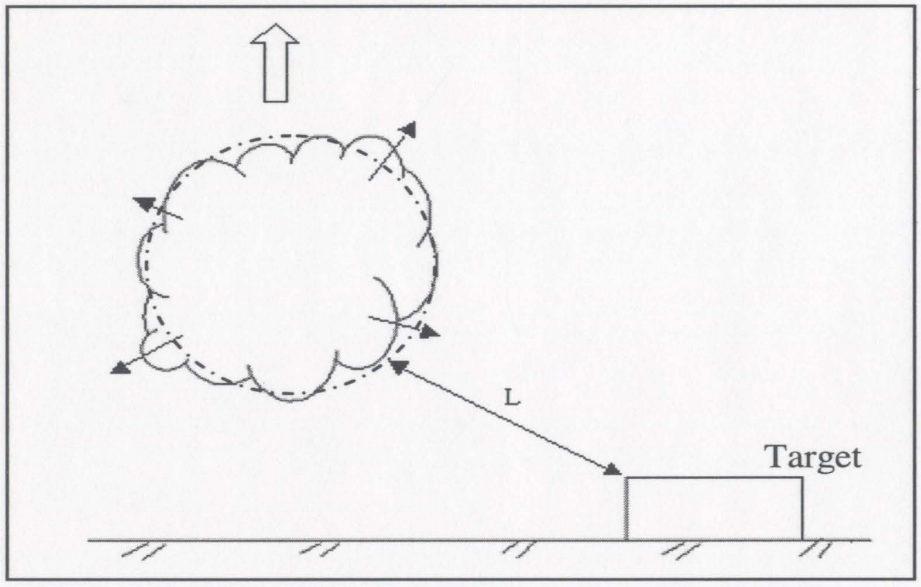

Figure 4.3. Flame geometry for an expanding, rising fireball

4.3.1 FIREBALL MODEL

A fireball, as the name represents is modeled as a spherical ball of flame. The solid flame model for a fireball comprises of correlations like fireball duration, diameter, lift-off time and its elevation. A radiation model includes correlations like surface emissive power and radiation heat flux, details of which follow.

i) **Fireball duration**

It is the time taken by the fireball to reach its maximum diameter, usually correlated with mass of fuel (M) involved in combustion process as,

$$t = 0.825 \times M^{0.26} \tag{4.37}$$

ii) **Fireball diameter**

Although fireballs are not exactly spherical, it is the most conservative assumption. The diameter of the fireball (D) is related with mass of the fuel (M) involved in the combustion process as,

$$D = 6.48 \times M^{0.325} \tag{4.38}$$

iii) **Fireball lift-off time**

In general, hazard calculations assume that fireballs are spherical and touch the ground. However, in practice the fireballs start to lift off when buoyancy and entrainment are dominant and drift with wind. An empirical

equation for lift-off time, which has been correlated with the fuel mass, is given as,

$$t_{lo} = 1.1 \times M^{1/6} \tag{4.39}$$

iv) **Fireball elevation**

Fireball elevation is the height of the center of the fireball above the ground at the time of maximum diameter. This parameter is important because it determines the distance of the recipient from the center of the fireball. Elevation is again correlated with the fireball diameter as,

$$H = 0.75 \times D \tag{4.40}$$

4.3.2 Thermal Radiation Model

i) **Surface emissive power**

Large-scale experiments carried out by Roberts et al. (2000) with propane as the fuel, measured a maximum average surface emissive power ranging from 270 – 333 kW/m² up/downwind and 278 – 413 kW/m² crosswind. Average of these values can be used conservatively for risk assessment studies. Also, due to the high turbulence involved, a fireball can cause significant overpressures.

ii) **Radiation Heat flux**

The radiation heat flux incident on a target is evaluated in a similar way as for previous fire models by the product of atmospheric transmissivity (τ), geometric view factor (VF) and the surface emissive power (SEP) given as,

$$q = VF \times SEP \times \tau \tag{4.41}$$

Surface emissive powers measured experimentally by Roberts et al. (2000) are used, while view factors and transmissivity are evaluated using the correlations described in the Section 4.1.2.

4.4. FLASH FIRE

"A flash fire is a transient fire resulting from the ignition of a gas or vapor cloud, where a delay between the release of flammable material and subsequent ignition has allowed a cloud of flammable material to build up and spread out from its release point" (CCPS, 1994).

A flash fire is usually characterized by a "wall of flame" (Raj & Emmons, 1975 and CCPS, 1994) progressing out from the point of ignition at a moderate velocity until the whole flammable cloud has burned. Similar to fireballs, flash fires can occur either by ignition of a flammable vapor cloud formed from an instantaneous release, or by delayed ignition of a cloud from a continuous

release, provided the turbulence in the cloud is low enough that a fireball does not occur. The instantaneous or continuous releases considered in risk studies would physically correspond to a spreading transient puff or a long steady-state plume.

When the cloud ignites, the initial damage will be caused primarily by thermal radiation. However, flash fires may generate more damaging "knock-on" events, especially if they burn back to the source. The knock-on events can be a pool fire, jet fire, BLEVE etc. Further, the presence of obstacles along the pathway and the high degree of congestion on offshore platforms can lead to significant flame acceleration. Such increases in flame speed can in turn lead to significant overpressures and ultimately a partially confined or confined vapor cloud explosion. The effects of these escalation events are likely to be more severe than the flash fire itself.

Consequence modeling of a cloud fire in an uncongested/unconfined environment where overpressure is not a principal hazard has been well-documented (Raj & Emmons, 1975, CCPS, 1994, Rew et al., 1995, 1998 and Cracknell & Carsley, 1997). These flash fire models are based on gas dispersion modeling coupled with the probability of ignition, where the boundary of the fire is defined by the unignited cloud's downwind and crosswind dimensions at

flammable limit concentrations (usually the lower flammable limit, LFL, of the cloud). An instantaneously released gas disperses and forms a cylindrical cloud of radius R as shown in the Figure 4.4. The modeling of the dispersing cloud formed by instantaneous fuel release has been described earlier in Section 3.2.1.

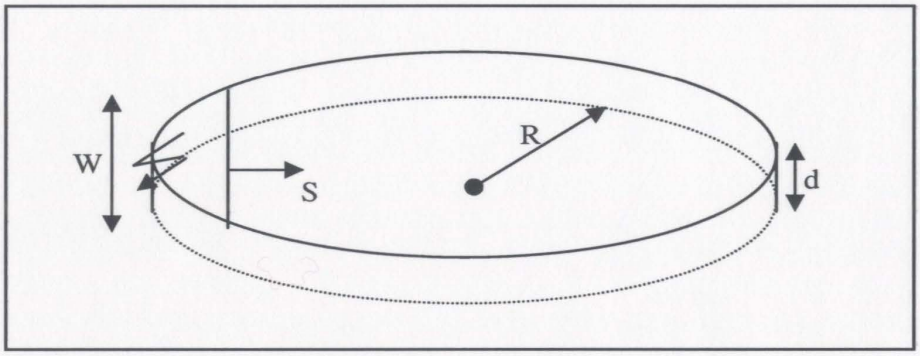

Figure 4.4. Flame geometry of a vapor cloud that burns as flash fire

4.4.1 FLASH FIRE MODEL

Flash fire is a transient event which may last for less than a minute depending on the size of the cloud and external conditions. When the vapor cloud is ignited at one end as shown in Figure 4.4, it burns rapidly like a wall of flame until the cloud is completely burned. The height of the flame is assumed constant through out the combustion process as the depth of the cloud is taken to remain the same within the cloud. However, width of the flame increases in the initial stage, reaches a maximum and then decreases. These are the main parameters which define the characteristics of a fire. The correlations for these and additional parameters like flame speed, burn time etc. are as follows:

i) **Flame Height**

Radiation effects from a flash fire can be determined if the geometry of the flame front is known. The height of the flame is given as,

$$H = 20d\left[\frac{S^2}{gd}\left(\frac{\rho_0}{\rho_a}\right)\frac{wr^2}{(1-w)^3}\right]^{1/3} \tag{4.42}$$

$$w = \frac{\phi - \phi_{st}}{\alpha(1-\phi_{st})} \quad \phi > \phi_{st} \tag{4.43}$$

$$w = 0 \quad \phi \leq \phi_{st} \tag{4.44}$$

where, H is visible flame height, d is cloud depth, S is cloud burning speed, ρ_0 is fuel-air mixture density, ρ_a is the density of air, r is stiochiometric mixture air-fuel mass ratio, α is constant pressure expansion ratio for stoichiometric combustion (typically 8 for hydrocarbons), ϕ is fuel-air mixture composition (fuel volume ratio) and ϕ_{st} is the stoichiometric mixture composition (fuel volume ratio).

ii) **Flame Width:**

The variation in the width of the flame with time is given as,

$$W = 2\sqrt{R^2 - (R - S \times t)^2} \tag{4.45}$$

where, R is the cloud radius, t is the time and W is the flame width.

iii) **Flame speed**

The flame speeds for natural gas and propane are obtained empirically and are quoted as 6 m/s and 12 m/s respectively (Cracknell & Carsley, 1997). After few experimental observations, Raj and Emmons(1975) found that burning speed was roughly proportional to ambient wind speed u and proposed an equation:

$$S = 2.3 \times u \tag{4.46}$$

However, the most widely used formula for flame speed is the one developed as a function of turbulent burning velocity and the expansion ratio of the gases, given as:

$$S = E \times U_t \tag{4.47}$$

where, E is the expansion ratio and U_t is the turbulent burning velocity. Empirically determined values for these parameters can be obtained from the literature for variety of gases (Lees, 1996).

iv) **Flame burning period:**

Following the determination of flame speed, flame burning period estimation becomes rather simple, given as,

$$t = \frac{D}{S} \tag{4.48}$$

where, D is the diameter of the cloud and S is cloud burning speed.

4.4.2 THERMAL RADIATION MODEL

i) **Surface Emissive Power**

From the Coyote and Maplin tests (HSE, 2001), a surface emissive power of 220 kw/m^2 has been obtained for propane and LNG flash fires. This value is considered to be a reasonable estimate when compared with other test results.

ii) **Radiation Heat flux**

The radiation heat flux incident on a target is evaluated in a similar way as for previous fire models by the product of atmospheric transmissivity (τ), geometric view factor (*VF*) and the surface emissive power (*SEP*):

$$q = VF \times SEP \times \tau \tag{4.49}$$

Surface emissive powers measured experimentally by Coyote and Maplin tests (HSE, 2001) are used, while view factors and transmissivity are evaluated using the correlations described in the Section 4.1.2.

4.5. SMOKE AND TOXICITY EFFECTS

In most offshore fires, the main effects are due to heat radiation, but in a few events the effect of smoke has been significant, and these events have resulted in many fatalities (e.g. *Piper Alpha*). The Cullen report (Cullen, 1990) following this incident recommended the operators to carry out four key studies, assessment of smoke generation, its ingress into the accommodation block and subsequent effects was one among them. Therefore it is necessary to study the effects of smoke and toxic combustion gases on the personnel in order to complete a comprehensive consequence study.

Smoke is generated by burning any hydrocarbon, gases or liquids, but in an offshore scenario, a significant amount is produced by burning liquids such as crude oil. Hence, pool fires and crude oil jet fires are considered to be the main sources for smoke generation. However, gas fires hold a minor contribution. Combustion gases consist mainly of a mixture of nitrogen, carbon dioxide, carbon monoxide and water vapor. Because of the high proportion of nitrogen in air, hot nitrogen tends to dominate in the combustion products. The concentration of toxic gases in the smoke is important because of their potential impact on personnel. For modeling purposes, it is necessary to know the initial concentration close to the fire. This task can be fulfilled by using basic

stiochiometric formulae. For example, the stochiometric ratio for most hydrocarbon fuels for combustion is 15 kg air per kg of fuel. Thus, in well ventilated fires with sufficient air for complete combustion, the smoke production rate is 16 times the fuel burning rate (Spouge, 1999).

Meanwhile, CO is generated due to incomplete combustion of gases, which in turn is due to reduced ventilation (insufficient supply of air). There are few experimental results available (Spouge, 1999) for CO and CO_2 concentration, but they are very uncertain and cannot be universally considered for all cases. However, the values depicted in Table 4.1 can be used as guidance in consequence studies. Traces of other toxic gas like HCN, H_2S etc are also released during combustion. However, they are not considered within this study.

Table 4.1. Initial Gas Concentrations in Smoke (Spouge, 1997)

GAS	CONCENTRATION IN SMOKE (vol %)			
	WELL VENTILATED FIRE		UNDER VENTILATED FIRE	
	GAS FIRE	LIQUID FIRE	GAS FIRE	LIQUID FIRE
CO	0.04	0.08	3	3.1
CO_2	10.9	11.8	8.2	9.2

With the concentration of main toxic gases in smoke e.g. CO, CO_2 known, concentration at any downwind distance can be determined by using a gas dispersion model such as a Pascal Gifford plume model discussed in Section

3.2.2. Thus, the effects of smoke and toxic gases on the personnel can be evaluated. The proportions of products in smoke for 1kg of heavy oil are illustrated in Figure 4.5. These estimates can guide the assessment of the consequences of smoke exposure.

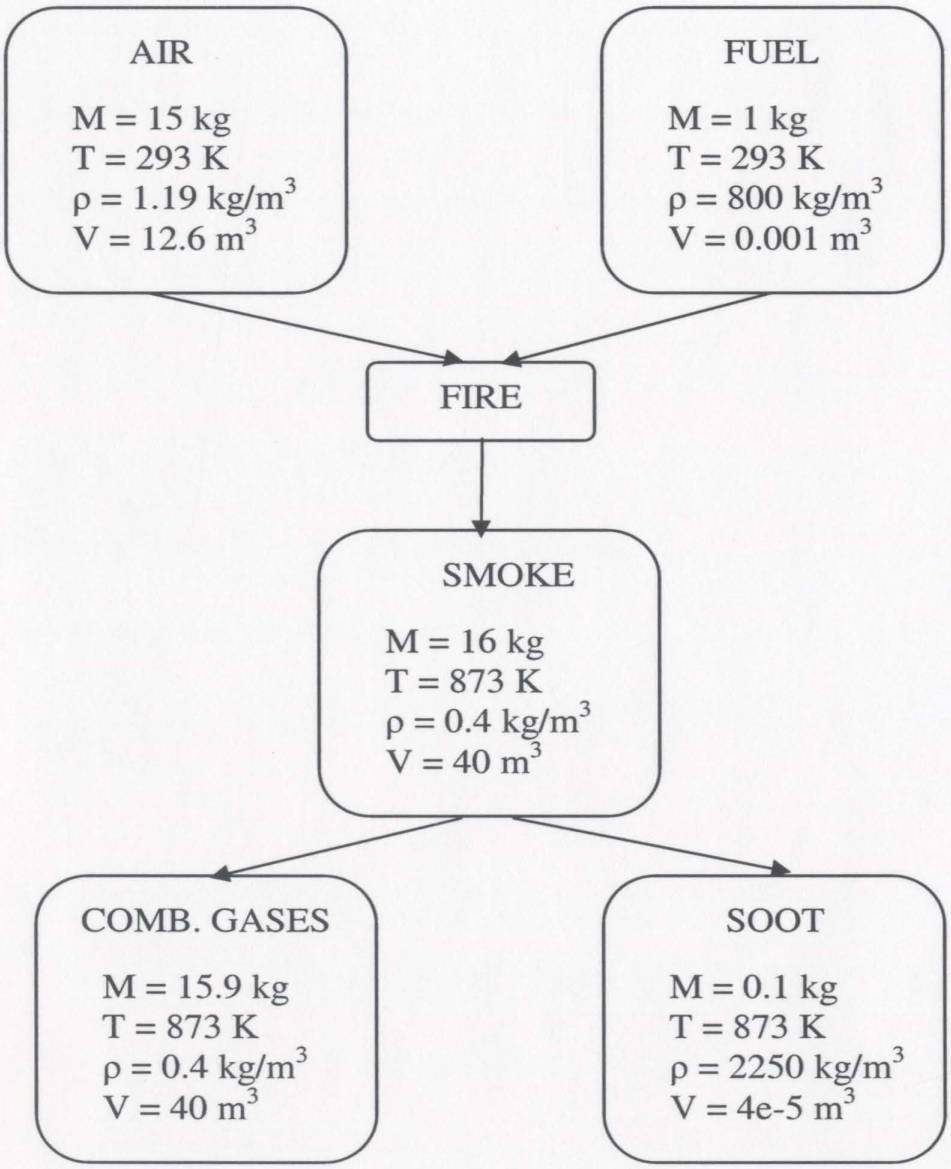

Figure 4.5. Smoke production per kg of Heavy oil

4.6. FIRE OVERPRESSURE MODEL

The importance of overpressure caused due to the fires, when occurring in a confined or semi-confined space has been highlighted by Wighus (1994). However, there appears to be no attempt to quantify this phenomenon. Therefore, a model has been developed to investigate the overpressure effects from the fires caused by the highly energized combustion gases released in a congested and confined compartment. This model has been developed by utilizing the ideal gas law and radiative heat transfer equations with the following assumptions.

a) negligible convective heat transfer,

b) ideal gas behavior of the combustion gases,

c) small compartment openings, and

d) linear distribution of temperature variation within the defined space.

As mentioned before, the purpose of formulating this model was to investigate the possibility of blast effects from fires on personnel, equipment and the platform structure. The model can further be used to study the characteristics of external fires by estimating parameters such as the amount of unburned gases released from a vent and its corresponding release rate (from the predicted

overpressure), and to verify the design of vents, module sizes and a combination of these in terms of tolerable overpressures.

The algorithm for overpressure calculation is as follows:

1. Calculate the flame temperature, T_{flame}, using the correlation for radiation heat transfer as (assuming black body):

$$SEP = \sigma \left(T_{flame}^4 - T_o^4 \right) \tag{4.50}$$

2. Similarly calculate the temperature at one corner of the compartment, T_{cc}, and using assumption (d) mentioned earlier, estimate the average temperature of the gases, T_{gases}:

$$T_{gases} = \frac{T_{flame} + T_{cc}}{2} \tag{4.51}$$

3. Finally, use the ideal gas law to estimate an approximate value of the overpressure, P_o, generated by the gases in the compartment:

$$P_o = \frac{nRT_{gases}}{V_{room}} \tag{4.52}$$

where SEP is the surface emissive power (heat emitted by the flame per unit area), σ is the Stefan-Boltzmann constant ($5.669*10^{-8}$ W/m^2K^4), T_o is the initial compartment temperature, n is the moles of combustion gases in the compartment, R is the gas constant, and V_{room} is the volume of the compartment under study.

4.7. HUMAN IMPACT MODELS

The consequences of fires and explosions are usually expressed in terms of thermal radiation intensity; smoke concentrations and explosion over pressures received by the personnel, equipment or structure. In order to estimate risk, it is useful to convert these effects into impacts causing damage. Dose response evaluation is used to quantify the damage (fatality) from thermal radiation and overpressure. To facilitate this analysis, personnel harm is expressed in terms of probit functions (Khan & Abbasi, 1998), which relate the percentage of people affected in a bounded region of interest by a normal distribution function.

4.7.1 RADIATION PROBIT EQUATIONS

The probability of death from radiation heat flux or overpressures received by human beings can be computed from the well defined probit relations. For the likelihood of fatality from heat radiation, the probit function (Lees, 1996) is given as,

$$Pr = -36.38 + 2.56\, ln(\, tq^{4/3}\,) \qquad (4.53)$$

where q is the radiation heat flux and t is the time of exposure.

4.7.2 TOXICITY PROBIT EQUATIONS

The probit function for likelihood of death due to toxic load caused by inhalation of toxic gases like CO, CO_2 etc, (Lees, 1996) is given as

$$Pr = a + b\ln(C^n t) \tag{4.54}$$

Where a, b, n are constants and C is the gas concentration in mg/m^3. The values of constants vary with the toxic gases. E.g. for CO a=1, b=-7.4 and n=1 (Lees, 1996).

Finally the probability (percentage), P, of damage is correlated with the probit values obtained from the above mentioned equations in a way given as (CCPS, 2000):

$$P = 50\left[1 + \frac{Pr-5}{|Pr-5|}erf\left(\frac{|Pr-5|}{\sqrt{2}}\right)\right] \tag{4.55}$$

where *erf* is the error function.

Chapter 5

EXPLOSION CONSEQUENCE MODELING

This chapter provides an overview of explosion consequence modeling for gas explosions and boiling liquid expanding vapor explosions. A comprehensive literature review carried out related to each explosion consequence model has been discussed in their respective sections. A new probabilistic model developed to analyze the impact of missile on the process area and the people is also discussed.

Reviewing the predictive models for analyzing the blast consequences from gas explosions, it was found that there are several models available, varying from simple empirical models to complex fluid dynamic models. These models are categorized as follows:

i) **Empirical models**: These models have a limited range of applicability, cannot deal with complex geometries and have simplified the physics considerably. Nevertheless, these methods are useful for quick order-of-magnitude calculations and for screening of scenarios for further investigation with more

sophisticated tools. Some of the empirical models are TNO Multi-energy model (Van den Berg, et al. 1997, 2000), Baker Strehlow model (Baker et al. 1998, 2000, 2004), (CAM 2) Congestion Assessment method 2 (Puttock, 1999).

ii) **Phenomenological models**: These models are slightly more complex than the empirical models and have a less limited range of applicability than them. These are essentially differential and algebraic equations, which are developed in a way to understand the physical process involved in gas explosions. Wherever necessary, the equations are fitted to experimental data to obtain the unknown parameters and are found to have a lower level of uncertainty than empirical models. The models are relatively easy to use, with modest computational requirements and therefore are suitable for use where large numbers of calculation runs are required. Examples of this type of model include SCOPE (**S**hell **C**ode for **O**ver-pressure **P**rediction in gas **E**xplosions) (Puttock et. al. 2000), CLICHE (**C**onfined **LI**nked **CH**amber **E**xplosion) (Catlin, 1990)

iii) **Computational Fluid Dynamic models**: CFD models are based on numerical solutions of the Navier-Stokes equations of fluid flow (i.e. a description of the conservation of mass, momentum and scalar quantities in flowing fluid, by means of a set of partial differential equations). Compared to the

phenomenological and empirical models, CFD offers the prospect of greater accuracy and flexibility, however computational run times are long and the scope for errors is greater. Examples of this type of model include FLACS, EXSIM, AUTOREAGAS, CFX, COBRA, Imperial College code (Lea et al. 2002).

After reviewing these models empirical models and phenomenological models were found to be appropriate for the current study. These models are easy to use, have short run times and are well suitable for being embedded in a quantitative risk assessment toolkit. As identified earlier, the explosions that commonly occur on offshore platforms are categorized as gas explosions (partially confined gas explosion, confined gas explosion and vented explosion) and Boiling Liquid Expanding Vapor Explosions. In the subsequent sections, literature review carried out for individual explosion models has been provided followed by the description of modeling details of the selected ones.

5.1. GAS EXPLOSIONS

A gas explosion is a sudden generation and expansion of gases due to rapid burning of a flammable mass. The level of congestion and confinement in the area covered by the gas cloud usually characterizes a gas explosion. High

congestion in the form of obstacles causes the turbulence level in the flow to increase the fluid flow past the objects, resulting in increased flame acceleration, and overpressures. Gas explosions are further divided into two categories, which are described as follows.

5.1.1 UNCONFINED/PARTIALLY CONFINED EXPLOSIONS

Partially confined and highly congested conditions are typical of the process area of an FPSO (Floating Production Storage and Offloading) vessel and some offshore modules. Ignition of any vapor cloud under such conditions will lead to an explosion referred to as a partially confined explosion. In this case, overpressure generation is mainly due to turbulence generated by the obstacles, such as process equipment in the path of the expanding gas. Available empirical models can be used for modeling this kind of explosion as they have been tested and validated for partially confined and highly congested conditions. A review of all the empirical models and their comparison with experimental data has been presented by Fitzgerald (2001). It was recommended that Congestion Assessment Method (Puttock, 1999) could be used if one wants to study a worst-case scenario and TNO Multi-energy model (Van den Berg, et al. 1997, 2000) if one wants to predict the average result for a set of explosion conditions. The former was chosen for explosion analysis in the present study.

The Congestion Assessment method comprises of two main steps for analyzing the consequences of gas explosions:

- Determination of the source overpressure and
- Dissipation of the obtained overpressure over a predefined area so that pressure experienced at various distances from the explosion center can be estimated.

i) **Source Overpressure estimation**

A correlation has been derived for estimating the source overpressure from a series of experimental tests in a gas-filled region of congestion comprising regular rows of cylinders with a central ignition source. The region is of length and width of 2L, and height L. To reach the open space the flame passes a number of similar grids in each direction. The correlation was developed in such a way that explosion overpressure is dependent on parameters such as type of fuel, number of rows of obstacles in each direction, area blockage ratio, obstacle diameter, spacing between the rows of obstacles etc, and is given as:

$$P = a_0\left(U_0(E-1)\right)^{2.71} \times d^{0.55} \times n^{a_1} \times exp(a_2 b) p_d^{a_3} \qquad (5.1)$$

where, a_0, a_1, a_2, a_3 are constants (determined from experimental measurements), U_0 is the laminar burning velocity, E is the expansion ratio $\frac{\rho_u}{\rho_b}$, ρ_u is unburned

gas density, ρ_b burned gas density, n is the number of rows of obstacles in each direction counting from the centre, b is the blockage of rows of obstacles.

However, with the increased congestion i.e. more rows of obstacles, the expression predicts very high overpressures (>10bars) which is beyond reality, as the experimental results (Fitzgerald, 2001) showed pressures no more than 8 bars. Therefore a new parameter has been introduced, called the Severity Index (SI) and used instead of overpressure (P) in the previous correlation. The expression is similar to equation (5.1), given as.

$$SI = a_0\left(U_0(E-1)\right)^{2.71} \times d^{0.55} \times n^{a1} \times exp(a_2 b) p_d^{a3} \qquad (5.2)$$

Severity index is in turn correlated with overpressure as shown in Figure 5.1, so that explosion overpressure is close to 8 bars for any degree of congestion.

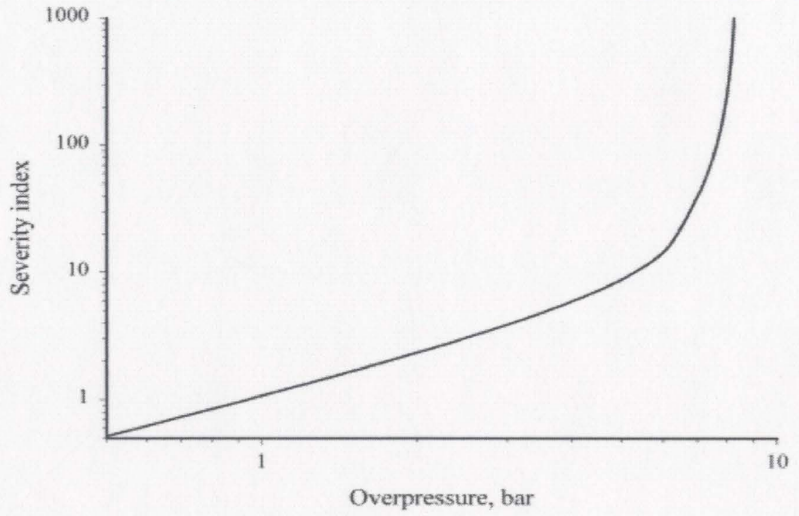

Figure 5.1. Severity Index and Overpressure relationship (Puttock, 1999)

It is clear that Severity index is equal to pressure at low overpressure, but increases rapidly as an overpressure of just over 8 bars is approached. By making an accurate curve fit, correlation in equation (5.3) was obtained, which is a nonlinear algebraic equation and has to be solved iteratively to obtain source overpressure P.

$$SI = P\,exp\left(0.4\frac{P}{E^{1.08}-1-P}\right) \tag{5.3}$$

ii) **Overpressure estimation at a receiver**

A receiver distance 'r' from the center of the cloud is the sum of the distance from the edge of the cloud to the cloud radius, given as,

$$r = R_0 + r' \tag{5.4}$$

$$R_0 = \sqrt[3]{\frac{3V_0}{2\pi}} \tag{5.5}$$

where, R_0 is the radius of the cloud and r' is the distance from the edge of the cloud to the receiver and V_0 is the volume of the gas cloud.

Thus, pressure at the receiver is,

$$P_{receiver} = min\left(\frac{R_0}{r}P, P_1\right) \tag{5.6}$$

where P_1 is a parameter given as,

$$log\, P_1 = 0.081_r^4 - 0.5921_r^4 + 1.631_r^2 - 3.281_r + 1.39 \quad (5.7)$$

$$l_r = log\frac{r}{R_0} + 0.2 - 0.02P_0 \quad (5.8)$$

With the help of these correlations the source overpressure and the overpressure at the point of interest can be evaluated.

5.1.2 Confined And Vented/External Explosions

Confined explosions, or confined vapor cloud explosions, usually occur in a largely confined space, such as inside enclosed modules, or in an oil tank, or a leg of a concrete platform. Overpressure is usually created by the expansion of gas in a confined volume as it burns and exceeds the vent capacity of the space. The presence of obstacles in the path will further enhance the overpressure generation and destruction. The phenomenological models SCOPE (Shell Code for Overpressure Prediction in gas Explosions) and CLICHE (Confined LInked CHamber Explosion) were specially developed for confined explosions in offshore modules. SCOPE 3, the most recent version of SCOPE, was selected for the present study due to its capability of handling mixed scale objects, rear

venting, and an improved combustion model. It has been validated against more than 300 experiments.

Vented/External explosion occurs in conjunction with confined explosions. During a confined explosion, unburned gas is released through the vents. On ignition, the release will lead to an external/vented explosion. The consequence modeling of external explosions is usually combined with confined explosions. SCOPE 3 handles vented explosions as well. Similar to the explosion model described in section 5.1.1, this model also has similar steps, source overpressure prediction and overpressure dissipation. However, the modeling approaches are different, as explained in the details as follows:

i) **Source overpressure estimation**

The explosion geometry (an offshore compartment) is approximated by a box of length *L*, width *W*, height *H* and cross-sectional area *A* with the obstacles represented in the form of shadings (Figure 5.2). At one end of the box is the main vent of area *Av*. Ignition occurs at the centre of the face opposite to the explosion vent, which corresponds to the worst possible case. The flame is assumed to be hemispherical until it reaches the walls of the box, at which point it ceases to increase in size and propagates along the box with a roughly

hemispherical shape. In order to correctly predict the relationship between pressure generation and vent flow, the model records two variables with time, the amounts of burnt and unburned gas inside the box.

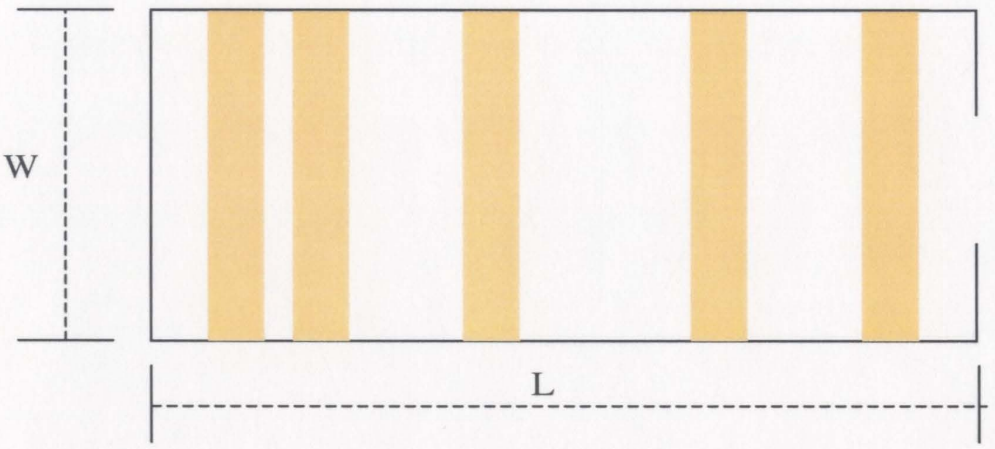

Figure 5.2. Geometry of an offshore module with obstacles

The equations for mass of burnt and unburned gases are:

$$\frac{dM_u}{dT} = -sAU_t\rho_u - U_v c_D A_v \rho_u \tag{5.9}$$

$$\frac{dB}{dT} = P^{1/\gamma} sAU_t E \tag{5.10}$$

where M_u is the mass of unburned gas inside the box, sA is the flame area , c_D is the vent discharge coefficient, U_v is the velocity of the unburned gas through the vent, P is the pressure inside the box, and E is the expansion ratio.

The parameter B is given by the following expression,

$$B = P^{1/\gamma} V_b \tag{5.11}$$

where, V_b is the volume of burnt gas inside the box. The pressure and flame position is determined by the quantity of burnt and unburned gas in the box. It is also possible to keep track of the mass of gas emitted M_e from the main vent that can be used later for external explosion calculations:

$$\frac{dM_e}{dT} = U_v c_D A_v \rho_u \tag{5.12}$$

All the parameters like turbulent burning velocity, laminar burning velocity, expansion ratio, grid effects (sharp edged obstacles), obstacle complexity, vent flow (main, side, rear vents) are obtained empirically or semi-empirically (Puttock et. al. 2000).

Vented/external explosion overpressure is correlated empirically with the pressure, when flame has covered 70% of the distance in the compartment given as,

$$\frac{P_{ext}}{P_{0.7}} = 3.75\left(\frac{A_v}{V^{2/3}}\right)^{0.85} \tag{5.13}$$

Therefore the maximum source overpressure is a relation between emerging pressure (pressure when flame reaches the vent) and the external pressure as:

$$P_{max} = P_{emerg} + 0.7P_{ext} \tag{5.14}$$

This is the maximum source pressure generated due to gas explosion in a compartment.

ii) **Overpressure estimation at a receiver**

Pressure at the receiver (overpressure dissipation) can be obtained in a similar fashion as described in Section 5.1.1.

5.2. BOILING LIQUID EXPANDING VAPOR EXPLOSION (BLEVE)

When a fire such as a pool or jet fire impinges on a vessel containing pressure-liquefied gas, liquid vaporizes and expands, raises the pressure in the vessel and weakens the vessel wall. This phenomenon can eventually cause a catastrophic failure of the vessel with the release of the entire inventory, which is called a BLEVE. There are empirical models (CCPS, 1994 and Lees, 1996) as well as dynamic response simulation codes (Salzano et al., 2003) for peak overpressure prediction. The procedure for predicting the blast effects from

BLEVE has been well addressed in CCPS (1994) and was employed in the current study. A description of the procedure follows.

i) **Collection of data:**

Data of some necessary parameters such as the vessel failure pressure, ambient pressure, volume of the vessel, liquid fill ratio and shape of the vessel have to be collected. These parameters are utilized while performing thermodynamic calculations to estimate the explosion energy.

ii) **Calculation of explosion energy**

The specific initial energy of superheated liquid stored in a vessel is determined using thermodynamic calculations in which it is obtained by the difference between the internal energies of the initial and expanded states of the fluid. The total explosion energy is then obtained by multiplying the specific initial energy by the mass of fluid released,

$$E_{ex} = m_l(u_1 - u_2) \tag{5.15}$$

where, u_1 is the specific internal energy of the fluid in the initial state, u_2 is the specific internal energy in the expanded state and m_l is the mass of fluid released.

iii) **Calculation of non-dimensional distance ($\overline{R}$)**

The correlation used to calculate the non-dimensional distance of the target, $\overline{R}$ is given as,

$$\overline{R} = r\left[\frac{P_a}{E_{ex}}\right]^{1/3} \tag{5.16}$$

where, r is the distance at which blast parameters are to be determined and P_a is the ambient pressure.

iv) **Determination of non-dimensional overpressure ($\overline{P_t}$)**

Using the parameter $\overline{R}$ and the plot for "Non-dimensional overpressure versus non-dimensional distance for overpressure calculations" (Figure 6.21 of CCPS, 1994), non-dimensional overpressure $\overline{P_t}$ corresponding to $\overline{R}$ is calculated.

v) **Adjustment of non-dimensional overpressure ($\overline{P_t}$) for geometric effects:**

This procedure produces blast parameters applicable to a completely symmetrical blast wave, such as that would result from the explosion of a hemispherical vessel placed directly on the ground. In practice, vessels are either spherical or cylindrical and placed at some height above the ground. This influences blast parameters. To adjust for these geometry effects, $\overline{P_t}$ should be multiplied by some adjustment factors derived from experiments with high

explosive charges of various shapes. Tables 5.1 and 5.2 give multipliers for adjusting scaled values for cylindrical vessel of various $\overline{R}$ and for spheres elevated slightly above the ground, respectively.

Table 5.1. Adjustment factors for $\overline{P_t}$ for cylindrical vessels of various $\overline{R}$ (CCPS, 1994)

Non-dimensional distance $\overline{R}$	**Multiplier for $\overline{P_t}$**
<0.3	4
$\geq 0.3 \leq 1.6$	1.6
$>1.6 \leq 3.5$	1.6
>3.5	1.4

Table 5.2. Adjustment factors for spherical vessels slightly elevated above ground (CCPS, 1994)

Non-dimensional distance $\overline{R}$	**Multiplier for $\overline{P_t}$**
<1	2
>1	1.1

vi) **Calculation of actual overpressure:**

The adjusted value of non-dimensional overpressure $\overline{P_t}$ is then transformed to actual overpressure using the following correlation.

$$P_t = P_a + \overline{P}_t \times P_a \tag{5.17}$$

where, $\overline{P}_t$ is the adjusted non-dimensional overpressure at the target and P_t is the actual pressure. This procedure allows calculating the overpressures at various target distances.

Other types of explosions that are not dealt within this study include physical explosions (caused by excess pressure in a vessel), internal explosions (within a flare stack), mist explosions and solid phase explosions (e.g. associated with the use of well completion explosives). The modeling of internal explosions, mist explosions, and solid phase explosions is not well understood and needs further research efforts.

5.3. MISSILE IMPACT ANALYSIS – A PROBABILISTIC MODEL

This section focuses on the probabilistic model developed to analyze the missile impacts on the people and the process area. The model quantifies the probability of a missile strike at an object and hence can aid in assessing the possible chances of escalation of accidental events. The details of the methodology are presented in the following sections.

5.3.1. INTRODUCTION

The total energy released during a physical explosion or a BLEVE is shared for overpressure and fragment generation. The fraction of energy imparted to the fragments by the blast wave causes the fragments to become air borne and act as missiles. They can cause direct injuries to the people or can damage the structures. Missile effects are considered to be a serious issue in the safety of process plants. Some of the recent explosion incidents occurred in Haltern, Germany in 1976, Texas City in 1978 and Mexico City in 1984 (CCPS, 1994). These incidents are disastrous and involved the effects of missiles causing vast damage to the personnel and the plant.

The main concern with missiles lies in its capability of enhancing the accident effects (or enabling escalation in the accident events), a phenomenon often referred as domino effect. Earlier, Khan and Abbasi (2001) worked on the issue of quantifying the probability of domino effect. They developed a computer automated tool, known as DOMIFFECT that does the necessary probabilistic calculations and embedded it in their consequence analysis toolkit MAXCRED.

The possibility of escalation arises when missiles strike equipment located in the vicinity with impact energy greater than the strength of the vessel. It should be noted that not all the missiles are involved in the process of collision.

In fact, there are no deterministic models available that can predict which missiles can collide with an object. Hence, the overall analysis is to be considered as probabilistic. The impact energy that causes an escalation is, therefore, defined as the product of "probability of a missile striking a vessel" and "the impact energy should it strike". There are correlations available in the literature to determine the impact energies (Lees, 1996) that are based on missile characteristics such as mass, shape and its velocity. However, there seems to be comparatively little work done in the area of quantifying the probability of strike from missiles.

Recently, Hauptmmans (2001) developed a procedure for analyzing the flight of missiles ejecting from bursts of spherical and cylindrical vessels by making use of Monte Carlo simulation technique. The calculations for estimating the probability of a missile hitting an individual in the surroundings were performed and the results were plotted as contours around the exploding vessel. However, no attempt was made to demonstrate the actual mathematical formulation. Earlier, Scilly and Crowther (1992) proposed a methodology for assessing the risk of missile impact on a process plant that involved the estimation of probability of a strike from the missiles for a given target close to the explosion source. The only scenario considered in their approach was that

"missiles strike an object only when they fall in a predefined area whose length dimension (range) is called effective range interval".

Emphasis is given only on the missiles ejecting from the burst of a cylindrical vessel placed horizontally on ground. Cases involving spherical vessels and vertical cylinders are not considered for time being. While formulating the methodology, two credible scenarios are taken into account. They are: Any object in the vicinity of explosion source gets struck by the missiles,

- When the missiles fall within the defined Vulnerable Area (VA) or
- When the missiles collide with the target before reaching their final destination (a distance father than the vulnerable area).

Probabilities of strike from these two scenarios are analyzed and combined together to put forth the overall probability of strike. During the process of probabilistic analysis, a Monte Carlo simulation technique has been employed to perform simulation experiments for representing the parameters of interest as statistical distributions.

5.3.2. METHODOLOGY FOR PROBABILITY OF STRIKE

The methodology for quantifying the probability of a strike from the missiles for a given target is based on the fact that any object in the vicinity of an explosion source has two possibilities for a missile strike. They are:

- When the missiles travel a distance exactly equal to that of an object and falls on the object or
- When the missiles collide with the object on its way before reaching its final destination, a distance farther than the object.

However, to be more conservative, instead of referring the strike due to missiles falling exactly on the object, it can be said that a missile strike is possible when the missiles reach an area where the object is placed. This area is termed as the Vulnerable Area (VA), which is representative of danger to the object from the missiles, should they reach it.

Consider a case where a cylindrical storage vessel placed horizontally on the ground is the explosion/missile source and a spherical storage vessel is the target object placed in the neighborhood of the source. A top view of this particular scenario has been represented in Figure 5.3. The dotted circular area around the spherical target is the Vulnerable Area (VA). Any fragment falling in this area would possibly have chances of striking the target. The obvious question that arises is "How do we define this area?" It can be defined by

assuming that the vulnerable area takes the shape of the target object and has a diameter 'x' times that of the target, where 'x' is subject to variation and depends on how conservative one wants to be in ones missile risk calculations. Any value in between 1 to 1.5 should be conservative for a spherical target.

With this background, the two possibilities mentioned earlier are modified. Instead of considering missiles falling on the object, missiles reaching the VA are given primary importance. For the new scenarios, a missile strike can be expected.

1. When missiles reach the VA, or
2. When missiles collide with the object before reaching its final destination, a distance beyond the VA.

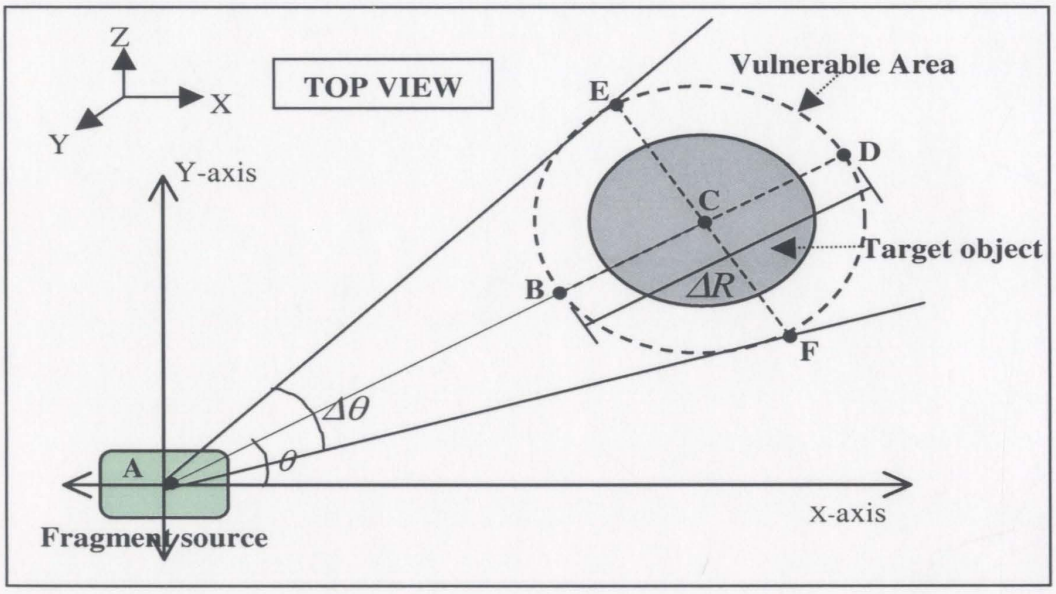

Figure 5.3. Top view of the source, target scenario

Scenario 1: While analyzing the missiles reaching the VA, two new terms are defined called Effective Range Interval (ERI) and Effective Orientation Interval (EOI). ERI is the diameter of the vulnerable area and EOI is the angle between the two tangents drawn to either sides of the VA from the center of the source as shown in Figure 5.3. After defining these two parameters, it can be said that missiles fall in the vulnerable area, when they fall within the ERI, provided they orient within the EOI. It should be noted that these two parameters dictate the dimensions of the vulnerable area.

For computational purposes, mathematical formulae have been provided to estimate ERI and EOI. From Figure 5.3, $AC = R$ is the distance between source and the target object, $\angle BAX = \theta$ is the orientation of the target object with respect to explosion source. $BD = \Delta R$ is the Effective Range Interval (ERI) and $\angle EAF = \Delta\theta$ is the Effective Orientation Interval (EOI).

The parameters ΔR and $\Delta\theta$ are estimated with the following equations,

$$\Delta R = xD_t \tag{5.18}$$

$$\frac{\Delta\theta}{2} = \left(\frac{\pi}{2} - tan^{-1}\left(\frac{AC}{EC}\right)\right) \tag{5.19}$$

$$\Delta\theta = 2 * \left(\frac{\pi}{2} - tan^{-1}\left(\frac{R}{\Delta R/2}\right)\right) \tag{5.20}$$

Where, D_t is the diameter of the spherical target object, R is the distance between the source and the target object and x as mentioned before is any value within 1–1.5. A conservative value of 1.5 has been chosen here.

Probabilistic analysis for scenario 1: Probability of strike due to fragments falling within the vulnerable area is given by the product of "probability of fragments falling within the ERI or ΔR" and "probability of fragments orienting within the EOI or $\Delta\theta$".

i) The probability of fragments falling within the ERI is then given by the difference between the cumulative probabilities for the fragments reaching a distance $R+0.5\Delta R$ and those reaching $R-0.5\Delta R$ as,

$$P(\Delta R) = P(r<(R+0.5\Delta R)) - P(r<(R-0.5\Delta R)) \qquad (5.21)$$

ii) The probability of fragments orienting within the EOI is given by the difference between the cumulative probabilities for the fragments orienting at an angle $\theta+0.5\Delta\theta$ and those orientating at $\theta-0.5\Delta\theta$ as,

$$P(\Delta\theta) = P(\theta<(\theta+0.5\Delta\theta)) - P(\theta<(\theta-0.5\Delta\theta)) \qquad (5.22)$$

Thus, the probability of a strike from this scenario 1 is,

$$P_1(strike) = P(\Delta R)\times P(\Delta\theta) \qquad (5.23)$$

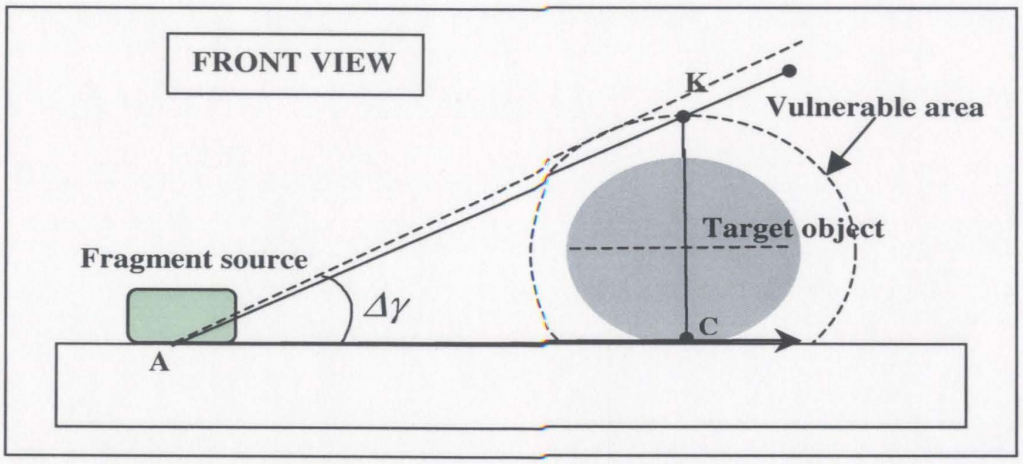

Figure 5.4. Front view of the source, target scenario

Scenario 2: While analyzing the missiles colliding with the object before reaching their final destination, another term is introduced called as Effective Trajectory Interval (ETI), where ETI is defined as the angle between the horizontal and the tangent, drawn from the center of the source to the top of the VA, shown as a dotted line in Figure 5.4 and given by $\Delta\gamma$. However, to simply the calculations for evaluation of ETI, the solid line is taken as a basis instead of the dotted line. It should be noted that Figure 5.4 represents the front view of the same source target scenario shown in Figure 5.3. Similar to the previous scenario, VA is the dotted circular area around the target object. Missiles traveling with an angle of trajectory less than or equal to the ETI would pass through the VA, provided they orient within the EOI and posses enough initial momentum that can drive them beyond the VA. Only these missiles pose danger to the target object.

From Figure 5.4, $\angle KAC = \Delta\gamma$ is the Effective Trajectory Interval (ETI). For computational purposes, $\Delta\gamma$ is estimated as:

$$tan(\Delta\gamma) = \frac{KC}{AC} \tag{5.24}$$

For $\Delta R = 1.5D_t$, $\Delta\gamma$ is given as,

$$tan(\Delta\gamma) = \frac{(D_t/4) + D_t}{R} \tag{5.25}$$

$$\Delta\gamma = tan^{-1}\left(\frac{(D_t/4) + D_t}{R}\right) \tag{5.26}$$

where D_t is the diameter of the spherical target object.

Probabilistic analysis for scenario 2: Probability of a strike due to collision of fragments with the target before reaching their final destination is given by the product of "probability of fragments falling beyond the ERI or ΔR" and "probability of fragments orienting within the EOI or $\Delta\theta$" and the "probability of them flying within the ETI or $\Delta\gamma$".

i) The probability of fragments falling beyond the ERI is given as:

$$P(\Delta R') = 1 - P(r < (R + 0.5\Delta R)) \tag{5.27}$$

ii) The probability of fragments orienting within the EOI is,

$$P(\Delta\theta) = P(\theta < (\theta + 0.5\Delta\theta)) - P(\theta < (\theta - 0.5\Delta\theta)) \quad (5.28)$$

iii) The probability of fragments flying within the ETI is given as,

$$P(\Delta\gamma) = P(\gamma < (\Delta\gamma)) \quad (5.29)$$

Thus, the probability of strike from this scenario 2 is,

$$P_2(strike) = P(\Delta R') \times P(\Delta\theta) \times P(\Delta\gamma) \quad (5.30)$$

Overall probability of strike

The overall probability of strike depends on both the scenarios defined above. They being independent events, union of probabilities of scenario1 and scenario2 is eventually the sum of their probabilities (equations 5.23, 5.30), given as,

$$P(strike) = P_1(strike) + P_2(strike) \quad (5.31)$$

From these probabilistic formulations it is evident that there is a necessity for cumulative distribution functions for range, orientation and trajectory of the fragments, which can be obtained by representing each of the parameters by statistical distributions, the details of which are discussed in the following section.

5.3.3. PROBABILISTIC MODELING AND ANALYSIS OF MISSILE IMPACT

The analysis carried out by Baker et al. (1978) on 25 accidental vessel explosions for mass and range distribution was considered to be the most complete statistical analysis in the open literature to date. As a result, log normal distributions were proposed for both mass and range of the fragments. However, there was no attempt to study the statistical characteristics of orientation and trajectories of the missiles. Also, there was not much emphasis on the shapes of the vessels involved in explosions. Although, accidents in cylindrical vessels were analyzed separately, they were not particular about whether these were placed horizontally or vertically. Therefore it may not be a sensible decision to follow the log normal distributions for mass and range of fragments universally for any vessel geometry. The focus of this work being on horizontal cylinders the distributions were re-evaluated based on simulation experiments carried out using a Monte Carlo simulation technique. The details of the input parameters for this approach are described below.

i) Orientation of fragments

The orientation of fragments when a large number of fragments is generated is not very well defined in the literature. The common assumption is that the fragments are projected uniformly in all directions. Alternatively, the

more conservative approach may be adopted in which the spatial density of the fragments is assumed to be greater in the direction of the vulnerable targets. Holden and Reeves (1985) analyzed 11 incidents involving 15 vessels containing mainly LPG. It was reported that about half of the fragments were projected into one third of the total area, in arcs of 30^0 to either side of the vessel's front and rear axial directions. Assuming the fragments are equally shared, 25%of fragments fall in each of the four regions corresponding to angles 345^0-15^0, 15^0-165^0, 165^0-195^0, and 195^0-345^0 respectively. This information is good enough to formulate a statistical distribution for orientation of fragments. With 25% of the fragments falling in the smaller regions corresponding to angles 345^0-15^0 and 165^0-195^0, a higher probability of strike may be expected in these regions.

ii) Angle of trajectory of fragments

No deterministic models exist to predict the angle of trajectory in the case of bursting of a vessel into a large number of fragments. However, for horizontal cylinders, most of the fragments are expected to take a small initial angle of trajectory, usually between 0 to 10^0 degrees (CCPS, 1994). This is because of the higher probability of generation of end caps than any other missile shapes. To be on the conservative side, a range of 0-20^0 was assumed and has been distributed uniformly as there is no evidence of any particular distribution cited in the literature.

iii) Range of fragments

With the assumption of negligible fluid dynamic forces, the only force acting on the fragment is that of gravity. Therefore, the range of fragment is given as:

$$R = \frac{v_i^2 \sin(2\gamma_i)}{2g} \tag{5.32}$$

where, v_i is the initial fragment velocity and γ_i is the fragment angle of trajectory.

While analyzing the fragments for their flight (range), there are parameters that need to be understood and which are often considered to be highly stochastic in nature. They are: energy of fragmentation, number of fragments generated, fragment shape, mass and energy distributions, wind and drag effects. These parameters have great influence on the flight of the missile and hence need extra attention. The stochastic nature or uncertainty of these parameters can be taken care of by representing them as statistical distributions. The details are as follows.

a. Energy for fragmentation

The initial energy of superheated liquid stored in a vessel is determined by a procedure illustrated by CCPS (1994). This is based on thermodynamic

calculations in which the energy is obtained by the difference between the internal energies of the initial and expanded states of the fluid.

Another important parameter is the fraction of total internal energy contributing to fragmentation. This energy is often referred to as kinetic energy since this is the energy which provides the initial momentum in the fragments turning them into missiles. From the experiments conducted by Baum (1984), the fraction translated to kinetic energy was found to be in between 0.2 to 0.5 of the total internal energy. It can be any value in the given range; therefore, the fraction is assumed being uniformly distributed with a constant probability density function.

b. Number of fragments

Baker et al. (1978) and Holden and Reeves (1985) discussed incidents involving 15 cylindrical vessels, the number of fragments resulted from which were then fitted by a log–normal distribution with a mean of 0.855 and a standard deviation of 0.525. By analyzing this statistical distribution, it was evident that there were chances of up to 20 fragments. However, in the case of BLEVE events, it was cited that the number of fragments are far fewer than mentioned above (CCPS, 1994). Any number between 2 to 10 is explainable. Therefore, besides using a log normal distribution, an option of employing a

right-sided triangular distribution was incorporated, with minimum and maximum number of fragments of 2 and 10 respectively.

c. Mass and Energy distribution of the fragments

Using the experimental results of Baker et al. (1977), Hauptmanns (2001) has estimated the mass distribution of fragments to follow a Beta distribution with parameters a=0.412 and b=1.39. However, introducing additional uncertain input variables will increase the complexity involved in calculations, which may deviate the results away from reality. Therefore, the mass of all the fragments was assumed to be the same here, which in turn lead to an assumption of equal energy distribution among the fragments.

d. Initial velocity of the fragments

The initial velocity of the fragments is used to calculate either the range of fragment travel or the impact velocity, if fragments collide with an obstacle before attaining maximum range. A great deal of work has been carried out in this area and CCPS, 1994). The formulation proposed by CCPS (1994) for fragment initial velocity is based on the kinetic energy E_{ki} imparted to a fragment and its mass, given as

$$v_i = \left[\frac{2E_{ki}}{M_i}\right]^{0.5} \tag{5.33}$$

Where, v_i is the initial fragment velocity, E_{ki} is the kinetic energy imparted to the fragment and M_i is mass of the fragment. As the mass of fragments is equally distributed, the velocity of each fragment remains the same.

e. Statistical Distribution for Range

A Monte Carlo simulation approach has been employed to conduct simulation experiments by making use of the equations, assumptions and considerations mentioned earlier. Each trial run is a simulation experiment. A large number of trial runs have been carried out for better convergence of the results. These experiments resulted in a set of data for the parameters of interest such as orientation, trajectory and range of fragments, which was further analyzed to obtain statistical distributions for each of them.

Having obtained the statistical distributions for orientation, trajectory and range of missiles, the implementation of the methodology described in section 5.3.2, for quantifying the probability of strike is straightforward. A case study considered to illustrate the capability of the proposed methodology has been discussed in chapter 7.

5.4. HUMAN IMPACT MODELS

The importance of human impact models was already discussed in section 4.7. In a nutshell, these models convert the overpressure and missile effects into consequences to humans via estimation of percentage fatalities. The corresponding probit equations for overpressures and missile effects are given below.

5.4.1. OVERPRESSURE PROBIT EQUATION

The probit function for likelihood of death due to overpressure (lung rupture) caused by explosions (Lees, 1996) is given as

$$Pr = -77.1 + 6.91 ln(P_o) \tag{5.34}$$

where P_o is the overpressure in Pa.

5.4.2. MISSILE EFFECTS PROBIT EQUATION

The data obtained based on animal experiments (Lees, 1996) was analyzed and a probit equation was formulated for penetration of a missile (causing wounds). It is given as

$$Pr = -8.35 + 0.61 ln(M_f \times u_f) \tag{5.35}$$

For fatal and serious injuries Gilbert, Lees and Scilly (1994) proposed a probit equation of the form

$$Pr = -0.24 + 1.96 \ln(M_f{}^{0.4} \times u_f) \tag{5.36}$$

where M_f is the mass of the fragment and u_f is the fragment velocity.

Chapter 6

SIMULATION - GRID BASED APPROACH

This chapter focuses on the computer code development for performing fire and explosion consequence analysis. A comparison of the models used in the present approach with that being used by existing software packages has been discussed. The use of grid based approach during the simulation process is highlighted within this chapter.

6.1. INTRODUCTION

Literature review of the existing fire and explosion consequence models and the selection of most suitable models for offshore conditions have been discussed so far in chapters 3, 4 and 5. In addition, a couple of new models such as a fire overpressure model and a probabilistic model for missile impact have been developed and discussed. A comparison of these models with the ones used by the existing software packages for fire and explosion consequence studies has been depicted in Table 6.1. It is evident from the table that most of the models

employed here are more advanced than the counterpart. This should produce enhancement in the results.

Table 6.1. Models for fire and explosion consequence study used in existing software packages and in the current work

S.No	FIRE CONSEQUENCE MODELS	USED IN EXISTING SOFTWARE PACKAGES	USED IN CURRENT WORK
1	RELEASE MODELS	Empirical correlations	Empirical correlations
2	DISPERSION MODELS	Empirical models	Empirical models
3	IGNITION MODEL	COX model	**Enhanced onsite Ignition model**
4	FIRE MODELS	Point source models/CFD codes	**State-of-the-art solid flame models**
5	OVERPRESSURE MODEL	N/A	**Model developed and used**
6	SMOKE MODEL	Neutrally buoyant gas dispersion model/CFD codes	Neutrally buoyant gas dispersion model
7	TOXICITY EFFECTS MODEL (CO, CO_2)	N/A	Stoichiometric Mass balance equations
8	EXPLOSION MODELS	Empirical or Phenomenological models/CFD codes	**State-of-the-art Empirical and Phenomenological models**
9	RADIATION AND EXPLOSION DISSIPATION MODEL	Point/area model	**Multipoint grid-based model**

10	MISSILE EFFECTS MODEL	Empirical model	**Probabilistic model developed using Monte Carlo simulation**
11	HUMAN IMPACT MODELS	Probit models	Probit models

6.2. SIMULATION USING GRID BASED APPROACH

With the required consequence models and the simulation algorithms available in hand, computer codes were developed in MATLAB 6 for simulating the fire and explosion consequence models. While simulating the models a sequence should be followed. For a fire consequence study the order of simulation of the models is shown in Figure 6.1 and for explosion consequence study it is shown in Figure 6.2. A grid-based modeling approach has been employed during this process which enables better modeling and analysis of radiation and overpressure impacts at different locations in the process area. During grid-based simulation, the process area under study as shown in Figure 6.3 is divided into a specific number of grids, and the hazard potentials and consequences are then evaluated at each end of the grid, finally plotting the results as contours.

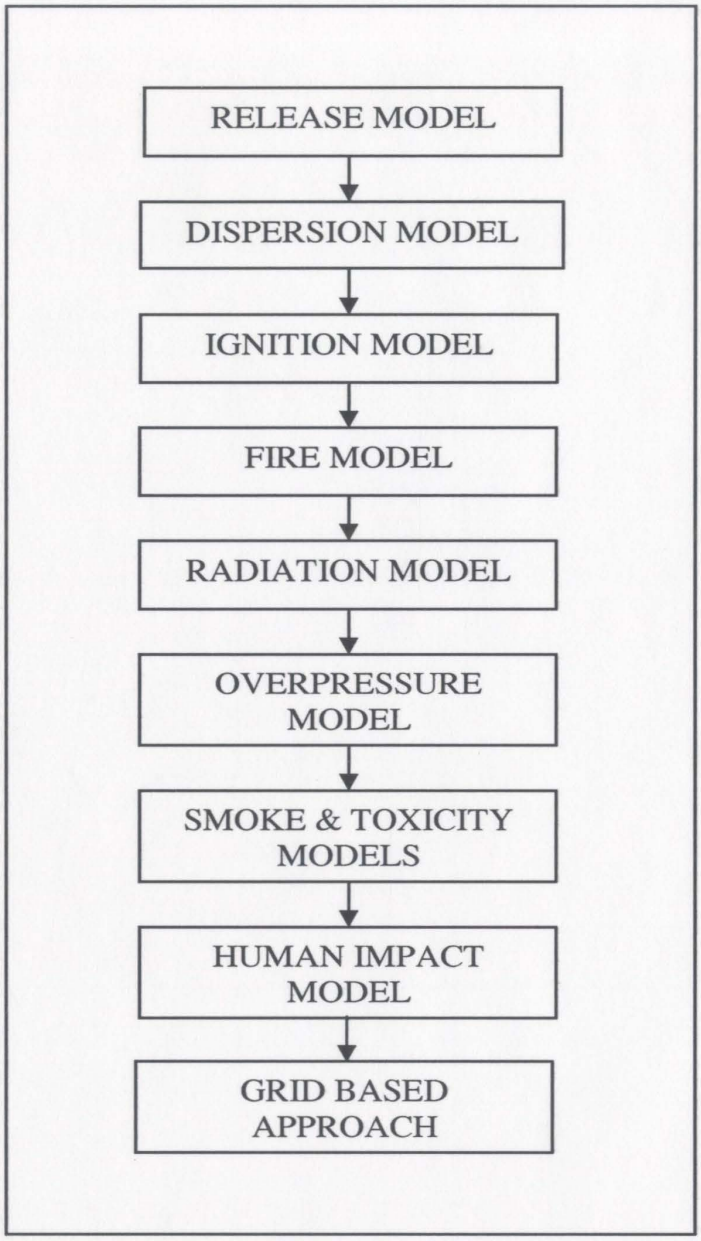

Figure 6.1. Simulation sequence of models for fire consequence study

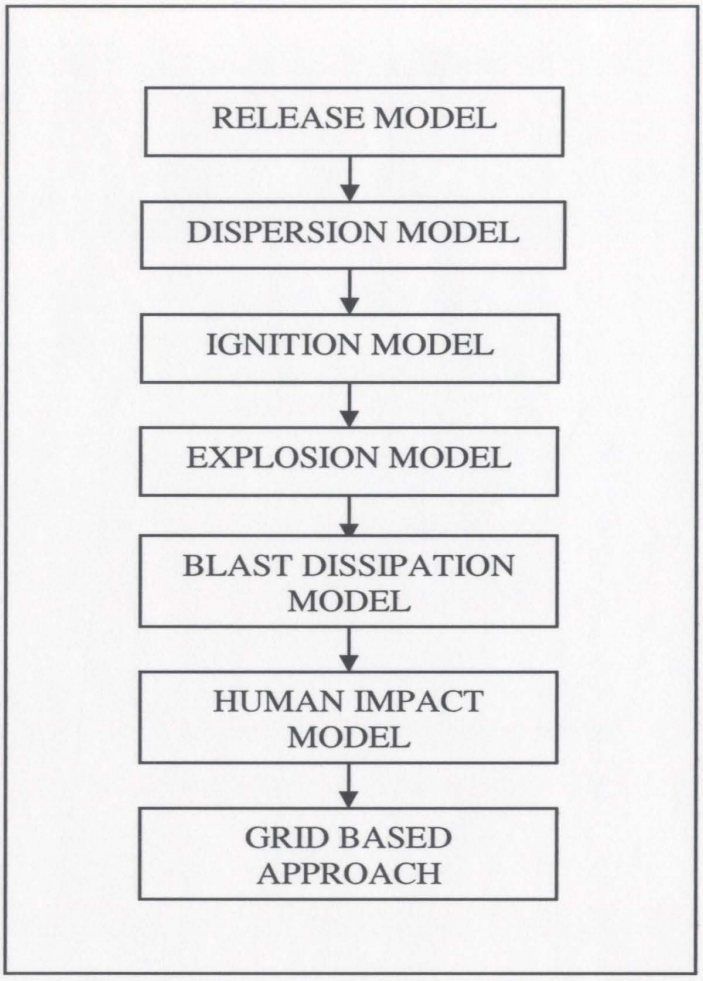

Figure 6.2. Simulation sequence of models for explosion consequence study

Contour plotting is a more user-friendly representation than the ordinary line plots obtained by other software packages. A question that arises is "into how many grids should the space be divided?" After extensive trial runs to study the effect of number of grids on two factors: the precision of results for plotting, and the computational time, 50 ×50 = 2500 grids turned out to be the optimal

setting that could ensure an optimal balance between precision and computational time.

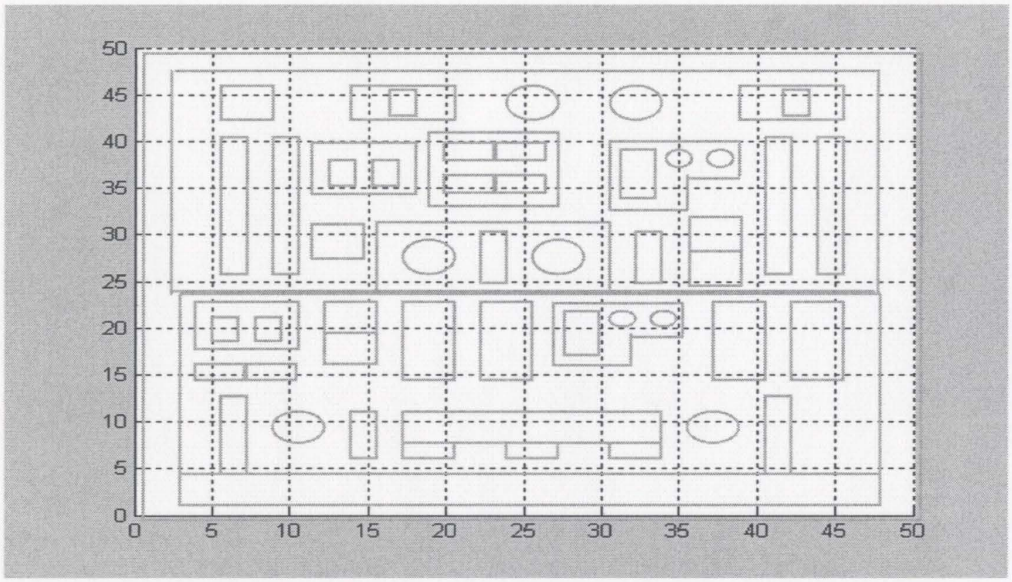

Figure 6.3. Plant layout that is divided into grids

Additionally, the analysis of radiation heat and blast waves is uncertain if the presence of obstacles (partial barriers, e.g. process equipment and solid barriers e.g. Passive Fire Protection walls, explosion proof walls) is not taken into account. This issue does not arise when using CFD models, as application of appropriate boundary conditions will solve the problem. However, it appears to be difficult to resolve this issue while using semi-empirical models, unless a grid-based approach is used. Also, the damage contours obtained by adopting a grid-based approach permit the development of a clear picture of potential impact

zones. This can facilitate proper selection and specification of safe separation distances to prevent injury to people and damage to nearby equipment.

Chapter 7

RESULTS AND DISCUSSIONS

This chapter presents and discusses the results obtained by carrying out fire and explosion consequence analysis. Various fire and explosion scenarios occurring on an offshore platform were identified and simulated. The results obtained from this work were compared with that of commercial software packages and are elaborated here. Also discussed are the results of missile effects.

7.1. OFFSHORE FIRES: CREDIBLE SCENARIOS

In this section, various credible scenarios are studied for pool fires, jet fires and fireballs occurring in a 50 m × 50 m × 10 m compartment on an offshore platform. These scenarios are then simulated using the suite of models for fire consequence analysis discussed in chapter 2, in a sequential order. The consequences from radiation heat fluxes and overpressures generated by the combustion gases in the compartment were then analyzed. The simulation

results for each of the fires are presented graphically in two different ways: radiation heat flux contours and radiation damage (% fatality) contours.

For flash fires, a separate scenario was identified, in which a flash fire occurs due to ignition of a vapor cloud formed over an imaginary process area (100×100 m^2) of a typical offshore platform. The radiation and fatality results are then plotted as contours over this area just to have a clear picture of safer zones and vulnerable zones. However, the obstacle effects on thermal radiation are not considered.

Scenario 1: Pool Fire

The liquid spill at a volumetric rate 0.04 m^3/s, from a storage tank containing 100-kg crude oil, placed in the center of a compartment forms a pool and catches fire, leading to a ***pool fire***. Wind conditions are 5 m/s in the easterly direction.

Simulation Results:

Maximum pool diameter = 3.3 m

Height of pool fire = 4.8 m

Angle of tilt from vertical = 57 degrees

Surface emissive power of lower clear flame = 105 kW/m^2

Surface emissive power of upper smoky flame = 24 kW/m^2

Radiation Effects

The steady state radiation heat flux in the compartment is represented by the contours shown in Figure 7.1. Similarly, lethality (radiation damage) contours in the same space are represented in Figure 7.2. As the pool fire is tilted 57 degrees from the vertical toward the downwind direction, the radiation and hence the damage must be higher downwind than upwind. This is evident from the contours in Figures 7.1 and 7.2. These contours confirm that most of the compartment is prone to lethal effects. Safe areas are apparent from Figure 7.2 and are located at corners of the compartment.

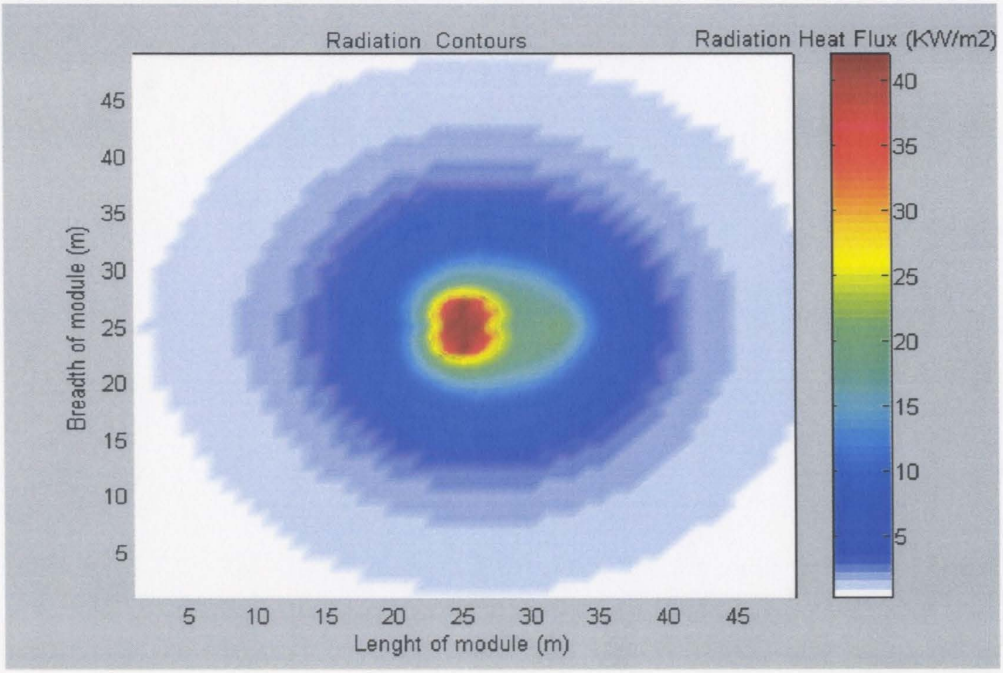

Figure 7.1. Radiation contours for the pool fire scenario

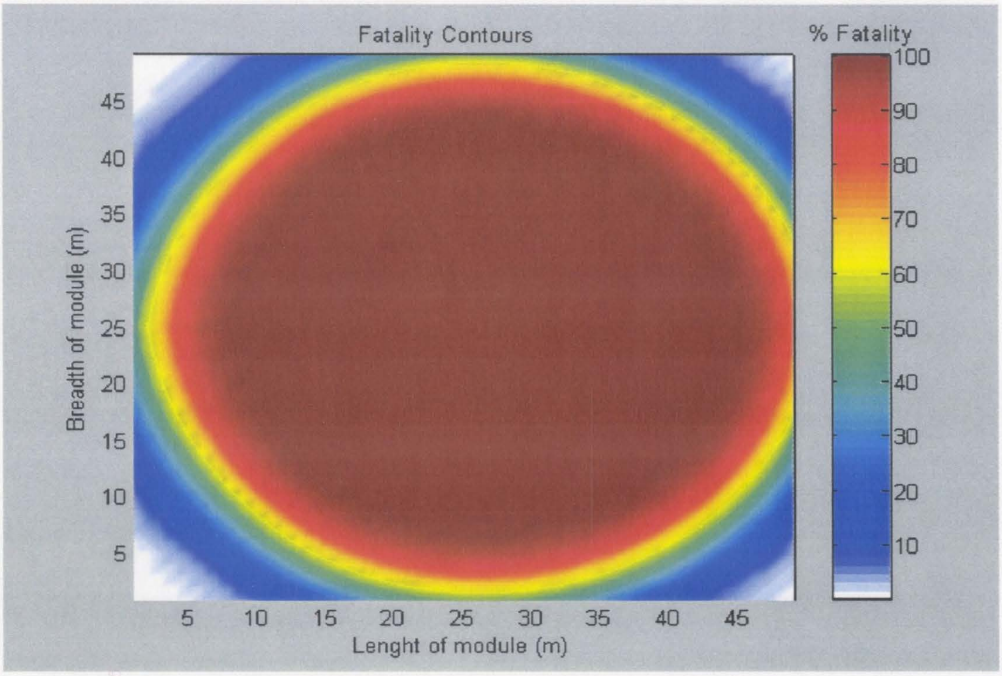

Figure 7.2. Lethality contours for the pool fire scenario

Overpressure Effects:

Overpressure generated from the hot combustion gases released during a pool fire in the compartment was calculated as 0.25 kPa, which has negligible impact. Possible effects are loud noise, sonic boom, glass failure and breakage of small windows under strain (CCPS, 2000). However, it must be remembered that this result is for a fuel loading of 100 kg. Larger fuel inventories, such as are routinely found on offshore installations, have the potential for generating higher overpressures.

Scenario 2: Horizontal Jet Fire

A leak of 0.152-m diameter in a 100-m^3 pressurized natural gas storage tank placed at one end of the compartment causes the inventory to exit as a horizontal jet at a rate of 11.2 kg/s. The fuel ignites immediately after release and results in a ***horizontal jet fire.*** Wind conditions are 5 m/s in the easterly direction.

Simulation Results:

Burning time = 17 s

Length of flame = 38 m

Frustum length = 26 m

Angle of tilt from vertical = 80 degrees

Surface emissive power from sides of flame = 223 kW/m^2

Surface emissive power from end of flame = 242 kW/m^2

Radiation Effects:

The steady state radiation heat flux in the compartment is represented by the contours in Figure 7.3. Although, the flame length is 38 m, the burning time of 17 seconds reduces the amount of damage in the defined space. The lethality (radiation damage) contours are represented in the same area as shown in Figure 7.4. The contours shown in Figures 7.3 and 7.4 are elliptical, as is expected from the initial and boundary conditions that define the physical scenario. This

confirmation facilitates the reliable prediction of consequences, which in turn provides an opportunity to identify safer zones for escape when an unwanted event occurs. The lethality contours illustrate that 100% lethality is predicted in most parts of the compartment. Safe zones in all directions are apparent from the lethality contours in Figure 7.4.

Overpressure Effects:

The overpressure generated by the combustion gases in the compartment was calculated to be 2.1 kPa. Limited minor structural damage and at times slight damage to window frames (CCPS, 2000) can occur due to this pressure.

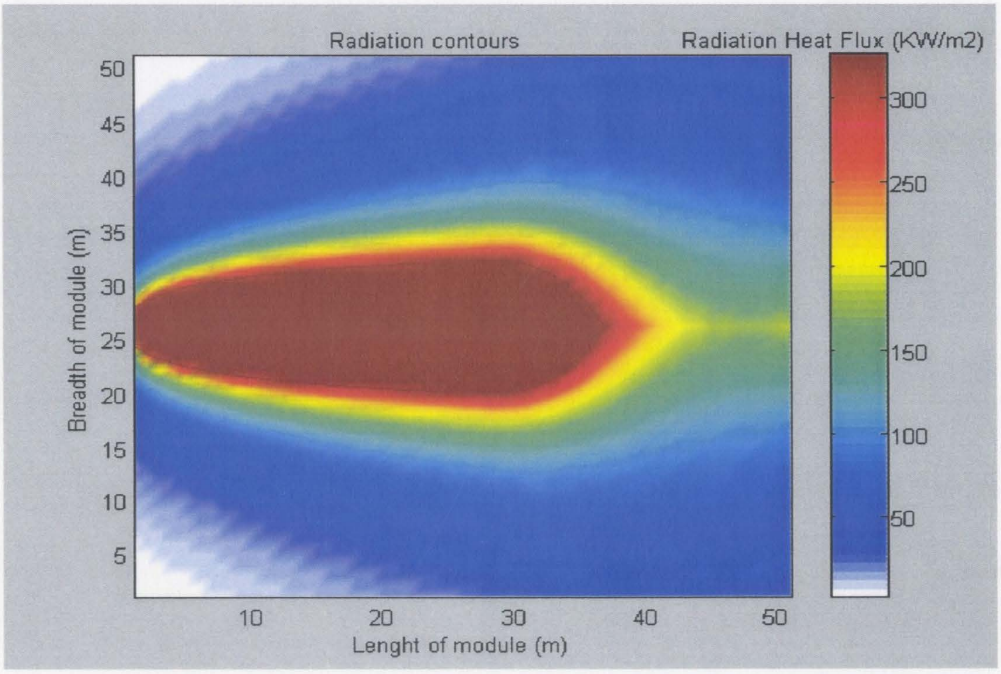

Figure 7.3. Radiation contours for the horizontal jet fire scenario

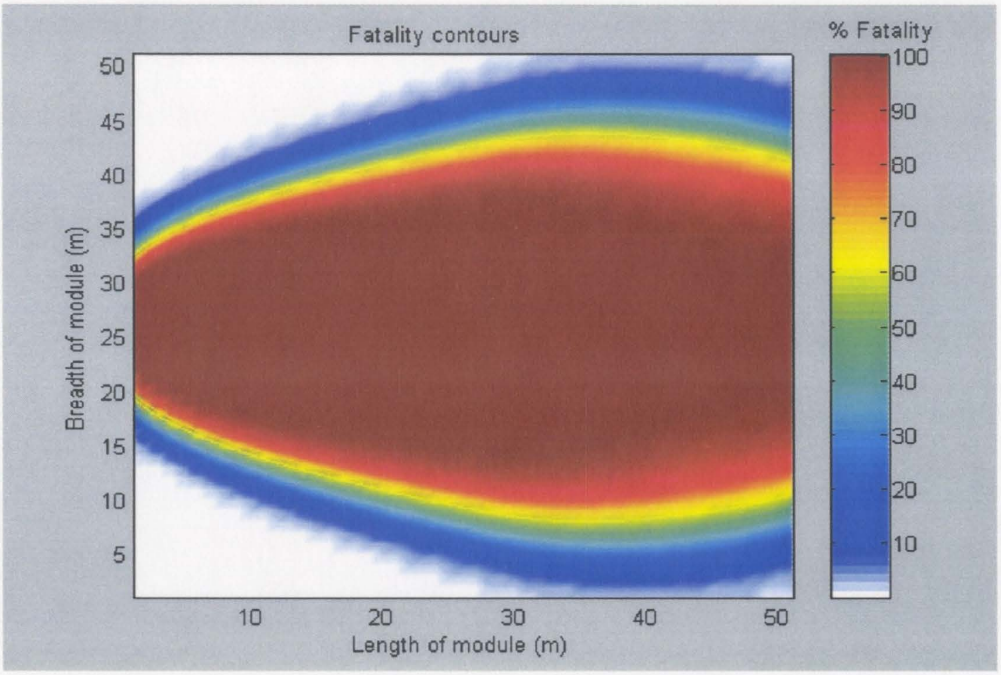

Figure 7.4. Lethality contours for the horizontal jet fire scenario

Scenario 3: Fireball

Fire impingement on a propane gas storage tank causes a pressure rise inside the tank and eventually leads to a BLEVE. A fuel mass of 1272 kg is released and ignited, resulting in a ***fireball***.

Simulation Results:

Diameter of fireball = 66 m

Time of existence of fireball = 7.9 s

Height of fireball center above ground = 49.5 m

Surface emissive power from the fireball = 320 kW/m^2

Radiation Effects:

The steady state radiation contours in the compartment are shown in Figure 7.5. Lethality (Radiation damage) contours are plotted on the same area as shown in Figure 7.6. Although the fireball lasts for only about 8 seconds, the large amount of fuel released results in ~90 % lethality close to the fireball with minor damage persisting at all other areas of the compartment. No zones are identified as 100% safer. Therefore, fewer chances are available for escape in the event of such a fireball.

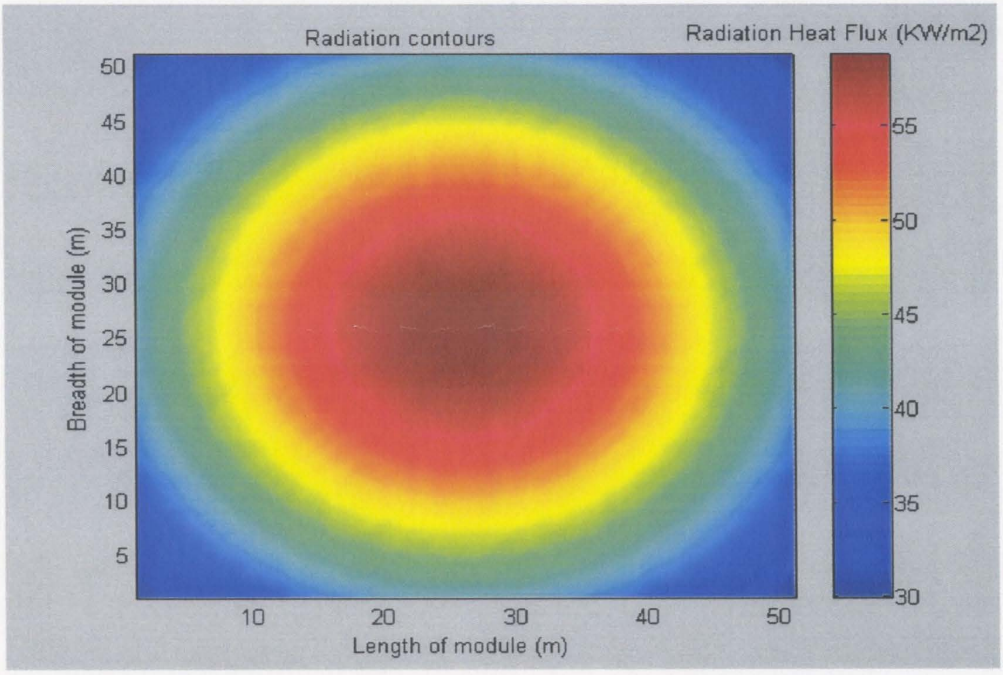

Figure 7.5. Radiation contours for the fireball scenario

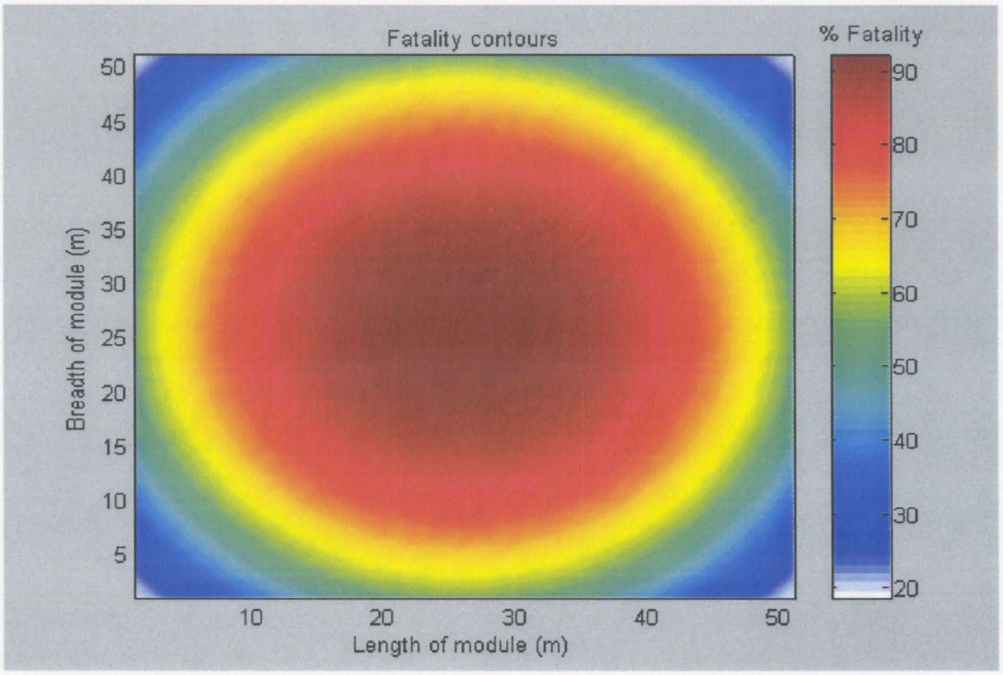

Figure 7.6. Lethality contours for the fireball scenario

Overpressure Effects

The overpressure created by the fireball in the compartment was calculated as 2.4 kPa, again a value which is approaching the point at which personnel mobility is affected. The fact that the fireball overpressure is higher than that predicted for the pool fire (scenario 1) is explainable in part by the much higher mass of fuel released in the fireball scenario.

Scenario 4: Flash fire

Two scenarios are considered within flash fires. They occur as a result of ignition of a propane gas cloud formed by instantaneous and continuous releases. The scenario details are as follows:

i) An instantaneous release (IR) of 1000 kg of propane gas over the process area forms a vapor cloud which upon ignition burns as a flash fire.

ii) A continuous release (CR) of propane gas at 10 kg/s due to a leak in a storage tank. The cloud formed due to this release, upon ignition results in a flash fire.

As mentioned before, the radiation and fatality results are plotted as contours over an imaginary process area (100×100 m^2) of a typical offshore platform.

Simulation Results

Table 7.1. Flash fire simulation results

Type of release	SLAB dispersion model		Ignition model		Radiation model			
	Cloud Radius (m)	Cloud Height (m)	Prob. of Ignition	Time for Ignition (s)	Flame height (m)	Flame speed (m/s)	Maximum '*q*' (kW/m^2)	Cloud burn time (s)
Instantaneous (1000 kg)	36.83	1.13	0.52	19	44.54	6	42.50	13
Continuous (10 Kg/s)	33.60	1.47	0.76	33	24.14	6	32.91	8

Radiation Effects:

The gas that is released (instantaneously or continuously) forms a cloud and disperses with initial momentum in low wind conditions. The dispersion of these clouds was simulated using a SLAB dispersion model to estimate the dimension of the cloud. Probability of ignition (P) was estimated using an onsite ignition model when the cloud concentration is within the flammability limits. The variations of P and cloud size with time, as well as P and cloud concentration with time, were plotted for the IR scenario in Figures 7.7 and 7.8 respectively. It is clear from the figures that an increase in the cloud size with time would lead to an increase in P and decrease in cloud concentration.

The results obtained from the SLAB model (cloud radius, height), and the ignition model (P, time of ignition after release) were used in the Flash Fire radiation model to obtain the fire dimensions and characteristics. These results are presented in Table 7.1 for both IR/CR scenarios. Further, radiation contours and fatality contours were plotted over the process area and are represented in Figures 7.9 and 7.10 for IR and in Figures 7.11 and 7.12 for CR. Radiation and fatality contours from the IR scenario show that most of the plant area is affected, whereas the contours from the CR scenario show that a relatively small part of the plant is affected. With this we can conclude that flash fire from an IR is the more dangerous event. However, the effects of escalation events (e.g. pool fire,

jet fire, BLEVE, VCE etc) that result when the cloud burns back during a CR, are likely to be more severe than the flash fire itself.

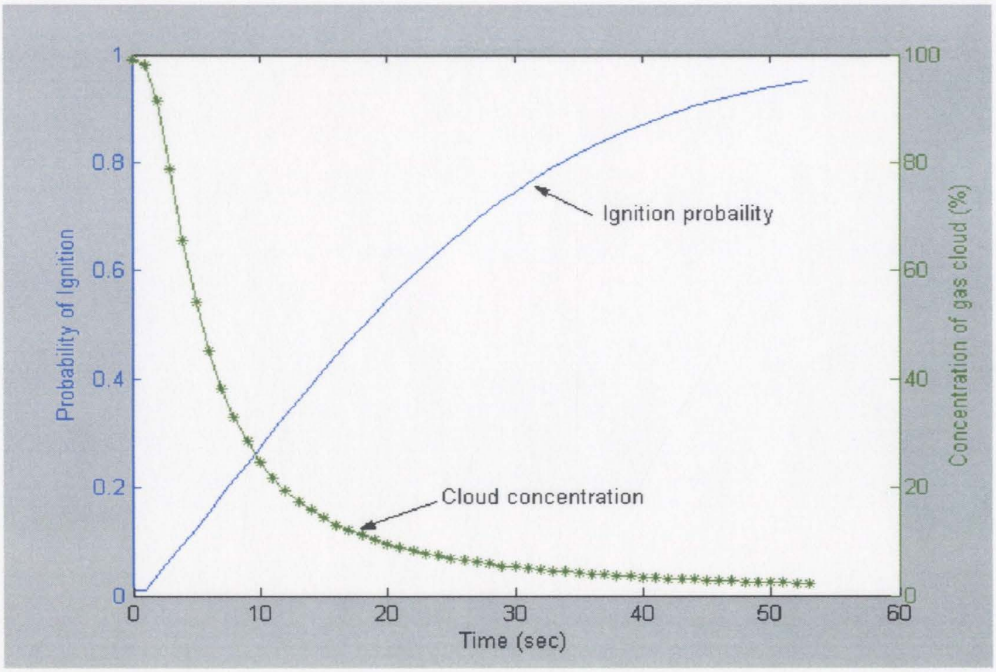

Figure 7.7. Variation of Probability of Ignition and cloud concentration with time

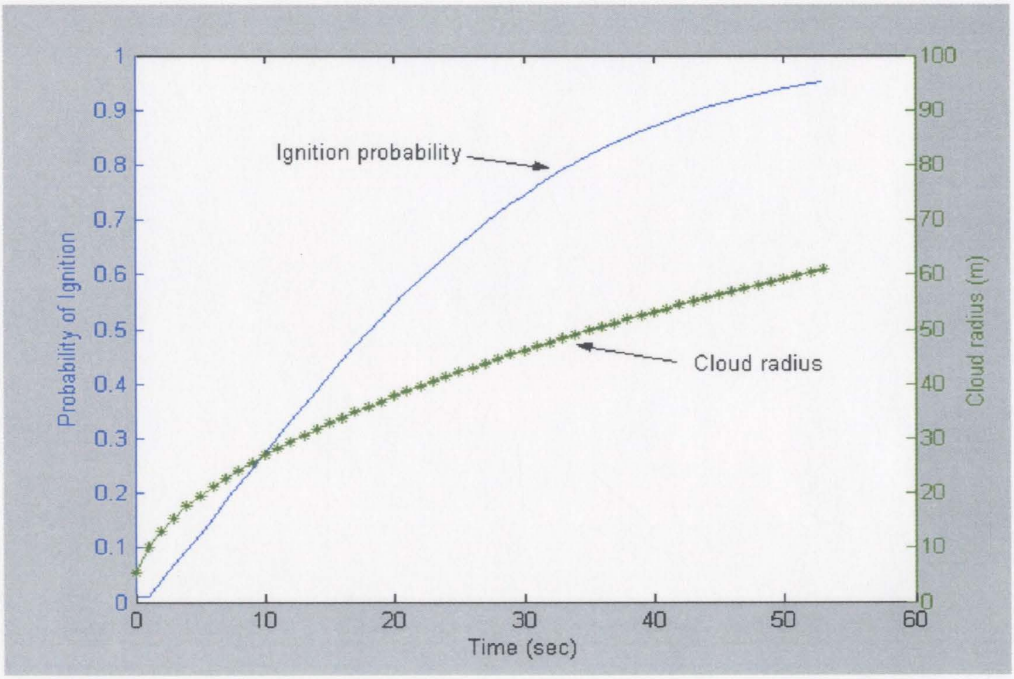

Figure 7.8. Variation of Probability of Ignition and cloud radius with time

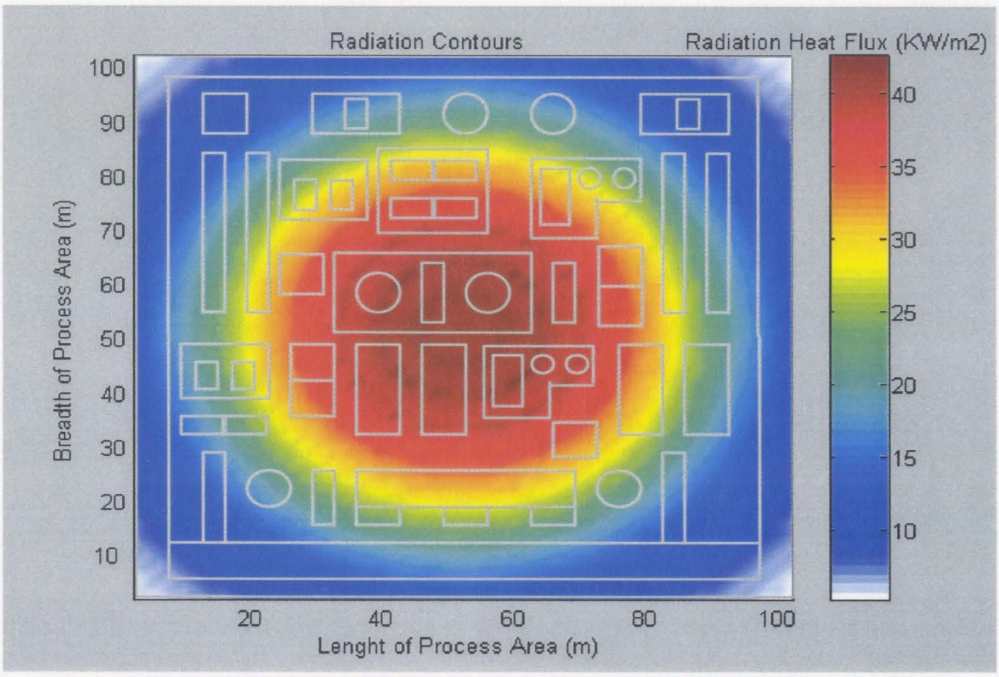

Figure 7.9. Radiation contours for the instantaneous propane release flash fire scenario

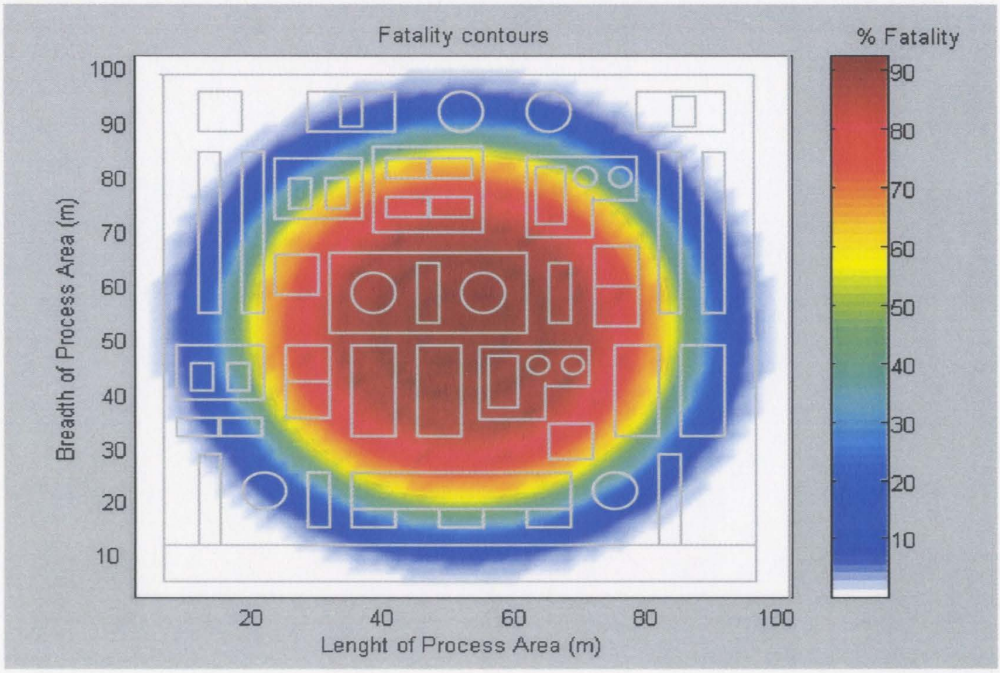

Figure 7.10. Lethality contours for the instantaneous propane release flash fire scenario

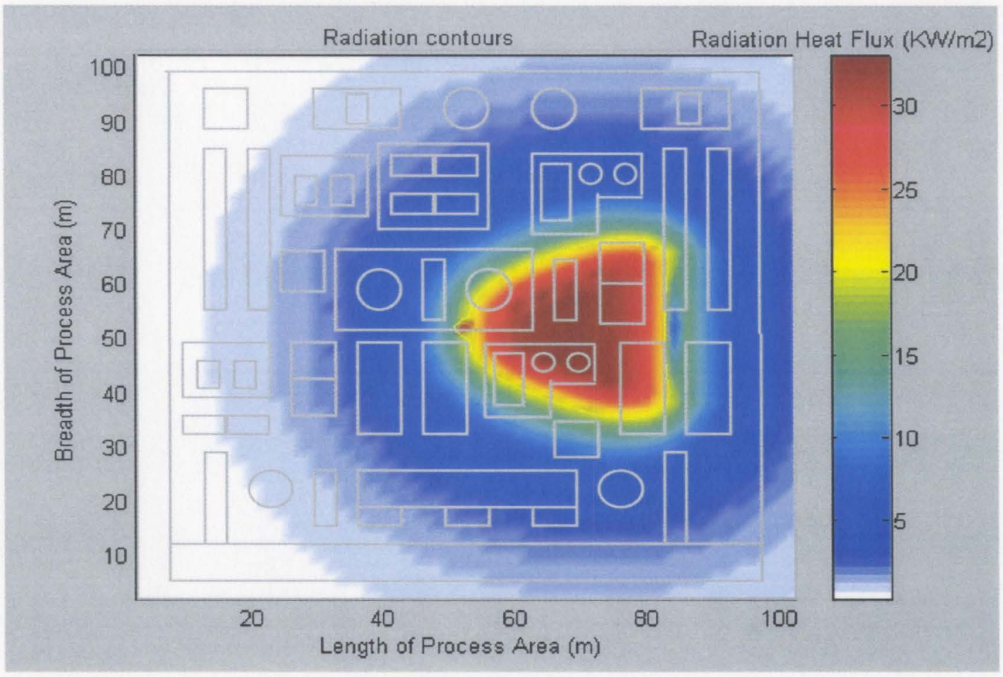

Figure 7.11. Radiation contours for the continuous propane release flash fire scenario

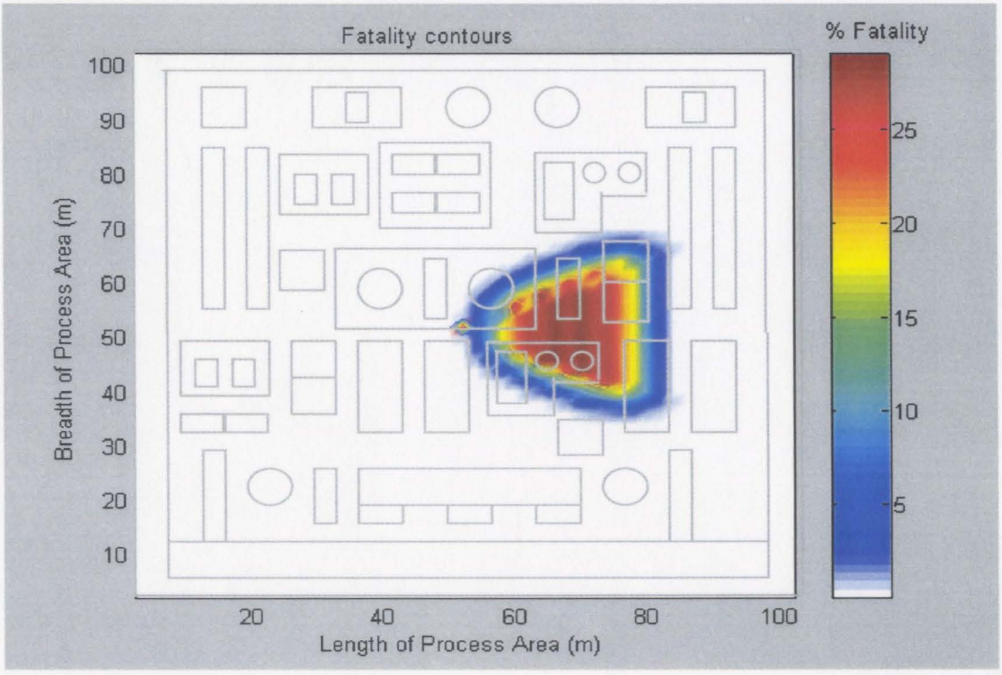

Figure 7.12. Lethality contours for the continuous propane release flash fire scenario

7.2. OFFSHORE EXPLOSIONS: CREDIBLE SCENARIOS

In this section, various credible scenarios for gas explosions and BLEVE are identified. Among gas explosions emphasis is given to only partially confined vapor cloud explosion, confined vapor cloud explosion and external explosion. The scenarios identified are simulated using the suite of models mentioned in chapter 2 for explosion consequence analysis, in a sequential order. The results are presented graphically in two different ways: overpressure decay contours and overpressure damage (% fatality) contours plotted over an imaginary (100×100 m^2) process area.

Scenario 1: Partially Confined vapor cloud explosion

A 1000 kg of Propane gas released into a process area that is highly congested and partially confined, results in a vapor cloud explosion upon ignition. The simulation was carried out using Congestion Assessment Method. Congestion in the process area is characterized by the blockage caused by process equipment in the length, breadth and height dimensions of the process area, usually referred as blockage ratio. Input values of 0.3 along the length dimension, 0.4 along the breadth dimension and 0.2 along the height dimension have been considered in this scenario.

Simulation Results:

Table 7.2. Congestion Assessment Method simulation results

SLAB dispersion model		Ignition model		CAM2 explosion model		
Cloud Radius (m)	Cloud Height (m)	Prob. of Ignition	Time for Ignition (s)	Source Volume (m^3)	Source Radius (m)	Source Pressure (bar)
36.83	1.13	0.503	19	37392	26.14	7.73

The simulation procedure is similar to that used for flash fires discussed in section 7.1 except that here, the results obtained from the SLAB and ignition models were used as input to the CAM2 explosion model to estimate the source overpressure, and then an overpressure decay model was used to obtain the blast waves. The results from the simulation are presented in Table 7.2, and the decay of the source pressure is plotted as contours over the process area in Figure 7.13. It is evident from the results (Figure 7.13) that the lethal overpressure engulfs the complete process area. The impact to human beings due to the blast waves is represented as fatality contours in Figure 7.14. Contours engulfing the entire process area further support the earlier prediction.

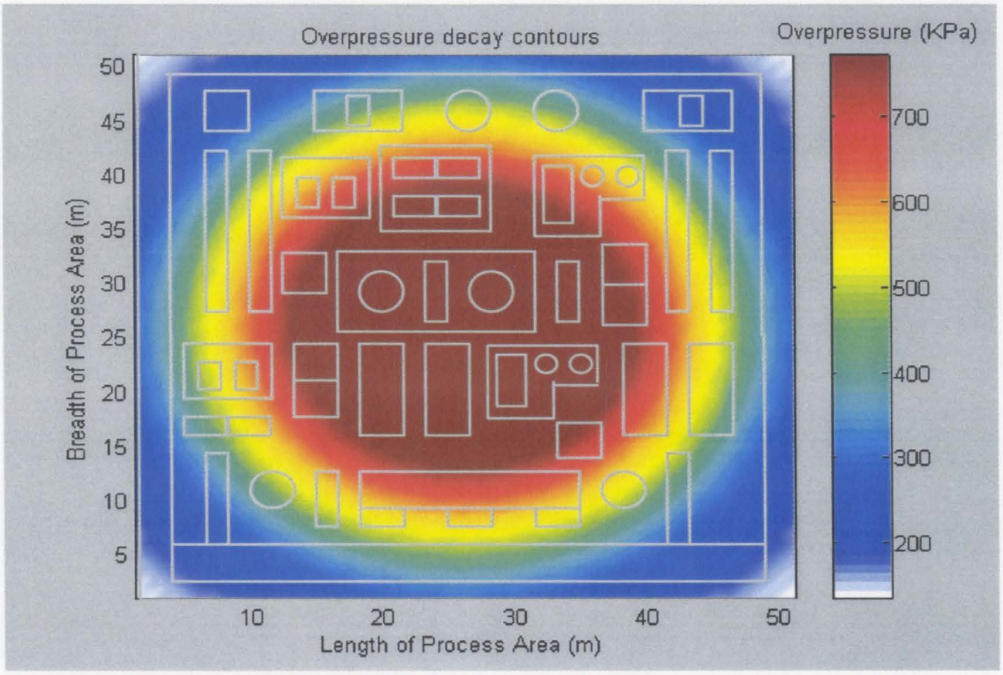

Figure 7.13. Blast waves from a partially confined vapor cloud explosion

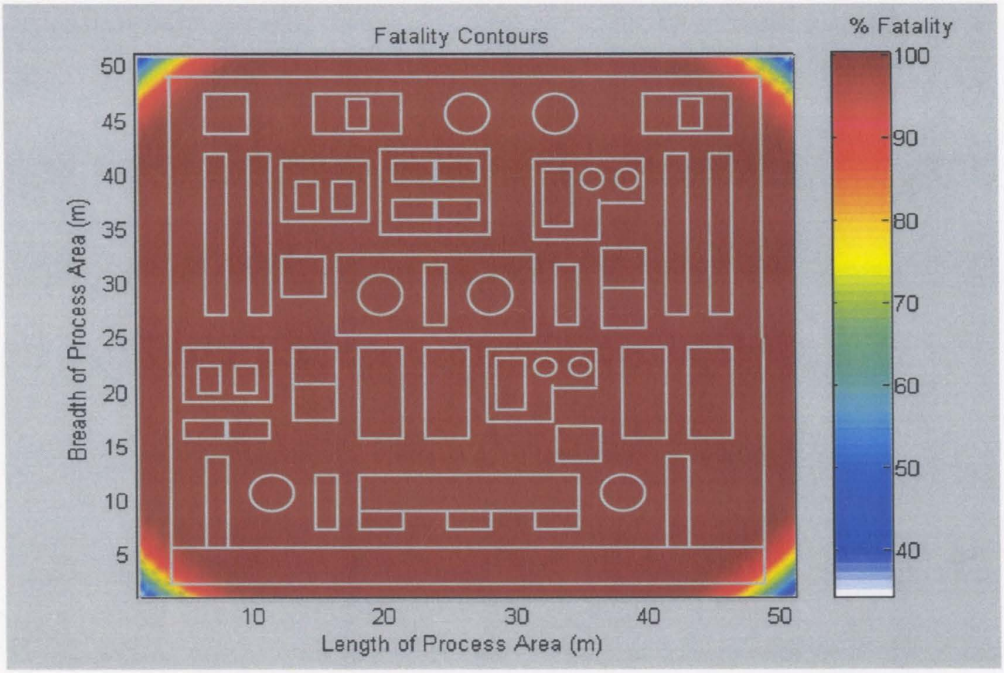

Figure 7.14. Lethality (overpressure) contours from a partially confined vapor cloud explosion

Scenario 2: Confined vapor cloud explosion

An offshore module ($10\times5\times5$ m^3) is completely filled with a stoichiometric amount of propane gas. The presence of obstacles at distances 1, 2, 4, 7 and 9 meters (see Figure 7.15) from one end of the wall, causes the gases to burn rapidly leading to a confined vapor cloud explosion. This particular scenario was simulated using SCOPE 3 and the results are shown in Table 7.3. The results in the table show how the turbulence intensity, drag coefficient, flame speed and overpressure vary after passing over each grid of obstacles. Turbulence, flame speed, and overpressure increase as the unburned gases pass over obstacles, which are reflected in the tabulated results. Precisely, the profile of variation of overpressure with time is shown in Figure 7.16, which shows that the gas in a $10\times5\times5$ m^3 volume is burnt in just 0.13 seconds leading to the development of high pressure. However it was found that only 28% of the gas was burned inside the module while the rest was vented out and combusted as an external explosion. Also, the variation of overpressure with flame position in the module is shown in Figure 6.17. The overpressure due to the gas burned in the module was 4.14 bar, whereas from the gas vented out was 2.04 bar. Thus the approximate maximum source overpressure generated by the combination of confined and vented explosion ($P_{max} = P_{module} + 0.7P_{vented}$) is 5.56 bar.

Simulation Results:

Table 7.3. SCOPE 3 simulation results

Grid number	Grid position (m)	Turbulence intensity (m/s)	Drag coefficient	Flame speed (m/s)	u'^* (m/s)	Overpressure (bar)	Reynolds number
1	1	0.64	4.09	1.16	0	0.02	74
2	2	1.10	4.08	7.94	0.23	0.04	159
3	4	3.12	4.08	44.87	1.62	0.51	1105
4	7	7.47	3.98	107.61	9.21	1.03	6277
5	9	11.24	3.48	161.85	23.37	1.97	15918
6	10	13.84	3.08	199.25	38.19	4.14	26019

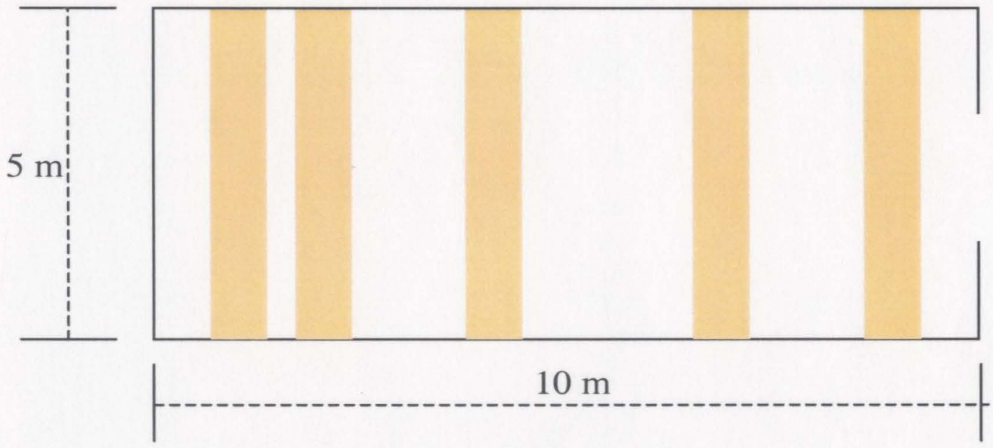

Figure 7.15. Geometry of an offshore module with a vent and obstacles at 1,2,4,7 and 9 meters

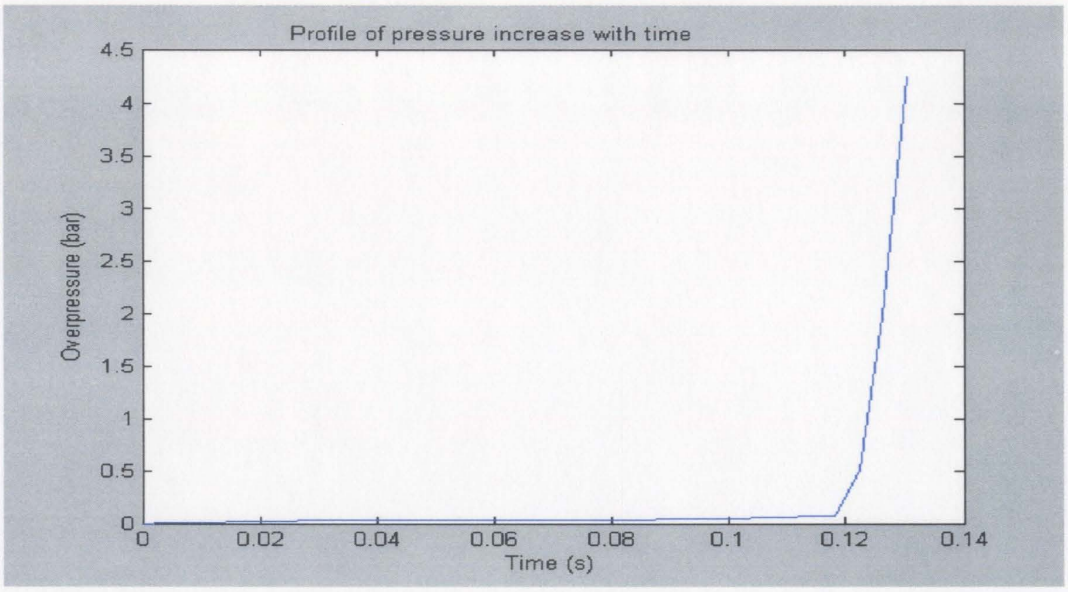

Figure 7.16. Variation of overpressure with time

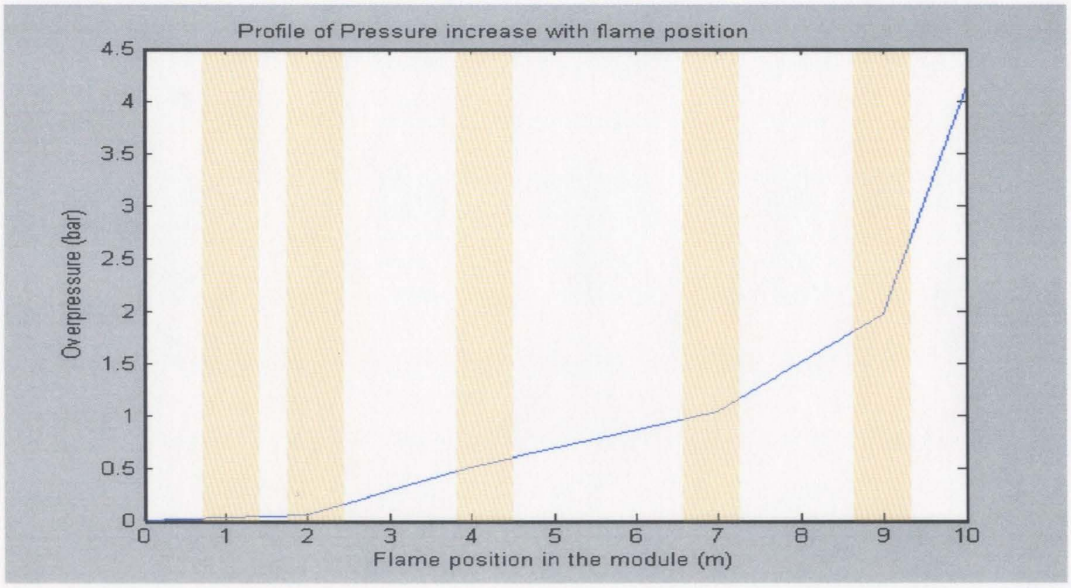

Figure 7.17. Variation of overpressure with the flame position in the module

Scenario 3: BLEVE followed by a fireball in an oil separator

High-pressure development in the 25 m^3 separator due to external fire impingement causes the unit to fail as a BLEVE. The vapor cloud formed due to BLEVE on ignition causes a fireball.

Simulation Results:

Maximum overpressure = 1.2 bar

Diameter of fireball = 66 m

Time of existence of fireball = 7.9 s

Height of fireball center above ground = 49.5 m

Surface emissive power from the fireball = 320 kW/m^2

The simulation results are represented as blast waves obtained from BLEVE and as radiation contours from the resulting fireball, shown in Figures 7.18 and 7.19 respectively. It is clear from the figures that the effect of BLEVE is concentrated in the near field, whereas the fireball radiation is widespread over most of the process area. The impact to human beings (%fatality) due to the cumulative effect of overpressure and heat load is then represented in Figure 7.20. It was found that the impact due to the fireball is greater than the blast waves and encompasses the entire process area.

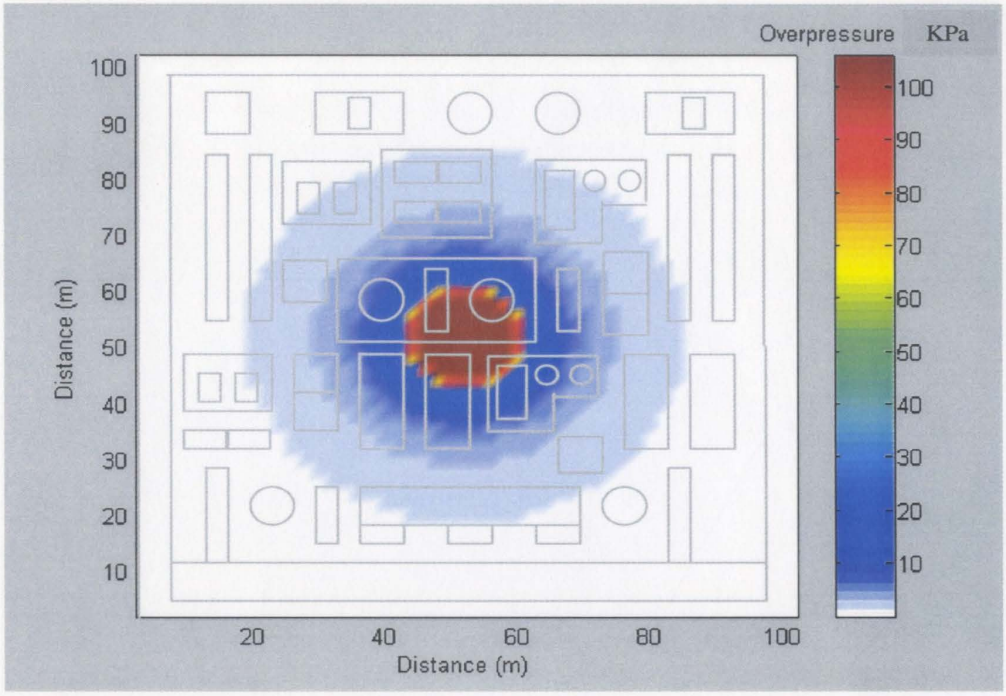

Figure 7.18. Blast waves from a BLEVE in oil separator.

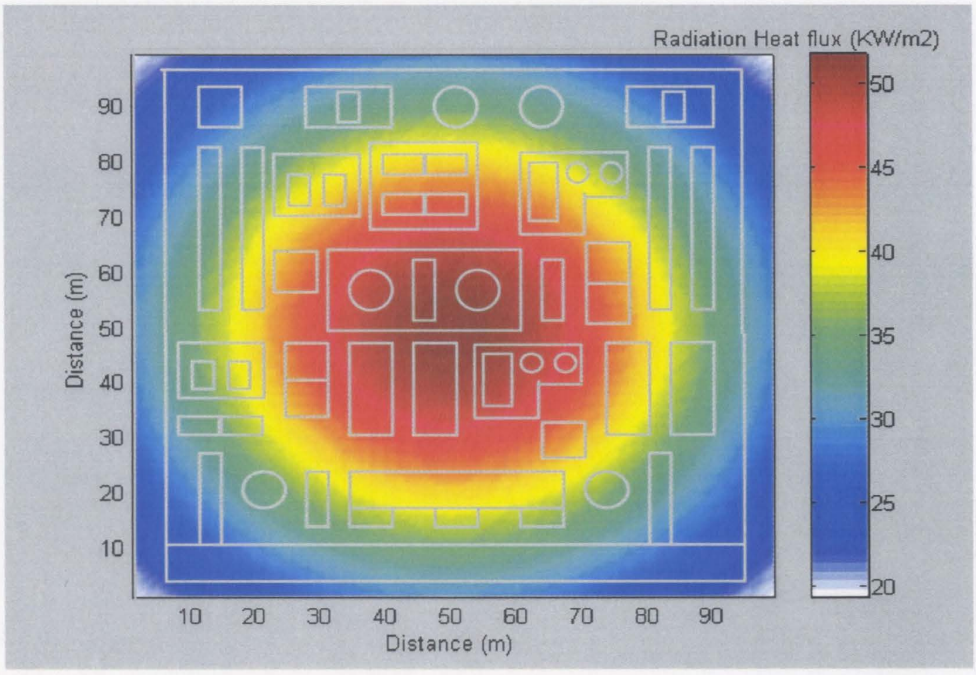

Figure 7.19. Radiation contours from a fireball

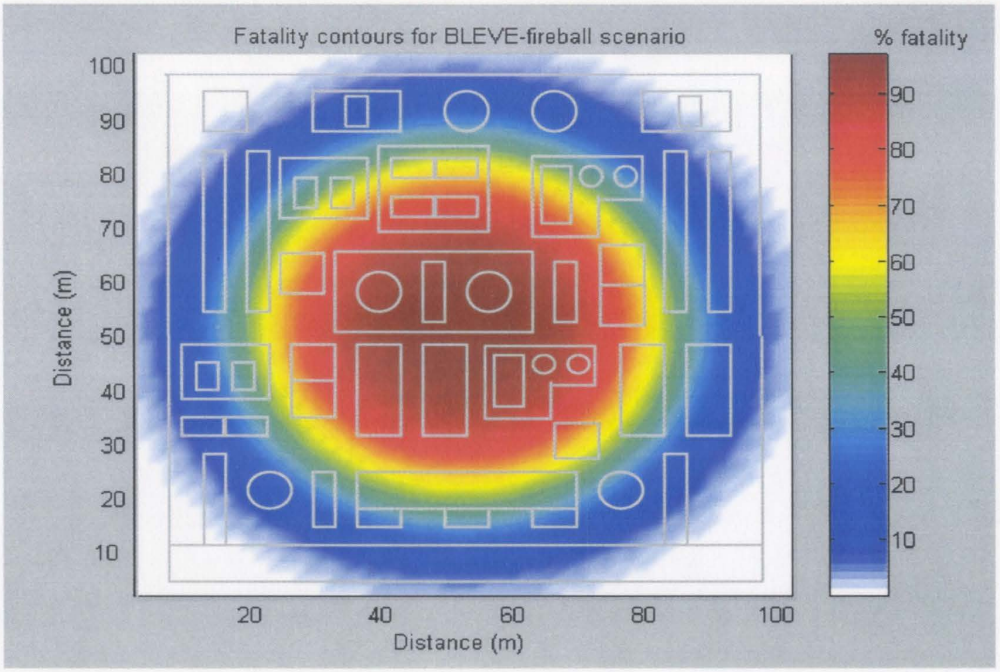

Figure 7.20. Lethality (overpressure & radiation) contours from a BLEVE - fireball scenario

7.3. MISSILE IMPACT SCENARIO

In this section, a scenario has been considered to illustrate the capability of the newly developed probabilistic model for assessing the missile impacts, the methodology being discussed earlier in section 5.3.

Scenario: A 25 m^3 cylindrical propane storage vessel is placed horizontally on the ground. It is filled with 80% liquid propane. Due to engulfment of the vessel in fire, it bursts as a BLEVE. Fragments generated as a result of the explosion from the vessel turn into missiles and pose danger to the equipment in its vicinity.

Consider a spherical storage tank, 15 m diameter, 150 m away from the exploding vessel, oriented at angle of 30^0. It is intended to find the probability of strike of missiles at this spherical target object. Upon simulating this scenario, the following results were obtained.

Simulation results:

BLEVE explosion energy = 7.14e4 KJoules.

Effective Range Interval (ERI) = 22.5 m

Effective Orientation Interval (EOI) = 8.58 degrees

Effective Trajectory Interval (ETI) = 7.125 degrees

The probability density function and the cumulative distribution function obtained for the range of fragments as a result of Monte-Carlo simulation are shown in Figures 7.21 and 7.22 respectively.

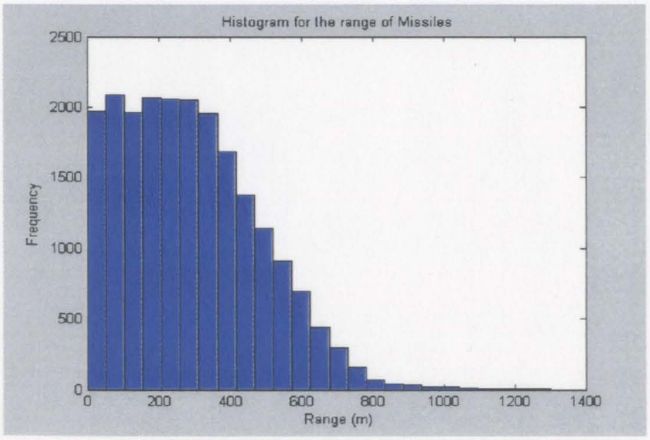

Figure 7.21. Probability density function for Range of missiles

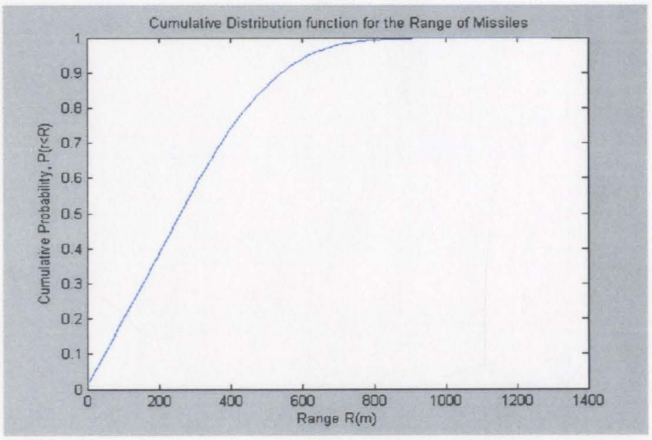

Figure 7.22. Cumulative distribution function for Range of missiles

The probability of strike results follows:

Probability of strike due to fragments falling within the vulnerable area:

The probability of fragments falling within the ERI = 0.0428

The probability of fragments orienting within the EOI = 0.0209

The probability of strike from this scenario = 8.9356e-004

Probability of strike due to collision of fragments with the target before reaching their final destination:

The probability of fragments falling beyond the ERI = 0.6935

The probability of fragments orienting within the EOI = 0.0209

The probability of fragments flying within the ETI = 0.3937

The probability of strike from this scenario = 0.0057

Overall probability of missile strike = 0.00089+0.0057

= **0.0066**

To provide a more interactive representation of the results, a multipoint grid based approach (Pula et.al., 2004) was used along with the probabilistic approach proposed here. The probability of strike results evaluated at various points in a defined area were obtained as a two dimensional matrix which was subsequently plotted as contours as shown in Figure 7.23. It is clear from the figure that for cylinders horizontally placed on the ground; the probability of

missile strike is much higher in the axial directions than in any other directions. This is close to reality because of the fact that the fragments such as end caps generated from the rupture of horizontal cylinders fall in the axial directions. Therefore, it can be concluded that symmetry of probability of strike around the object, as was obtained in (Hauptmmans, 2001) is incorrect for horizontal cylinders as explosion source. There may be that this symmetry holds true for spherical and vertical cylinders, however it needs to be justified.

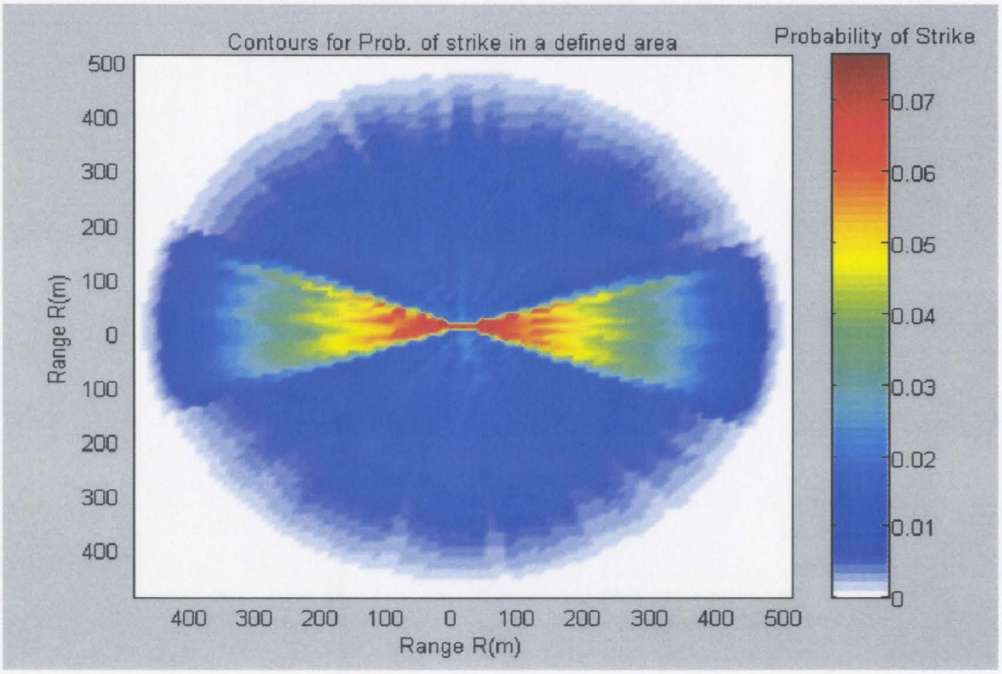

Figure 7.23. Probability of missile strike contours

These calculations can be further combined with the consequence calculations to obtain missile risk contours, which can then be used in designs of safer process layouts.

7.4. COMPARISON OF RESULTS WITH OTHER PACKAGES

In this section, the results from the pool fire and jet fire consequence models discussed in section 6.1., scenarios 1 and 2, are compared with their corresponding point source models (such as used in the commercial software PLATO©, a well-known package for simulating hydrocarbon leakage and ignition on offshore installations). A description of the modeling approaches for pool fires, jet fires and fireballs that are embedded in this package is given by Jones & Irvine (1997). These pool fire and jet fire point source models were simulated for the same data and specifications as in scenarios 1 and 2 in section 7.1. The results are represented as radiation contours and radiation damage contours in Figures 7.24 – 7.27.

Scenario 1: Pool fire results comparison

Comparing the results of the pool fire consequence model as shown in Figures 7.1 and 7.2 with those in Figures 7.24 and 7.25 indicates that:

- The radiation contours from the point source model (used in PLATO©) are circular, whereas the revised model gives elongated contours due to the actual physical mechanism of flame tilt.
- The point source model (used in PLATO©) over-predicts the thermal radiation damage relative to the revised pool fire model used in the

present approach. This is to be expected given the point source approach in the former model and the use of a solid flame in the latter. Hence the use of point source models brings in a large amount of uncertainty in the results.

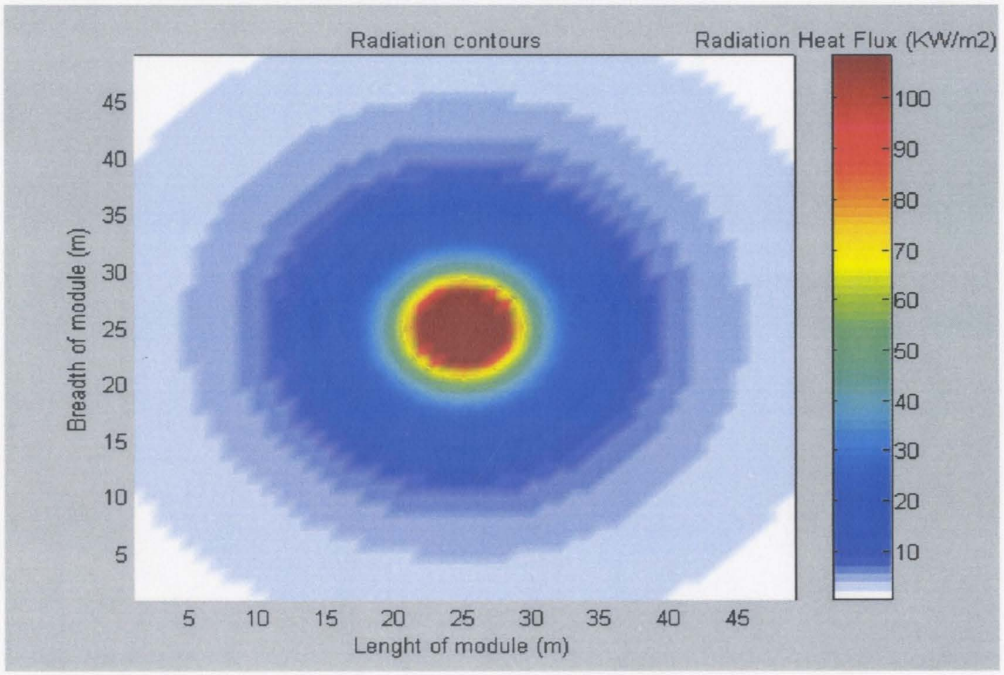

Figure 7.24. Radiation contours from point source pool fire consequence model

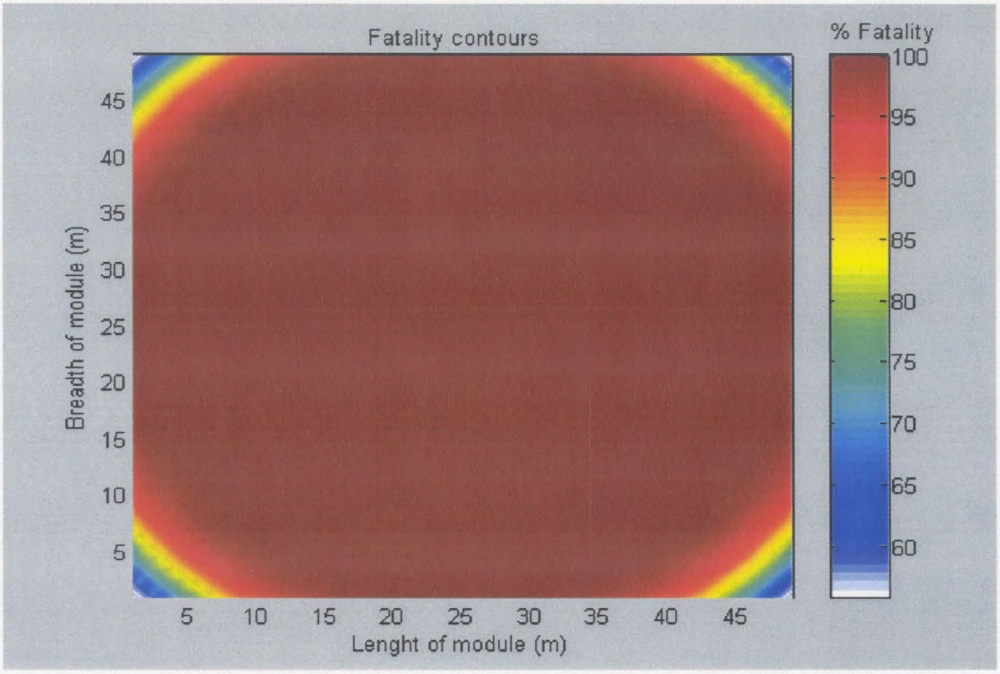

Figure 7.25. Percentage lethality (thermal radiation) contours from point source pool fire consequence model.

Scenario 2: Jet fire results comparison

Comparing the results of the jet fire consequence model as shown in Figures 7.3 and 7.4 with those in Figures 7.26 and 7.27 indicates that:

- The radiation contours predicted by the revised model are elliptical in shape, whereas those from the point source model are concentric circles.
- The damage contours display the same features as the radiation contours described in the previous point.
- The over-predictions as a result of using a point source model are clear from the damage contour plots.

Although the comparisons above are admittedly limited, it is felt that the ability of the pool fire and jet fire consequence models adopted here to simulate aspects of physical behavior has been demonstrated. These aspects include pool fire flame tilt due to the prevailing wind direction and the elliptical shape of a horizontal jet fire due to the momentum impulse created in such a scenario. In addition to radiation impact consequences, the overpressure impact caused by hot expanding combustion gases and unburned fuel gases was also considered by the consequence models employed in the current work.

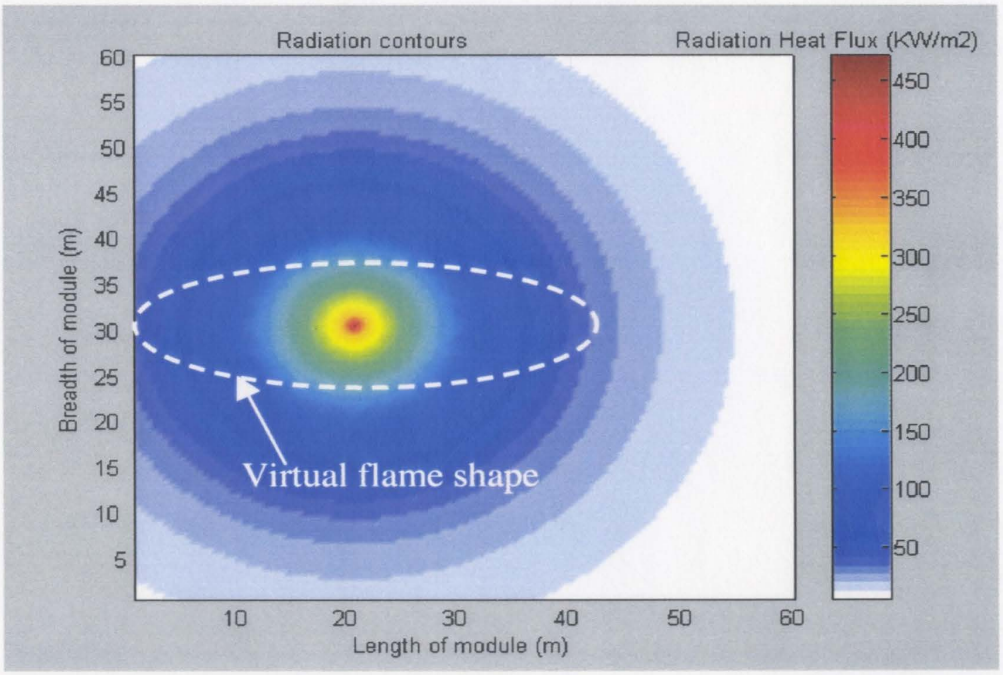

Figure 7.26. Radiation contours from point source jet fire consequence model.

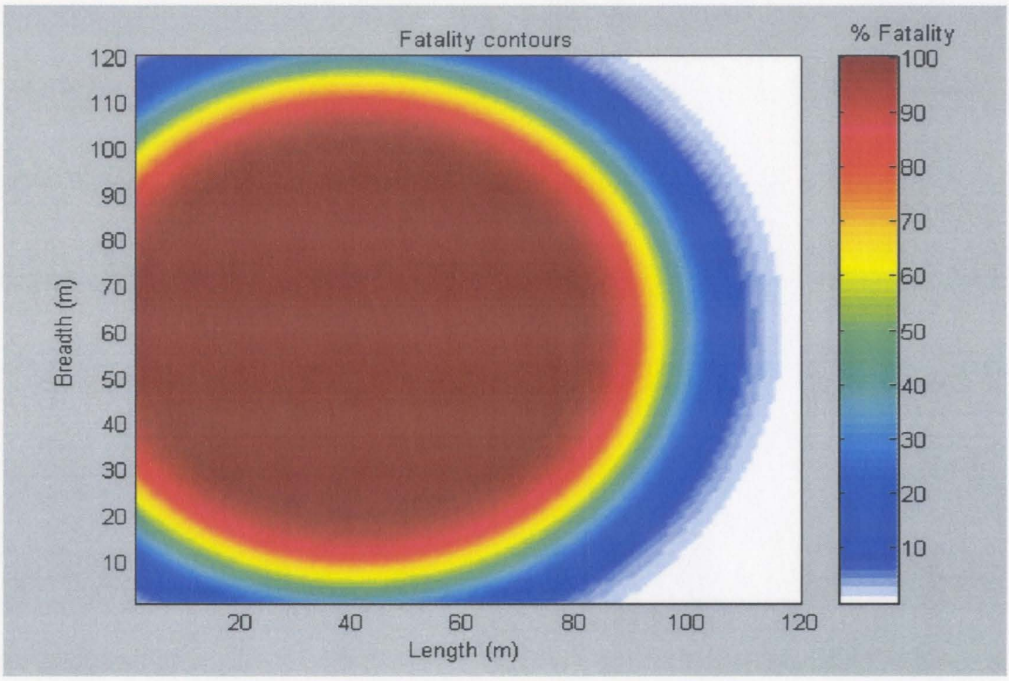

Figure 7.27. Percentage lethality (thermal radiation) contours from point source jet fire consequence model.

7.5. SUMMARY

In this chapter, the results obtained by simulation of a variety of scenarios for all the types of fires and explosions discussed in the work have been discussed. Consequences from these accidents were plotted as percentage fatality contours over the imaginary process area of a typical offshore platform. These contours provide an ability to develop a clear picture of potential impact zones and the safer zones. This can facilitate proper selection and specification of safe separation distances to prevent injury to people and damage to nearby

equipment. A limited comparison of these results with those obtained from models used in commercial software packages has also been made. The comparison justified the accurate predictions of the realistic radiation and damage contours using the models used in this approach. The results obtained from the probabilistic model developed to predict the probability of missile impact on a target object were also discussed. The probability of missile strike contours from "BLEVE in a horizontal cylinder" scenario has proved to be close to reality as well.

Chapter 8

CONCLUSIONS AND RECOMMENDATIONS

8.1. CONCLUSIONS

This work has been mainly focused on developing a computer automated toolkit that can assist the execution of consequence analysis of process related accidents such as fires and explosions, which commonly occur on offshore platforms. A methodology has been proposed for offshore consequence analysis and computer codes were subsequently developed using the proposed methodology and the consequence models discussed in chapters 3, 4 and 5. The following revisions were incorporated in the present methodology and consequence models in comparison with those used in available software packages:

- An enhanced onsite ignition model was used in the current study.
- The state-of-the-art fire and explosion consequence models were employed that closely match the physical characteristics of fire scenarios which arise on offshore installations.

- A fire overpressure model was employed to investigate the possibility of blast effects from fires occurring in confined offshore modules.
- A new probabilistic model was developed and used to characterize the effects of missiles on the escalation of accidents.
- A grid-based approach was adopted to enable better modeling and analysis of radiation and overpressure impact.

To illustrate the capability of the computer codes, a variety of credible accident scenarios was considered. The simulation results obtained from these scenarios were presented as hazard and damage contours by using the proposed grid based approach. These damage contours permit the development of a clear picture of potential impact zones over the process area. This can facilitate proper selection and specification of safe separation distances to prevent injury to people and damage to nearby equipment. This can also help in the design of protective layers (barriers between accident and receptors) and effective emergency response plans.

Overpressure generation from fires has also been shown to be a critical consideration in developing the impact zone map for an offshore facility. Also, missile impact analysis is found to be crucial in devising protective measures

against missiles and in designing the layout of the process area such that missile impact on the nearby equipment or the surrounding of its premises becomes improbable.

Finally, this work highlights the implementation of a grid based approach for offshore fire and explosion consequence analysis, which is found to be effective for contour plotting and analyzing the results in a better way. The kind of analysis carried out in this work can be used to predict the consequences from the hazardous events on offshore platforms.

8.2. RECOMMENDATIONS

i) **Comparison and validation of results:** In order to make the consequence models more reliable and the computer codes competitive with the existing ones it is necessary that the simulation results be properly compared and validated with the experimental results from large scale studies. Therefore, the first recommendation is to compare and validate the simulation results with the experimental results.

ii) **Sensitivity analysis:** Most of the inputs and the outputs from consequence studies are uncertain to some degree. In some cases, the

uncertainties may be very large, and the conclusions of the overall QRA may be sensitive to possible variations in the inputs or modeling assumptions. These uncertainties form one of the main limitations and it is important that they are understood and accounted for explicitly. Therefore, sensitivity analysis is one of the future directions for improvement of the current work.

iii) **Development of a user friendly software using Visual Basic:** Finally, a user friendly software package needs to be developed in Visual Basic making use of the computer codes developed during this work. This package can be subsequently combined with the supporting software packages for hazard identification and frequency analysis to come up with a comprehensive offshore QRA toolkit.

REFERENCES

Baker, Q.A. & Tang, M.J. (2000). Comparison of blast curves from vapor cloud explosions. *Journal of Loss Prevention in the Process Industries*, **13**, 433-438.

Baker, Q.A., Doolittle, C.M., Fitzgerald, G.A. & Tang, M.J. (1998). Recent Developments in the Baker-Strehlow VCE analysis methodology. *Process Safety Progress*, 17, **4**, 297-301.

Baker, Q.A., Pierorazio, A.J., Thomas, J.K., & Ketchum, D.E. (2004). An update of the Baker-Strehlow-Tang vapor cloud explosion prediction methodology flame speed table. *38th Loss Prevention Symposium*, AIChE.

Baker, W.E., Kulesz, J.J., Richer, R.E., Westine, P.S., Parr, V.B., Vargas, L.M., & Moseley, P.K. (1978). Workbook for estimating the effects of Accidental Explosions in Propellant handling systems. *NASA CR-3023. Washington:NASA Scientific and Technical Information office.*

Baum, M.R. (1993). Velocity of a single small missile ejected from a vessel containing high pressure gas. *Journal of Loss Prevention in Process Industries*, 6, 251-264.

Baum, M.R. (1995). Rupture of a gas-pressurized cylindrical vessel: the velocity of a detached end cap. *Journal of Loss Prevention in Process Industries*, 8, 149-161.

Baum, M.R. (1998). Rocket missiles generated by failure of a high pressure liquid storage vessel. *Journal of Loss Prevention in Process Industries*, 11, 11-24.

Carsley, A.J. (1994). A model for predicting the probability of impingement of jet fires. *IChemE Symposium Series No. 139*, 177-193.

Catlin, C.A. (1990). CLICHÉ - A generally applicable and practicable offshore explosion model. *IChemE Symposium Series No. 68*, Part B, 245-253.

CCPS (1994). *Guidelines for evaluating the characteristics of vapor cloud explosions, flash fires and BLEVEs*. New York: American Institute of Chemical Engineers.

CCPS (1996). *Guidelines for use of vapor cloud dispersion models*. New York: American Institute of Chemical Engineers.

CCPS (1998). *Estimating the flammable mass of a vapor cloud*. New York: American Institute of Chemical Engineers.

CCPS (2000). *Guidelines for chemical process quantitative risk analysis*. New York: American Institute of Chemical Engineers.

Chamberlain, G.A. (1987). Developments in design methods for predicting thermal radiation from flares. *Chemical Engineering Research and Design*, **65**, 299-310.

Chamberlain, G.A. (1996). Hazards posed by large-scale pool fires in offshore platforms, *Process Safety and Environmental Protection*, **74**, 81-87.

Chamberlain, G.A. (2002). Controlling hydrocarbon fires in offshore structures. *Proceedings of Annual Offshore Technology Conference*, 1211-1218.

Chamberlain, G.A., & Persaud, M.A.. (1997). A model for predicting the hazards from large-scale compartment jet fires. *IChemE Symposium Series No. 141*, 163-174.

Cox, R.A. & Carpenter, R.J. (1980). Further development of a dense vapor cloud dispersion model for hazard analysis. *Heavy Gas and Risk Assessment (Hartwig, S.)*, 55.

Cracknell, R.F., & Carsley, A.J. (1997). Cloud fires – a methodology for hazard consequence modeling. *IChemE Symposium Series No. 141*, 139-150.

Cracknell, R.F., Davenport, J.N., & Carsley, A.J. (1994). A model for heat flux on a cylindrical target due to the impingement of a large-scale natural gas jet fire. *IChemE Symposium Series No. 139*, 161-175.

Crowl, D.A. & Louvar J.F. (2002). Chemical process Safety: Fundamentals with Applications. *Prentice Hall international series in the physical and chemical engineering sciences*, Prentice- Hall Inc., NJ 07458.

Cullen, H. L. (1990). The Public Inquiry into the Piper Alpha Disaster, Department of Energy, HMSO, London.

Davis, B.C., & Bagster, D.F. (1989). The computation of view factors of fire models. *Journal of Loss Prevention in the Process Industries*, **2**, 224-234.

DiMattia, D.G., Amyotte, P.R. & Khan, F.I. (2004). Determination of human error probabilities for offshore platform musters. *International Conference on Bhopal and its Effects on Process Safety*, IIT-Kanpur, India.

Ditali, S., Colombi, M., Moreschini, G., & Senni, S. (2000). Consequence analysis in LPG installation using an integrated computer package. *Journal of Hazardous Materials*, **71**, 159-177.

Fitzgerald, G.A. (2001). A comparison of simple vapor cloud explosions prediction methodologies. *Second Annual Symposium, Mary Kay O'Connor process safety center*, Texas A&M University, College Station, Texas.

Hauptmmans, U. (2001). A procedure for analyzing the flight of missiles from explosions of cylindrical vessels. *Journal of Loss Prevention in Process Industries*, **14**, 395-402.

Holden, P.L., & Reeves, A.B. (1985). Fragment hazards from failures of pressurized liquefied gas vessels. *The Assessment and Control of Major Hazards*, 263.

HSE (1996). Offshore accident/incident statistics reports. *OTO96.954*, Health and Safety Executive, London, UK.

HSE (2001). Experimental data acquisition for validation of a new vapor cloud fire modeling approach. *HSL/2001/15*, Health and Safety Executive, London, UK.

Johnson, A.D. (1992). A model for predicting thermal radiation hazards from large scale LNG pool fires. *IChemE Symposium Series No. 130*, 507-524.

Johnson, A.D., Brightwell, H.M., & Carsley, A.J. (1994). A model for predicting the thermal radiation hazards from large-scale horizontally released natural gas jet fires. *Process Safety and Environmental Protection*, **72**, 157-166.

Johnson, A.D., Ebbinghaus, A., Imanari, T., Lennon, S.P., & Marie, N. (1997) Large-scale free and impinging turbulent jet flames: numerical modeling and experiments. *Process Safety and Environmental Protection*, **75**, 145-151.

Jones, J. C., & Irvine, P. (1997). PLATO© software for offshore risk assessment: a critique of the combustion features incorporated. *Journal of Loss Prevention in the Process Industries*, **10**, 259-264.

Khan, F. I., & Abassi, S.A. (1998). Rapid quantitative risk assessment of a petrochemical industry using a new software package MAXCRED. *Journal of Cleaner Production*, **6**, 9-22.

Khan, F. I., & Abassi, S.A. (2001). DOMIFFECT (DOMIno eFFECT): a new software for domino effect analysis in chemical process industries. *Environmental Modeling and Software*, **13**, 163-177.

Khan, F.I., & Amyotte, P.R. (2002). Inherent safety in offshore oil and gas activities: a review of the present status and future directions, *Journal of Loss Prevention in the Process Industries*, **15**, 279-289.

Khan, F.I., Sadiq, R., & Husain, T. (2002). Risk based process safety assessment and control measures design for offshore process facilities, *Journal of Hazardous Materials*, **94**, 1-36.

Krueger, J., & Smith, D. (2003). A practical approach to fire hazard analysis for offshore structures. *Journal of Hazardous Materials*, **104**, 107-122.

Lea, C.J., & Ledin, H,S. (2002). A review of the state-of-the-art in gas explosion modeling. *HSL Report 2002/02*, London, UK.

Lees, F.P. (1996). *Loss prevention in the process industries*. London: Butterworths.

Mansfield, D., Poulter, L., & Kletz, T.A. (1996b). Improving inherent safety: a pilot study into the use of inherently safer designs in the UK offshore oil and gas

industry. *HSE Offshore Safety Division Research Project Report*, HSE Office, London, UK.

Mansfield, D.P., Kletz, T.A., & Al-Hassn, T. (1996a). Optimizing safety by inherent offshore platform design. *Proceedings of 1996 OMAE Conference - Volume II (Safety and Reliability)*, June 16-20, 1996, Florence, Italy.

Phillips, W.G.B. (1994). Simulation models for Fire Risk Assessment. *Fire Safety Journal*, **23**, 159-169.

Pritchard, M.J., & Binding, T.M. (1992). FIRE2: A new approach for predicting thermal radiation levels from hydrocarbon pool fires. *IChemE Symposium Series No. 130*, 491-505.

Prugh, R.W. (1994). Quantitative evaluation of fireball hazards. *Process Safety Progress*, **13**, 83-91

Pula, R., Khan, F.I., Veitch, B. & Amyotte, P. (2004). Revised Fire Consequence Models for Offshore Quantitative Risk Assessment. *International Conference on Bhopal and its Effects on Process Safety*, IIT-Kanpur, India.

Pula, R., Khan, F.I., Veitch, B. & Amyotte, P. (2005). A Grid Based Approach for Fire and Explosion Consequence Analysis. Submitted for publication in *Process Safety and Environmental Protection.*

Puttock, J.S. (1999). Improvements in guidelines for prediction of vapor cloud explosions. *International conference and workshop of modeling the consequences of accidental releases of hazardous materials*, San Francisco, CA.

Puttock, J.S., Yardley, M.R., & Cresswell, T.M. (2000). Prediction of vapor cloud explosions using the SCOPE model. *Journal of Loss Prevention in the Process Industries*, **13**, 419-431.

Raj, P.P.K., & Emmons, H.W. (1975). On the burning of a large flammable cloud. *Joint Technical Meeting of the Western and Central States Sections of the Combustion Institute*, San Antonio TX.

Rew, P.J., & Daycock, L. (2004). Development of a method for the determination of on-site ignition probabilities. *HSE Contractor Report WSA/226*, HSE Books, London, UK.

Rew, P.J., Hulbert, W.G., & Deaves, D.M. (1997). Modeling of thermal radiation from external hydrocarbon pool fires, *Process Safety and Environmental Protection*, **75**, 81-89.

Rew, P.J., Spencer, H., & Daycock, L. (2000). Offsite ignition probability of flammable gases. *Journal of Hazardous Materials*, **71**, 409-422.

Rew, P.J., Spencer, H., & Madison, T. (1998). Sensitivity of risk assessment of flash fire events to modeling assumptions. *IChemE Symposium Series No. 144*, 265-278.

Rew, P.J., Spencer, H., Hockey, S.M., & Lines, I.G. (1995). Review of flash fire modeling. *HSE Contractor Report WSA/RSU8000/015*, HSE Books, London, UK.

Roberts, T., Gosse, A., & Hawksworth, S. (2000). Thermal radiation from fireballs on failure of liquefied petroleum gas storage vessels. *Process Safety and Environmental Protection*, **78**, 184-192.

Salzano, E., Picozzi, B., Vaciaro, S. & Ciambelli, P. (2003). Hazards of Pressurized Tanks involved in fires. *Industrial and Engineering Chemistry Research*, **42**, 1804-1812.

Scilly, N.F. & Crowther, J.H. (1992). Methodology for predicting domino effects from pressure vessel fragmentation. *Hazard Identification and Risk analysis, Human Factors and Human Reliability in Process Safety*, 1.

Spencer, H., & Rew, P.J. (1997). Ignition probability of flammable gases. HSE Books, London, UK.

Spouge, J. (1999). A Guide to Quantitative Risk Assessment for Offshore Installations, The Center for Marine and Petroleum Technology (CMPT) 1999, UK.

Thomas, P.H. (1963). The size of flames from natural fires. *Combustion*, **9**, 844.

Vachon, M., & Champion, M. (1986). Integral model of a flame with large buoyancy effects, *Combustion and Flame*, **63**, 269-278.

Van den Berg, A.C. & Mercx, W.P.M. (1997). The explosion blast prediction model in the revised CPR 14E (Yellow Book). *Process Safety Progress*, **16**, 3, 152-159.

Van den Berg, A.C. & Mercx, W.P.M., Hayhurst, C.J., Robertson, N.J., & Moran, K.C. (2000). Developments in vapor cloud explosion blast modeling. *Journal of Hazardous Materials*, **71**, 301-309.

Venart, J.E.S. (2001). Boiling liquid expanding vapor explosions (BLEVE); possible failure mechanisms and their consequences. *IChemE Symposium Series No. 130*, 491-505.

Vinnem, J.E. (1998). Evaluation of methodologies for QRA in offshore operations. *Reliability Engineering and System Safety*, **61**, 39.

Wayne, F.D. (1991). An economical formula for calculating atmospheric infrared transmissivites. *Journal of Loss Prevention in the Process Industries*, **4**, 86-92.

Wighus, R. (1994). Fires on offshore process installations. *Journal of Loss Prevention in the Process Industries*, **7**, 305-309.

Wilcox, D.C. (1975). Model for fires with low initial momentum and nongray thermal radiation, *AIAA Journal*, **13**, 381-386.

Appendix A - Simulation code for Jet fire consequence evaluation

```
% Simulation of horizontal jet fire consequence evaluation
clear all;
global density_air g G Ds W;

% momemtum flux G calculation
%*****************************************
Ts = 277;
gama_gas = 1.31;
Mdot = 11.2;
do = 0.152;
Wgk = 16.9*10^-3; %kg molecular weight of gas kg/mole (16.9 kg/kgmol)
density_gas_STP = 1.819;
Rc = 8.314 ;                %J.K/mol
Po = 101.3*10^3 ;           % N/m2
%*****************************************

% flame geometry variables
%*****************************************
density_air = 1.25;
g = 9.8;
W = 0.05;
Ua = 5;
Wa = 0;
%*****************************************

%ATMOSPHERIC TRANSMISSIVITY
%*****************************************
% RH = fractional relative humidity range(0-1)
% Smm = Saturated water vapor pressure in mm of Hg at the atmospheric temp T
% L = path length (m)

RH = 0.89;
Smm = 760;

T = 279;
Qc = 589822.48;% heat of combustion for methane is 890 Kj/gmol..
% Qc = Hc * Mdot/Mwt = 890*11.2/16.9e-3
%*****************************************

% thermal radiation variables
%*****************************************
k =0.4; % constant grey gas absorption coefficient m-1
%*****************************************


% CALCULATION OF MOMENTUM FLUX G

% calculation of Mach no for unchoked flow
%F = 3.6233*10^-5 * (Mdot/do^2) * sqrt( Ts/(gama_gas*Wgk) );
```

```
%Mach_jet = sqrt( (sqrt( 1+2*(gama_gas -1)*F^2 ) -1) / (gama_gas -1))

% Calculation of Temperature of the jet
% T_jet = ( 2 * Ts )/( 2 + (gama_gas -1) * Mach_jet^2 );

% Density of the expanded jet
% density_jet = density_gas_STP * 273/T_jet;

% velocity of the jet
% U_jet = Mach_jet * sqrt( (gama_gas*Rc*T_jet)/Wgk )

% diameter of the expanded jet
% D_jet = sqrt( (4*Mdot)/(pi*U_jet*density_jet) );

% momentum flux G
% G = ( pi * density_jet * U_jet^2 * D_jet^2)/4

% Ds = do * sqrt(density_jet/density_air)

% Calculation of Mach no for choked flow
Tc = (2*Ts)/(1+gama_gas)
Pc = 3.6713 * (Mdot/do^2) * sqrt( Tc/(gama_gas*Wgk) )
Mach_jet = sqrt( ((gama_gas+1)*(Pc/Po)^((gama_gas-1)/gama_gas) - 2) / (gama_gas-1) )

% Calculation of Temperature of the jet
T_jet = ( 2 * Ts )/( 2 + (gama_gas -1) * Mach_jet^2 )

% Density of the expanded jet
density_jet = density_gas_STP * 273/T_jet;

% velocity of jet
U_jet = Mach_jet * sqrt( (gama_gas*Rc*T_jet)/Wgk )

% diameter of the expanded jet
D_jet = sqrt( (4*Mdot)/(pi*U_jet*density_jet) );

% momentum flux G
G = ( pi * density_jet * U_jet^2 * D_jet^2)/4

Ds = D_jet * sqrt(density_jet/density_air);


% FLAME GOEMETRY

% calculation of flame length in still air
%options = optimset('Display','iter','TolFun',1e-5)
Lbo = fzero('calcLbo',[0.01 100])%,options)

GITA = ((pi*density_air*g)/(4*G))^(1/3) * Lbo
```

```
OHMx = sqrt(pi*density_air/(4*G))*Lbo*Ua      % Ua = wind speed in release direction (m/sec)
OHMz = sqrt(pi*density_air/(4*G))*Lbo*Wa      % Wa = wind speed perpendicular to release
(m/sec)

if(GITA <= 5.11)
   F_GITA = 0.55 + (1-0.55) * exp(-0.168*GITA);
elseif(GITA>5.11)
   F_GITA = 0.55 + (1-0.55) * exp(-0.168*GITA - 0.3*(GITA-5.11)^2);
end

if(GITA <= 3)
   r_GITA = 0;
elseif(GITA>3)
   r_GITA = 0.082*( 1-exp( -0.5*(GITA-3.3) ) );
end

% X position of the flame
X = Lbo * F_GITA *(1+ r_GITA * OHMx)

if(X>Lbo)
   X = Lbo;      % limit placed on the X position by setting a max value of X/Lbo = 1
end

h_GITA = (1 + (1/GITA))^-8.78
c_GITA = 0.02*GITA

% Y position of the flame
Y = Lbo * h_GITA * (1-c_GITA*OHMx)

Lbxy = sqrt(X^2 + Y^2)

% maximum width of the flame
W2 = Lbxy * ( -0.004 + 0.0396*GITA - OHMx*(0.0094 + 9.5*10^-7*GITA^5) )

% Flame lift off
b = 0.141 * sqrt(G*density_air)

% Minimum width of the flame
W1 = b*(-0.18 + 0.081*GITA)

% flame cannot become narrower than the forced convection limit and
% therefore W1/b has a minimum value of 0.12

if( W1/b < 0.12)
   W1 = 0.12*b
end

% Z position of the flame
```

```
Z = (X-b)*0.178*OHMz

Lbxz = sqrt(X^2 + Z^2);
%Lbxy = sqrt(Lbxz^2 + Y^2)

%calculation of angle of tilt with the vertical and the horizontal
theta_v = 90 - asin(Y/Lbxy)*180/pi
theta_h = asin(Z/Lbxz)*180/pi

% Room dimensions and grids
%*************************************************************************************************
coverage_distance = 100; %room area
% for radiation heat flux calculations, evaluation at each meter
if(coverage_distance>=50)
   n=51; % maximum number of grid for calcualtions.. just to reduce the execution time
else
   n = coverage_distance/1 + 1; % n meters = n+1 grids are required
end
%*************************************************************************************************


%ATMOSPHERIC TRANSMISSIVITY
%*************************************************************************************************
L_distance = relative_distance(coverage_distance,n,X);

  for i=1:n
      for j=1:n
         if(L_distance(i,j) == 0)
            Tou(i,j) = 1;
         else
            X_H2O(i,j) = RH * L_distance(i,j) * Smm * 2.88651*10^2 / T;
            X_CO2(i,j) = L_distance(i,j) * 273/T;
            Tou(i,j) = 1.006 - 0.01171 * log10(X_H2O(i,j)) - 0.02368 * log10(X_H2O(i,j))^2 -
0.03188*log10(X_CO2(i,j)) + 0.001164*log10(X_CO2(i,j))^2;
         end
      end
   end

%*************************************************************************************************

for i=1:n
   for j=1:n
      if(Tou(i,j)<0)
         Tou(i,j)=1;
      end
   end
end
```

```
% View factor calculation
%De = 2*sqrt(W1+W2)/Lbxy * ( Lbxy^2 + (W2-W1) )^(1/3)
De = (W1+W2)/2;
VF = viewfactor(theta_v,De,Lbxy,X,coverage_distance,n) ;
VFend = VF;
VFside = VF;

% surface emissive power
Fso = 0.21*exp(-0.00323*U_jet)+ 0.14;
RL = sqrt( (X-b)^2 + Y^2 ) ;
A = pi/4 * (W1^2 + W2^2) + pi/2 * (W1+W2) * sqrt( RL^2 + (W2-W1/2)^2 );
So = Qc*Fso/A;

Sside = So*(1-exp(-k*W2)) ;

Send = So*(1-exp(-k*RL)) ;

%Q = (Sside+Send).*VF .*Tou;
Q = (VFend*Send + VFside*Sside) .* Tou ;

x = 1:n;
y = x;
[X,Y] = meshgrid(x,y);
Z =  Q(x,y);%peaks(X,Y);
 pcolor(X,Y,Z);
 shading interp;
 hold on;
 contour(X,Y,Z);%,'k');
colorbar;
```

RELATIVE DISTANCE ROUTINE

```
function L = relative_distance(coverage_distance,n,flame_length);
%coverage_distance = 250;
%flame_length = 87.3;
%n=11; % no of grid points... usually 10m = 11 grids, distance b/w 2 grids = 1m

m = ceil(n/2);
k = 2*m-1; % to make a (m,2*m) matrix
X = zeros(m,k) ;

% first making a small compartment and then extending it
X(1,1) = coverage_distance/2; % right top compartment ...  125    ...  if coveragedist = 250m
X(m,k) = coverage_distance;  % right top compartment ...  0-250  ...
X(m,1) = 0;
```

```
% initializing the boundaries
horizontal_increment = (X(m,k)-0)/(k-1);
for i=2:k
   X(m,i) = X(m,i-1) + horizontal_increment; % filling the gaps between 0-250 depending on the
no. of grids
end

vertical_increment = ( X(1,1) - 0)/(m-1);
for i=2:m
   X(i,1) = X(i-1,1) - vertical_increment; % filling the gaps between 125-0
end

for i=1:m
   for j=2:k
      X(i,j) = sqrt( X(i,1)^2 + X(m,j)^2 );
   end
end

Y = X(1:m-1,:);
Y=flipud(Y);
X = [X;Y];   % Matrix which gives the relative distance from the location of fire


temp = coverage_distance - ceil(flame_length); % temporary variable for diff b/w room length
and fire length.

if(temp <=0)

   XX = zeros(m,k);
   XX(1,1) = coverage_distance/2;
   vertical_increment = ( XX(1,1) - 0)/(m-1);

   for i=2:m
      XX(i,1) = XX(i-1,1) - vertical_increment; % filling the gaps between 125-0 for first column
   end

   for i=2:k
      XX(:,i) = XX(:,1); %copying to all other columns
   end

   YY = XX(1:m-1,:);
   YY = flipud(YY);
   X = [XX;YY];
   L = X;

else

   FL_grids = ceil(flame_length/horizontal_increment)+1; %grids occupied by flame starting
from 0
```

```
Remaining_grids = n - FL_grids ;
X_copy = X(:,2:Remaining_grids+1);

XX = zeros(m,FL_grids);
XX(1,1) = coverage_distance/2;
vertical_increment = ( XX(1,1) - 0)/(m-1);

for i=2:m
   XX(i,1) = XX(i-1,1) - vertical_increment; % filling the gaps between 125-0 for first column
end

for i=2:FL_grids
  XX(:,i) = XX(:,1); %copying to all other columns
end

YY = XX(1:m-1,:);
YY = flipud(YY);
XX = [XX;YY];
X = [XX X_copy];
L = X;

end
```

VIEWFACTOR CALCULATION ROUTINE

```
% Viewfactor calculation at various grid points
function VF_target90 = viewfactor(theta,D,Len,flame_length,coverage_distance,n);
global L X_func theta_func

%*********************************************************************
% CALCULATION OF RELATIVE DISTANCES
%*********************************************************************

m = ceil(n/2);
k = 2*m-1; % to make a (m,2*m) matrix
X = zeros(m,k) ;
% first making a small compartment and then extending it
X(1,1) = coverage_distance/2; % right top compartment ...  125    ...  if coveragedist = 250m
X(m,k) = coverage_distance;   % right top compartment ...  0-250  ...
X(m,1) = 0;


% initializing the boundaries
horizontal_increment = (X(m,k)-0)/(k-1);
for i=2:k
   X(m,i) = X(m,i-1) + horizontal_increment; % filling the gaps between 0-250 depending on the
no. of grids
end
```

```
vertical_increment = ( X(1,1) - 0)/(m-1);
for i=2:m
   X(i,1) = X(i-1,1) - vertical_increment; % filling the gaps between 125-0
end

for i=1:m
   for j=2:k
      X(i,j) = sqrt( X(i,1)^2 + X(m,j)^2 );
   end
end

Y = X(1:m-1,:);
Y=flipud(Y);
X = [X;Y] ;  % Matrix which gives the relative distance from the location of fire


temp = coverage_distance - ceil(flame_length); % temporary variable for diff b/w room length
and fire length.

if(temp <=0)

   XX = zeros(m,k);
   XX(1,1) = coverage_distance/2;
   vertical_increment = ( XX(1,1) - 0)/(m-1);

   for i=2:m
      XX(i,1) = XX(i-1,1) - vertical_increment; % filling the gaps between 125-0 for first column
   end

   for i=2:k
      XX(:,i) = XX(:,1); %copying to all other columns
   end

   YY = XX(1:m-1,:);
   YY = flipud(YY);
   X = [XX;YY];
   Xdup = X;

else

   FL_grids = ceil(flame_length/horizontal_increment)+1; %grids occupied by flame starting
from 0
   Remaining_grids = n - FL_grids ;
   X_copy = X(:,2:Remaining_grids+1);

   XX = zeros(m,FL_grids);
   XX(1,1) = coverage_distance/2;
   vertical_increment = ( XX(1,1) - 0)/(m-1);
```

```
   for i=2:m
      XX(i,1) = XX(i-1,1) - vertical_increment; % filling the gaps between 125-0 for first column
   end

   for i=2:FL_grids
     XX(:,i) = XX(:,1); %copying to all other columns
   end

   YY = XX(1:m-1,:);
   YY = flipud(YY);
   XX = [XX;YY];
   X = [XX X_copy];
   Xdup = X;

end


%************************************************************************
%CALCULATION OF ANGLE OF TILT AT DIFFERENT GRIDS
%************************************************************************

Theta = zeros(m,k);
theta = 72;
for i=1:m
   for j=1:k
      if(i==1 & j==1)
         Theta(i,j) = theta ;
      else
         Theta(i,j) = acot((i-1)/(j-1));
         Theta(i,j) = Theta(i,j)*180/pi;
         Theta(i,j) = (theta/90)*Theta(i,j);
      end
   end
end
Theta;
temp = Theta(2:m,:);
temp = flipud(temp);
Theta = [temp;Theta];
%************************************************************************

r = D/2;
l = Len;
Theta =  Theta*pi/180 ;

L = l/r;
X = X./r;
Phi = asin(1./X);

b1 = sqrt( (X.^2 - 1).*cos(Theta).^2 + (1 - 1./X.^2).*sin(Theta).^2 );
```

```
a1 = (atan( (L - ((X-1)./X).*sin(Theta))./b1) + atan( (((X-1)./X).*sin(Theta))./b1) ).*(1./b1);

%for i=1:n
 %   for j=1:n
  %      a2(i,j) = integraleval(X(i,j),theta(i,j));
   %     a3(i,j) = integraleval3(X(i,j),theta(i,j));
    %    a4(i,j) = integraleval4(X(i,j),theta(i,j));

    %end
    %end

for i=1:n
    for j=1:n
        X_func = X(i,j);
        theta_func = Theta(i,j);
        a2(i,j) = quadl('fintegral',0,pi/2);
        a3(i,j) = quadl('fA3integral',0,pi/2) ;
        a4(i,j) = quadl('fA4integral',0,pi/2) ;

       % a2(i,j) = integraleval(X(i,j),theta(i,j));
        %a3(i,j) = integraleval3(X(i,j),theta(i,j));
        %a4(i,j) = integraleval4(X(i,j),theta(i,j));

    end
end
a2 ;
a3(floor(n/2),floor(n/2)+2);

%VF_target90 = (1/pi) * cos(theta).*( a1.*cos(Phi) + L.*a2 );
VF_target90 = (1/pi) *( sin(Theta) .* ( a1.*cos(Phi) + L.*a2 ) + (a3-a4) );

for i=1:n
    for j=1:n
        if(Xdup(i,j)<=r)
            VF_target90(i,j) = 0.7;
        end
    end
end

VF_target90 = abs(VF_target90);
```